DISSERTATION

Evaluation of the cardiac involvement of chronic inflammatory bowel diseases using cardiovascular magnetic resonance

Evaluierung der kardialen Mitbeteiligung chronisch entzündlicher Darmerkrankungen mittels kardiovaskulärer Magnetresonanztomographie

zur Erlangung des akademischen Grades Doctor medicinae (Dr. med.)

vorgelegt der Medizinischen Fakultät Charité – Universitätsmedizin Berlin

von

Endri Abazi

Erstbetreuung: Prof. Dr. med. Jeanette Schulz-Menger

Datum der Promotion: 29.11.2024

TABLE OF CONTENTS

LIST OF ABBREVIATIONS

5-ASA	5-aminosalicylic acid
ACM	Arrhythmogenic cardiomyopathy
AHA	American Heart Association
ANOVA	Analysis of variance
BMI	Body mass index
BSA	Body surface area
bSSFP	Balanced steady-state free precession
CD	Crohn’s disease
CDAI	Crohn's Disease Activity Index
CMR	Cardiovascular magnetic resonance
CRP	C-reactive protein
DCM	Dilatative cardiomyopathy
ECG	Electrocardiogram
ECMO	Extracorporeal membrane oxygenation
ECV	Extracellular volume
EDV	End-diastolic volume
EIM	Extraintestinal manifestations
ESV	End-systolic volume
FT	Feature tracking
GBCA	Gadolinium-based contrast agents
GCS	Global circumferential strain
GLS	Global longitudinal strain
GRS	Global radial strain
HCM	Hypertrophic cardiomyopathy
HV	Healthy volunteers
IBD	Inflammatory bowel disease
IC	Indeterminate colitis
IQR	Interquartile range
LGE	Late gadolinium enhancement
LVEF	Left ventricular ejection fraction
MINOCA	Myocardial infarction with non-obstructive coronary arteries
MOLLY	Modified look-locker inversion recovery
MPR	Multiplanar reconstruction
MRI	Magnetic resonance imaging
MVO	Microvascular obstruction
ROI	Region of interest
RVEF	Right ventricular ejection fraction
SCCAI	Simple Clinical Colitis Activity Index
SCD	Sudden cardiac death
SCMR	Society of Cardiovascular Magnetic Resonance
SES-CD	Simple Endoscopic Score for Crohn's Disease
UCEIS	Ulcerative Colitis Endoscopic Index of Severity

LIST OF TABLES

LIST OF FIGURES

ABSTRACT (ENGLISH VERSION)

Introduction:

Inflammatory bowel diseases (IBD) are associated with known extraintestinal manifestations, however cardiac involvement is poorly understood. There is evidence of increased cardiovascular risks in IBD patients and of systemic inflammation involving the heart. Our study aims to assess cardiac involvement in terms of inflammation in IBD patients using cardiovascular magnetic resonance.

Methods:

In this prospective study, 50 adults with IBD were screened and 44 of them, without known ischaemic heart disease, were included. They were categorized into active disease and remission groups, while 44 age- and sex-matched healthy volunteers served as controls. Disease activity scores (CDAI, SCCAI) and endoscopic assessments (SES-CD, UCEIS) were conducted, and exclusion criteria (contraindications to CMR, GFR<30ml/min, pregnancy and lactation) were applied.

Imaging was performed with 1.5 Tesla scanner. Cine and parametric mapping (T1, T2, ECV) images were acquired. LGE and fat/water imaging were obtained. Biventricular function and strain analysis were conducted. Quantitative analysis of mapping used a 16-segment AHA model. For the statistical analysis, a p-value <0.05 was considered significant.

Results:

The analysis included 44 scans, 26 with active disease and 18 in remission. Baseline characteristics did not differ between the groups. Ventricular function was normal in both groups without significant differences. Patients in remission had higher myocardial mass indices compared to the control group ($p = 0.018$). T2 values showed no significant differences between the three groups ($p = 0.605$). Patients with active disease had significantly higher global T1 values than control ($p < 0.001$). ECV analysis did not show any differences between active and remission stages, but a moderate correlation between disease activity scores, global T1 values ($p = 0.049$) and global ECV ($p = 0.042$) was seen.

A non-ischemic LGE pattern was detected in 7/43 patients and myocardial fat infiltration in 5/44 patients. Both findings did not differ statistically when comparing active and remission groups. Pericardial effusions were significantly more prevalent in the active group compared to control ($p = 0.017$). Pleural effusions showed no such difference.

Patients with active disease had significantly lower global radial and circumferential strain values than control (GRS:p =0.002; GCS:p <0.001).
There was no difference in global T1, T2, and ECV when IBD patients were separated according to the presence of mesalazine treatment or monoclonal antibody treatment.

Conclusions:

This study suggests evidence of myocardial involvement in IBD patients due to detected subclinical changes with preserved LVEF. While cardiovascular complications in IBD are not very common, CMR may identify at-risk patients for closer monitoring and inform treatment decisions. Further research is required to explore this area, including the impact of various IBD therapies on myocardial injury.

ABSTRACT (DEUTSCHE VERSION)

Einführung:

Chronisch entzündliche Darmerkrankungen (CED) zeigen bekannte systemischen Manifestationen, jedoch ist die Herzbeteiligung wenig verstanden. Es gibt Hinweise auf erhöhte kardiovaskuläre Risiken bei CED-Patienten. Ziel der Studie ist die Herzbeteiligung in Bezug auf Inflammation bei CED mithilfe von CMR zu bewerten.

Methoden:

In dieser prospektiven Studie wurden 50 erwachsene CED-Patienten gescreent, davon 44 ohne bekannte ischämische Herzerkrankung, eingeschlossen. Sie wurden in aktive Erkrankungs- und Remissionsgruppen unterteilt, während 44 alters- und geschlechtsangepasste gesunde Freiwillige als Kontrollen dienten. Krankheitsaktivitäts-Scores, endoskopische Scores wurden durchgeführt, und Ausschlusskriterien angewendet. Die Bildgebung erfolgte mit 1,5 Tesla-CMR. Cine- und parametrisches Mapping wurden aufgenommen. LGE- und Fett-/Wasser-Bildgebung wurden durchgeführt. Die biventrikuläre Funktion und Strain wurde analysiert. Die quantitative Analyse des Mappings verwendete ein 16-Segment-AHA-Modell. Für die statistische Analyse wurde ein p-Wert <0,05 als signifikant angesehen.

Ergebnisse:

Die Analyse von 44 Patienten, 26 mit aktiver CED und 18 in Remission, zeigte keine Unterschiede der Grundlinienmerkmale zwischen den Gruppen. Die ventrikuläre Funktion war in beiden Gruppen normal und ohne Unterschiede. Patienten in Remission hatten im Vergleich zur Kontrollgruppe höhere Myokardmassenindexe ($p = 0,018$). T2-Werte zeigten keine signifikanten Unterschiede zwischen den drei Gruppen ($p = 0,605$). Patienten mit aktiver CED hatten signifikant höhere globale T1-Werte im Vergleich zur Kontrolle ($p <0,001$). ECV zeigte keine Unterschiede zwischen aktiver CED und Remission, aber es wurde eine moderate Korrelation zwischen Aktivitäts-Scores und globalen T1- ($p = 0,049$) und ECV-Werten ($p = 0,042$) gesehen.

Ein nicht-ischämischer LGE-Muster wurde bei 7/43 Patienten und eine Fettinfiltration bei 5/44 Patienten nachgewiesen. Beide Befunde unterschieden sich statistisch nicht zwischen aktiven und Remissionsgruppen. Perikardergüsse waren in der aktiven Gruppe signifikant häufiger als in der Kontrollgruppe ($p = 0,017$). Pleuraergüsse zeigten keinen solchen Unterschied.

Aktive CED-Patienten hatten signifikant niedrigere globale radiale und zirkumferenzielle Strainwerte im Vergleich zur Kontrolle (GRS: $p = 0,002$; GCS: $p <0,001$).

Es gab keinen Unterschied in globalen T1-, T2- und ECV-Werten, wenn Patienten nach dem Vorhandensein von Mesalazinbehandlung oder monoklonaler Antikörperbehandlung getrennt wurden.

Schlussfolgerungen:

Aufgrund nachgewiesener subklinischer Veränderungen bei CED-Patienten trotz erhaltener LVEF zeigten sich Hinweise auf Myokardbeteiligung. Obwohl kardiovaskuläre Komplikationen bei CED selten sind, könnte die CMR hochrisiko-Patienten identifizieren und überwachen sowie Therapieentscheidungen ermöglichen. Weitere Forschung ist erforderlich, um diesen Bereich weiter zu erkunden, einschließlich der Auswirkungen verschiedener CED-Therapien auf Myokardschäden.

1. INTRODUCTION

Chronic inflammatory bowel diseases (IBD) are part of a group of polygenic autoinflammatory diseases characterized by chronic inflammation of the gastrointestinal tract. The main entities are Crohn's disease (CD) and ulcerative colitis (UC). While intestinal manifestation is the defining characteristic of chronic inflammatory bowel diseases, extraintestinal manifestations (EIM) can affect various organ systems, occur frequently, and may precede intestinal manifestation. The occurrence of EIM can influence patients' quality of life and decisions regarding diagnostic and therapeutic interventions. [1, 2]

Little is known about the occurrence of a cardiac manifestation. To our knowledge, there are currently no systematic prospective CMR studies investigating potential cardiac involvement in the context of chronic inflammatory bowel disease. However, retrospective cohort studies have shown an increased risk of cardiovascular events and mortality due to cardiovascular causes, especially during the active phase of the disease. CMR case reports also showed patients with IBD flare developing clinically relevant forms of myocarditis. [3] Echocardiographic studies have already shown impaired left ventricular strain with preserved ejection fraction and an increased rate of pericardial effusions in this group of patients. The reasons for these observed correlations are unclear and potential targets of current research. A few hypotheses consider the presence of a systemic inflammation involving the heart muscle and the coronary arteries, leading to myopericarditis and/or coronary artery disease followed by heart failure. Other hypotheses suggest a correlation between long-term use of systemic corticosteroids and a higher risk for ischemic heart disease. [3-8]

CMR is an established clinical routine technique with a high safety profile, used for diagnosing and helping to make treatment decisions for cardiovascular diseases, as well as the primary imaging method for myocardial tissue characterization. The number of indications for cardiovascular magnetic resonance in the current ESC guidelines has increased over the last decade. A major role in this was given to the characterization and risk assessment of cardiomyopathies. For the detection of myocarditis, CMR is considered a mandatory test in the current guidelines. In the setting of ischemic heart disease, adenosine-based stress testing using CMR has an equivalent role to other non-invasive testing techniques. In the diagnostic work-up for MINOCA, the leading role of this method is already recognized in the differentiation of pathologies causing this entity. The study of myocardial viability, valvular heart disease, congenital heart disease, cardiac tumors and great vessel disease are some of the

main indications for CMR. [9-11]These aspects will be discussed in further detail in Section 1.5.
In the oncologic field, the influence of CMR has been increasing as well. For instance, subclinical changes in cardiac function and inflammatory myocardial changes have already been demonstrated by CMR in patients undergoing chemotherapy. [12, 13]

Using various sequences, it is possible to make intramyocardial cell death and cell changes visible and quantifiable. Our research groups have demonstrated this in patients with acute myocarditis.[14] Advances in weighted and parametric mapping techniques (T1, ECV, T2, T2* mapping techniques) allow spatial representation and quantification of tissue characteristics and allow conclusions to be drawn about disease processes. T1 and T2 mapping techniques allow the visualization of edema, fibrosis, and hyperemia. [12] Late gadolinium enhancement (LGE) images after contrast agent administration enable the visualization of focal fibrosis and scar formation in ischemic and non-ischemic cardiomyopathies. [13, 15] With CMR, it is possible to distinguish between intracellular (e.g., iron overload in hemochromatosis, glycosphingolipid deposits in Anderson-Fabry disease) and extracellular (e.g., fibrosis, accumulation of amyloid proteins in amyloidosis) changes in the myocardium or a combination of both (e.g., in the context of myocarditis or acute infarction). Focal and diffuse changes can be identified. [15]
Therefore, CMR can already detect subclinical cardiovascular involvement in various systemic diseases and is used for clarification of such involvement. [16-19]

There are different treatment options for patients with IBD. These include immunosuppressive or immunomodulating therapies and biological agents. [20]
There is evidence of an increased risk of developing myocarditis in patients treated with mesalazine. New classes of drugs are being implemented and developed, but there is still not enough data yet on the possible subclinical and clinical effects of these medications on the heart. [21-25] The study of the correlation between these therapies and myocardial changes using CMR should be of great importance since it can guide therapeutic decisions.

Our study aims to investigate the potential cardiac involvement in chronic inflammatory bowel diseases using cardiovascular magnetic resonance. In order to do so, we formulated the following hypotheses.
Primary hypothesis:

Patients with IBD show signs of myocardial damage in the form of diffuse and focal fibrosis compared to an age- and gender-matched healthy control cohort, even with preserved left ventricular ejection fraction.
Secondary hypotheses:
The following MR parameters show relevant differences between the two above-mentioned groups: functional parameters such as stroke volume, ventricular and atrial dimensions, myocardial elasticity (myocardial strain), and left and right ventricular ejection fraction (LVEF and RVEF).
The MR inflammation parameters differ significantly between patients with active IBD, patients in remission, and the healthy control group.
Medication used in the treatment of patients with IBD has an influence on the observed myocardial changes.

1.1. Inflammatory bowel disease

1.1.1. Epidemiology, etiology and types of inflammatory bowel disease

Inflammatory bowel disease is a group of clinical entities characterized by a localized or diffuse bowel inflammation with or without systemic involvement. The two main pathological presentations include ulcerative colitis and Crohn's disease.
The clinical presentation of CD differs from UC, as does the therapeutic approach. These differences are mainly due to the localization of micro- and macroscopic changes, the pattern of the inflammation involving the gut, and the systemic inflammation involving other organs and tissues. The treatment usually requires a multidisciplinary approach of different healthcare workers and nutritionists combined with lifestyle adaptation. This implies non-pharmacological, pharmacological and surgical treatments. [20]
Up to 15% of the patients present mixed or undistinguishable patterns of the two diseases at different points in time, so they are considered to have indeterminate colitis (IC). This diagnosis can change in time and be converted to UC or CD. [26, 27]

Recent studies suggest a prevalence of 0.2-0.3% of the European population living with IBD, with the first peak between 20 and 40 years and the second one between 60 and 80 years of

age. There are also differences in incidence and prevalence between western and northern compared to eastern European countries, showing a higher prevalence in developed countries, even though the incidence in developing countries has been rising recently. One major Danish study estimated a prevalence of CD with a range from 1.5 to 213 cases per 100,000 and of the UC from 2.4 to 294 per 100,000. Another international study showed a higher prevalence in western countries for females for CD and no relevant difference between sexes for UC. [28-30]

The exact etiology of the disease is still unknown, but there are known predisposing factors to IBD. Aside from predisposing genes which were found to be associated with either UC or CD, there are other environmental factors like smoking, nutritional factors (western diet), pollution and especially dysbiosis. The latter refers to the intestinal barrier and all the elements that can alter its physiological microbiome. One example is the early use of antibiotics in children that can change the intestinal microflora. These factors could play a role in activating an autoimmune inflammatory response, including the release of cytokines like TNF-α, IFN-γ and IL-12. As a result of this extensive inflammation, mucosal tissue damage can occur in different parts of the intestine with a pathognomonic distribution pattern according to the type of IBD. [31]

Ulcerative colitis represents a chronic inflammation of the intestinal mucosae involving the rectum with proximal extension in the colon. In the vast majority of cases, there is a defined margin between the inflamed and non-inflamed tissue. The diagnosis is made with sigmoidoscopy, but an ileocolonoscopy is advised to exclude the involvement of the ileum. [32] Histologically, atrophy of the crypts can be seen with basal plasmacytosis and an irregular villous surface. These microscopic changes, however, are not diagnostic and pathognomonic for UC. [33]

Crohn's disease, on the other hand, has a more segmental involvement of the intestine, with alteration of inflamed and healthy segments of intestines. Typically, the terminal ileum is affected, with very different patterns affecting the small intestine and colon. The diagnosis is based on clinical signs, endoscopic findings of the ileocolonoscopy, blood and stool tests, and histologic patterns, and this is all combined with imaging (MRI enteropathy of Sellink). Histologically, a segmental inflammatory pattern is seen, with the formation of granulomas and crypt distortion. [20, 33, 34]

1.1.2. Clinical and endoscopic disease activity

The clinical presentation of IBD can be manifold, it depends on the pattern and degree of inflammation of the intestine, and also on the systemic involvement of other organs with extra-intestinal manifestation. Both UC and CD are characterized by periods of active disease or relapse and by periods of disease remission. [20]
As a result of the above-mentioned aspects, and because of the frequently nonspecific symptoms, there is usually a delay of diagnosis of 23 months from the onset of symptoms. Similar results were confirmed by different studies done in different countries.
During the active phase of the disease, patients with ulcerative colitis mostly develop abdominal pain, diarrhea with blood and mucus in stool, fecal incontinence and urgency. Pancolitis is associated with extensive disease. [29, 35]
Patients with Crohn's disease develop symptoms like chronic diarrhea with weight loss and abdominal pain, but also anemia and fever. A complicated course of the disease is characterized by the formation of anal fistula and intestinal strictures. [29, 35-37]
It was shown that IBD increases the risk of colorectal cancer and extra-intestinal malignancies. The overall risk for malignancy was higher in patients with UC. [38, 39]

Both entities are also characterized by a systemic autoimmune response with inflammation involving other extra-intestinal organs. Except for the pyoderma gangrenosum and primary sclerosing cholangitis, these manifestations are more common for CD than UC. The most frequent of which is musculoskeletal involvement led by arthropathies and followed by cutaneous changes like erythema nodosum, pyoderma gangrenosum, and aphthous stomatitis. In terms of ocular manifestation, uveitis is seen more rarely than episcleritis. [2, 29, 40, 41]

The diagnosis of relapse is based on clinical, imaging, endoscopic, and lab findings. In order to appreciate the severity of the disease at any point in time, clinical and endoscopic scores are used. Two of the main clinical scores are Simple Clinical Colitis Activity Index (SCCAI) for UC and Crohn's Disease Activity Index (CDAI) for CD. As for the endoscopic scoring systems, two of the most common ones are the Ulcerative Colitis Endoscopic Index of Severity (UCEIS) and the Simple Endoscopic Score for Crohn's Disease (SES-CD) for UC and CD, respectively. [20]
The SCCAI score for UC has been already validated in different studies for its accuracy and also for its correlation in the follow-up of patients in the remission phase. It includes six clinical variables and does not require invasive testing or lab findings. It can also be used by

the patients themselves in order to follow up on the progression of the disease and partly self-diagnose a relapse or remission of the UC. There is range of 0-19 points, and a score higher than 5 points indicates a relapse, whereas a score equal to or lower than 2 indicates remission. [42]

The endoscopic scoring system UCEIS for UC is based on three major macroscopic variables: vascular pattern, bleeding, and erosions and ulcers. This score was designed to improve reliability, but a certain degree of interobserver variability is its main limitation. The scoring system varies from 0 to 8 points, where a score under 1 point indicates remission and a score above 2 indicates a relapse grading from mild to moderate and severe, each stage having a 2-point difference from one another. [43, 44]

CDAI, being a clinical score for CD broadly used for clinical and research purposes, relies upon different clinical parameters, laboratory data, and imaging. A score under 150 points indicates remission, over 150 points indicates active disease, whereas above 450 points indicates severe disease. The main limitation is the more complex calculation, which weighs more towards diarrhea (which can have other causes) and cannot be used in patients after surgery of the intestine. [20, 45]

SES-CD offers an endoscopic evaluation of the stage of the disease for patients with CD. It is a scoring system based on endoscopic parameters such as the size of the ulcers, ulcerated surface, affected surface, and the presence of narrowing. Under 2 points the disease is considered in remission, while 3-6 points is mild, 7-15 points is moderate, and over 15 points is severe endoscopic activity. This scoring system is considered simple to calculate, reliable and reproducible. [46, 47]

Two other inflammation markers that can be used to titrate therapy are the C-reactive protein (CRP) and fecal calprotectin. Both these elements can be used to appreciate the activity of the disease and effectivity of the therapy in IBD patients. The use of these markers has so far shown improved results for the short term but not for the long term. [48]

1.1.3. Treatment strategies

There is still no known causal therapy and, therefore, no treatment that can completely heal patients with IBD. The therapy goal is to reach and maintain remission for as long as possible, and by doing so, also reduce the risk for complications, extra-intestinal involvement, and tumors. There is still no broad consensus whether the main goal of the treatment should be the clinical/symptomatic remission or the endoscopic and histological one. It was seen that the endoscopic remission was related to better long-term outcomes, reduced frequency of relapses, and the incidence of colorectal carcinoma in patients with UC. A combined clinical and endoscopic remission is the current advised approach with the highest consent among specialists. [20, 49-51]

Ulcerative colitis in the active phase of mild to moderate disease requires first-line therapy with 5-aminosalicylic acid (5-ASA, mesalazine). It can be given orally and/or topically and it can also be used to maintain remission with good evidence. In case of intolerance or side effects like nephrotoxicity, corticosteroids can be used. Prednisolone was superior to 5-ASA for achieving remission. Budesonide and beclomethasone are two other alternatives in treating patients with mild to moderate disease. In case of moderate to severe disease with failure of 5-ASA, an approach with intravenous corticosteroids is preferred. [52-55]
Immunosuppressive therapy with thiopurines (such as azathioprine) still plays a role in maintaining remission after it is induced using corticosteroids. [56] In recent years, however, it has been broadly replaced by biologic therapy. Infliximab (anti-TNF alpha) has its main indication in patients with active disease in which the corticosteroids or thiopurines failed to achieve remission. [57] Adalimumab (anti-TNF alpha) had comparable efficacy to Infliximab in treating moderate to severe disease. [58] In case of failure of this therapy, the next advised step is the use of Vedolizumab (Anti-alpha4beta7-Integrin). [59] Ustekinumab (anti-IL12 and anti-IL 23) should only be considered in case of failure of the all above therapies. [60]
Tofacitinib (JAK-1 and JAK-3 inhibitor) is another additional alternative when the other therapeutic approaches are not successful or not tolerated by the patients. [61]
In case of resistant disease, intolerance of the above medication or life-threatening complications such as bleeding, toxic megacolon and perforation, a surgical approach is needed. The surgery of choice is subtotal colectomy and end ileostomy. This can be achieved laparoscopically or through open surgery. Both approaches have shown good long-term results in terms of quality of life and functional outcomes. [62-64]

Crohn’s disease in an active stage of the disease requires as first-line therapy the use of corticosteroids to induce remission in mild, moderate, or severe disease. Budesonide was shown as effective as prednisolone to treat mild to moderate disease, but a severe stage requires the use of prednisolone. [65, 66] In patients with severe disease, the use of biological therapy should be considered early on, in order to reduce the probability of developing complications. As the first line treatment, infliximab should be considered followed by vedolizumab and ustekinumab. [20, 67] As maintenance therapy, thiopurines (azathioprine) or methotrexate should be considered as first-line, followed by biological treatment with infliximab or vedolizumab/ustekinumab in case of inefficiency of the first therapy. [20]
The surgical approach is mostly laparoscopic with ileocecal resection in patients non-responsive to medical therapy and is also considered cost-effective taking into consideration the costs of biological treatments. [68]

1.2. Systemic inflammation and evidence of cardiac involvement

Systemic inflammation is characterized by the evidence of inflammation of two or more organs at the same point in time. [69] There are two major groups of known and classified diseases which are divided into autoimmune and autoinflammatory diseases. The first group can be a monogenic or polygenic entity that involves the activation of T-cells, B-cells and dendritic cells with the formation of autoantibodies against specific self-antigens. The second group, autoinflammatory diseases, are characterized by spontaneous inflammation without evidence of high autoantibodies and the absence of activation of the above-mentioned cells. For the majority of these clinical entities, there is no such complete division between the two groups, but there is more of a mixed and overlapped pattern resulting from a combination of the above mechanisms. [70]

Cardiac involvement in systemic disease can show different patterns and is associated with worse clinical outcomes. [71] The inflammation can involve the myocardium, pericardium or endocardium with myopericarditis and further development in dilatative or hypokinetic non-dilatative cardiomyopathy, or endocarditis with or without endomyocardial fibrosis; the conduction system of the heart can be affected and lead to arrhythmias; furthermore, the involvement of cardiac vascular system can result in micro- or macrovascular dysfunction. In the worst setting, heart failure and life-threatening arrhythmias can be the defining prognostic factors. [18, 72-74]

The clinical signs and symptoms can vary and be nonspecific. Chest pain, dyspnea, palpitations, syncope, heart failure symptoms, and survived cardiac arrest should be considered as red signs for possible cardiac involvement in patients with known systemic disease. [73]

The diagnostic workup after the clinical examination should continue with electrocardiography (ECG) and cardiac biomarkers such as Troponin (high-sensitivity Troponin, hs-Tnt) and N-terminal prohormone of brain natriuretic peptide (NT-pro BNP) should be taken. The non-invasive imaging is mainly focused on echocardiography followed by cardiac magnetic resonance (CMR) for tissue characterization, positron emission tomography (PET) for specific inflammatory diseases (such as sarcoidosis), and computed tomography (CT) mostly being used for aortic and coronary involvement. Endomyocardial biopsy (EMB) should be considered in experienced centers to further identify the etiology in case of suspected myocarditis. [18, 75]

The treatment regimen is mostly focused on treating the underlying systemic inflammatory condition with disease-specific immunosuppressive and/or immunomodulatory therapy. In some cases, this therapy should also be titrated based on the degree of cardiac involvement. Other supportive and cardiac-focused therapies might be required in case of relevant cardiac injury. [71]

Some of the known systemic diseases with common cardiac involvement are systemic lupus erythematosus, systemic sclerosis, sarcoidosis, rheumatoid arthritis, granulomatosis with polyangiitis, inflammatory myopathies, ankylosis spondylitis, and myasthenia gravis, among others. Additionally, for inflammatory bowel disease, being a systemic disease, there is a certain degree of evidence of cardiac involvement. [18]

1.3. Relation between inflammatory bowel disease and cardiac disease, the present state of knowledge

Although the systemic involvement of joints, skin, liver and other organs has been confirmed in patients with IBD, the degree of myocardial involvement in this patient population is still unclear. A recent retrospective study showed a higher risk for heart failure in patients with systemic lupus erythematosus, systemic sclerosis, rheumatoid arthritis and acquired immunodeficiency syndrome (AIDS). [76] Like in other systemic inflammatory diseases, it is reasonable to assume a certain degree of cardiac involvement also in patients with IBD. Cardiovascular manifestations have been reported in patients with IBD - the most common ones were myopericarditis, arrhythmias, endocarditis and heart failure. [77]

The main studies which addressed this issue date back to the late nineties and had a retrospective approach. One major Danish study with a registry-based follow-up of 16 years showed an increased risk for myocarditis in patients with inflammatory bowel disease, which was partly also caused by the medication (such as mesalazine) used to treat these conditions. [78]

There are multiple case reports in the literature with patients in the active phase of the disease (CD or UC) with recurrent myocarditis confirmed by CMR or biopsy. In some of these cases, the cause could not be fully differentiated between drug toxicity or systemic inflammation with heart involvement. [3, 7, 8]

Different meta-analyses showed an overall increased risk of cardiovascular events (myocardial infarction, stroke, heart failure and cardiovascular death) in IBD patients with active disease compared to the general population. [5, 6, 79]

Another study identified 28 pediatric patients with IBD who developed myocarditis or pericarditis as an EIM or a consequence of drug toxicity. 50% of these patients were in an active phase of the IBD at the time of the diagnosis. The mechanism is unclear and possible correlations are still to be confirmed. It was reported that an anti-inflammatory therapy with corticosteroids used for the treatment of active IBD also improved the cardiac symptoms in these patients. Two of these patients needed pericardiocentesis and one developed fulminant myocarditis requiring extracorporeal membrane oxygenation (ECMO). The diagnosis, however, is usually difficult to make and remains a diagnosis of exclusion. Even if it is a rare complication of IBD, myocarditis can in some cases be a life-threatening condition that requires an early diagnosis and prompt therapy. [21]

1.4. Drug-induced cardiac disease in IBD patients undergoing therapy

IBD treatments' effects on cardiac function have already been considered in a few studies. 5-ASA (such as mesalazine) is the most commonly used medication to induce and maintain remission in patients with active mild to moderate ulcerative colitis. This drug also appears to be the leading cause of myocarditis and pericarditis in this group of patients according to some studies. The mechanisms that explain this correlation are still unknown. Some of the hypotheses are based on the humoral response of the organism, with the formation of autoantibodies against 5-ASA and cross-reaction with cardiac or pericardial cell-antigens, while others explain it as a hypersensitivity IgE-mediated reaction, or as a direct toxic effect of the drug itself on cardiac tissue. [21, 22, 80]

There is no broad consensus on whether the myocarditis is induced in the first 2-4 weeks after therapy or later. A major role in postponing the myocardial involvement seems to be played by the corticosteroid therapy, which is commonly given in the acute phase of UC together with 5-ASA. [81]

Infliximab was also reported to correlate with the development of myocarditis and/or pericarditis in patients with IBD undergoing this treatment. The mechanism is unknown, but it might involve a type 3 hypersensitivity reaction. [23]

Other studies and case reports showed a correlation between the development of myocarditis/pericarditis in patients being treated with methotrexate, azathioprine, etanercept, and adalimumab. The mechanisms are mostly unknown, and the diagnosis was made after pausing the administration of the drug, which was followed by clinical improvement. [24, 25, 82-84]

In some of the reported cases, the therapy was also based on the concomitant administration of steroids. The drug suspected to cause the inflammation was exchanged with a drug of another category. [21]

1.5. Role of cardiovascular magnetic resonance in detecting cardiac disease

Cardiovascular magnetic resonance has developed exponentially in the last 20 years and has become of crucial importance in the field of cardiovascular medicine. Its implementation is very broad as it offers a multitude of information regarding cardiac function, tissue characterization with the detection of subclinical myocardial changes, valvular disease, ischemic heart disease, cardiac masses, great vessel disease, congenital heart disease and more. New techniques are in development and CMR is in constant evolution. [13, 15]
Its role in detecting cardiac changes in systemic disease has already been supported and confirmed by different studies. The accuracy of measuring the myocardial volumes and mass left and right ventricular function has already been demonstrated. Using T1 and T2-weighted as well as mapping techniques with the help of contrast media-mediated imaging, myocardial inflammation, such as in the setting of myocarditis, can be detected. Local or diffuse fibrotic tissue involving the subendocardial, myocardial or epicardial layer can be differentiated. Using these techniques, it is possible to distinguish between ischemic and non-ischemic myocardial disease and also differentiate types of cardiomyopathies. One of the main advantages of CMR is that it can detect subclinical changes with still preserved left ventricular ejection fraction. The versatile character of CMR allows it to play an important role in cardiovascular research. [17, 19, 85]
In addition to the qualities mentioned above, the main advantages of CMR are based on it being a non-invasive and non-ionizing technique. It offers a competitive alternative to other imaging techniques used for the assessment of myocardial perfusion. The disadvantages include its availability and costs. Patient compliance with breath-holding and the restricted space inside the CMR scanner are other factors to consider in claustrophobic patients. For this purpose, non-breath-holding techniques were developed. Cardiac devices can either be a contraindication for CMR or can reduce image quality and interpretation. The same consideration should also be taken in patients with irregular heart rhythms. Additionally, in these cases, alternative methods such as real-time imaging were developed in order to make semiquantitative image interpretation possible. In case of devices, specific techniques such as wideband LGE can be used.
Chronic kidney insufficiency with a glomerular filtration rate (GFR) under 30ml/min is also another relative contraindication for the injection of gadolinium-based contrast media. [86]

The majority of clinical CMR are done using 1.5 Tesla systems, however, there is an increased usage of 3 Tesla systems, and each of them has its own advantages. Some of these differences between the two systems are:
The ECG-gating on 3T can be more problematic and unreliable than 1.5T; devices identified as safe on 1.5T may not be safe on 3T. Conversely, 3T may produce better image quality for perfusion imaging, tagging and 4D Flow. [87]

1.5.1. Cardiac dimensions and function

The measurement of left ventricular mass and volumes, as well as end-diastolic (EDV) and end-systolic volumes (ESV) is done with high accuracy using CMR, making it the gold standard imaging method for these measurements. These parameters were shown to be important predictors of the risk for cardiovascular events (LV mass) and ventricular remodeling (EDV, ESV). [88]
The assessment of left ventricular ejection fraction (LVEF) is done with high accuracy (higher or comparable with echocardiography) and is reproducible. It has a low interobserver variability and is done using Simpson's method. [89, 90]
CMR is the leading imaging method to perform the assessment of the right ventricular ejection fraction (RVEF). This was demonstrated through meta-analysis to have a relevant prognostic value in the prediction of cardiovascular events in patients with heart failure and in those with myocarditis. [91, 92] Another main indication in performing accurate measurement of RVEF is a suspected arrhythmogenic cardiomyopathy (ACM). [93]
The image acquisition is made using balanced steady-state free precession (bSSFP) as a first-choice method. It offers the highest signal-to-noise ratio and high myocardium/blood contrast. This method makes image acquisition possible with cines of long- and short-axis views produced during breath-hold. The long-axis cine images are divided into four-, two- and three-chamber views. The short axis view is acquired from the apex to the base of the left ventricle, with an average slice thickness of 6 to 8mm. Measurements of LV mass, volumes, and ejection fraction are done by contouring the endo- and epicardial lines in the four- and two-chamber views in the end-diastole and end-systole. For a more accurate evaluation of the right ventricle dimensions and function, an axial view with multiple thin slices should be considered. Due to the thin atrial walls, the measurement of area and volumes is done

following the endocardial contours in the four- and two-chamber views timed at the maximal filling of the atria before the opening of the atrioventricular valve.
In case of inability to hold breath by the patient or irregular heart rhythm, bSSFP can be susceptible to artefacts. An alternative is the ultra-fast acquisition of images called real-time imaging, which acquires many images a second and provides a cine sequence of a cardiac cycle. This is performed without the patient needing to hold their breath. It allows at least a visual assessment of the ventricular function and a semiquantitative assessment of heart-chamber dimensions since it offers lower image quality. [87, 94]

1.5.2. Tissue differentiation and parametric mapping

Tissue differentiation is made possible through CMR, which not only permits a visual appreciation of myocardial tissue changes but also a quantification of these changes. Using T1, T2, T2* relaxation times and ECV makes a distinction possible between intracellular and extracellular myocardial tissue changes and infiltrations. By doing so, it is possible to differentiate diseases with a known specific pattern of myocardial involvement. [12]
There are multiple applications for using parametric mapping in CMR. Some of them are in patients with suspected myocarditis, cardiomyopathies, heart failure, myocardial infarction, amyloidosis, Fabry disease, iron overload (hemochromatosis) and myocardial masses. [12, 95-101]
T1 represents a time constant of the recovery of longitudinal magnetization, whereas T2 is a time constant of the decay of transverse magnetization. In case of suspected local field inhomogeneities like iron overload, the T2* time constant is used. The ECV is acquired as a T1 time constant and is calculated based on the T1 times before and after contrast media administration by also taking into consideration the hematocrit of the patient. It is given as a percentage of extracellular volume. The calculation of ECV is done using this formula:
$ECV = (1 - \text{Hematocrit}) \times (\Delta R1_{\text{myocardium}} / \Delta R1_{\text{blood}})$, where $R1 = 1/T1$. [12]
Native T1 and ECV mapping are taken using the same slice and cardiac phase. ECV should be acquired 10-30 minutes after Gadolinium (0.1-0.2mmol/l) administration. [102]
The clinical interpretation of altered T1, T2 relaxation times and ECV values is based on a combined evaluation of all these three mapping techniques. Native T1 relaxation time can increase in a setting of increased acute or chronic free water content at an intra- or

extracellular level. Other causes of increased interstitial space prolong the T1 relaxation time. Diffuse interstitial fibrosis is one common condition that correlates with higher T1 values. [103] Particularly high values are seen in patients with cardiac amyloidosis as a result of interstitial infiltration of amyloid fibrils. Native T1 relaxation times can be very useful in determining the diagnosis. [97] Contrary to amyloidosis, Fabry disease with heart involvement is characterized by very low T1 relaxation times. In combination with specific LGE patterns in the basal inferolateral myocardial wall, it can make an early diagnosis of this condition possible.[98] Generally increased T1 time should be considered as a marker for pathological myocardium but not specific to the kind of pathology and activity of the disease. [104]

Since native T1 is sensitive to myocardial edema but less specific in differentiating acute versus chronic stages, it is recommended to combine it with T2 mapping for a better interpretation of myocardial changes. This is a very important marker in detecting the presence of edema in an acute setting. [105] It shows typically high values in the presence of edema in an acute ischemic setting, or if an ischemic injury is ruled out, it correlates with high accuracy with myocardial inflammation as seen in myocarditis. It has a high sensitivity of 89% in ruling out active myocarditis and it can discriminate between acute and healed myocarditis. [106, 107]

Conditions that increase the interstitial space, such as diffuse edema and fibrosis, increase ECV values. It is also typically increased locally in areas in which focal fibrosis is detected by LGE. Like native T1, ECV shows particularly high values (above 40%) in the case of amyloid disease of the heart. [108, 109]

The most common indication for parametric mapping is the suspected myocarditis. Histological changes are characterized by myocardial edema with hyperemia and capillary leakage, followed by necrosis and fibrosis. These changes can be detected with different techniques used in CMR. The widest consensus for the diagnosis of myocarditis using CMR is based on the implementation of the updated Lake Luise Criteria II of 2018. This represents a combination of T2-based imaging (myocardial edema) with T1-based imaging (non-ischemic myocardial injury) for the diagnosis of myocarditis. Supportive criteria such as pericarditis and systolic LV-dysfunction are also used for the diagnosis. [104, 110]

1.5.3. Late gadolinium enhancement

The use of late gadolinium enhancement for ischemic and non-ischemic heart disease has been validated for more than 20 years. It is the gold standard of all cardiac imaging for the evaluation of myocardial viability. Apart from its use in cardiac ischemic disease, the other main recommendations include different types of cardiomyopathies, myocarditis, and arrhythmogenic tissue differentiation providing guidance for interventional ablation therapy. [111-113]

Its implementation is based on the effect that gadolinium-based contrast agent (GBCA) has on shortening the T1 recovery time, its tissue-dependent distribution pattern, and the wash-in/wash-out effect. Gadolinium does not pass the cellular membrane but remains in the interstitial space. In the case of fibrosis with augmented interstitial space, GBCA requires more time to get distributed in the interstitium and stagnates longer than in other parts of healthy myocardial tissue. In case of acute myocardial damage with rupture of cell membranes, it can also enter the damaged cells. The image acquisition is done typically 10 minutes after GBCA administration, when the areas with accumulated contrast agents cause a shortening of T1 recovery time, which results in a delayed higher enhancement of the signal. [114-116]

In 2017, the use of linear GBCA was suspended due to concerns about cerebral deposition and it was replaced with macrocyclic GBCA, raising the safety profile of these contrast agents. [117]

The image acquisition is done by using myocardium-specific T1 times so that the longitudinal magnetization of the myocardium is null during signal acquisition. By doing so, the myocardium will appear dark, but blood and fibrotic tissue will be enhanced due to the relevant shortening of T1 relaxation time.

Three slices of the long axis (four-, three-, and two-chamber views) and multiple slices of the short axis are produced. The image interpretation is based on describing the localization of LGE (sub-, intra-, or epicardial), its extent and the presence of areas of microvascular obstruction (MVO). [116]

Ischemia-induced LGE starts at a subendocardial level spreading in the direction of the epicardial part with different degrees of transmurality. Non-ischemic LGE typically spares the subendocardial layer and it is located mostly in the intramyocardial or epicardial layers. LGE is also very useful in detecting myocarditis (Lake Luise Criteria II), differentiation between cardiomyopathies and in case of suspected heart involvement in systemic disease. [116]

The quantification of the LGE presence in patients with hypertrophic cardiomyopathies (HCM) has been shown to be an important risk stratification tool for the prediction of sudden cardiac death (SCD) in patients with preserved ejection fraction. A LGE>15% was associated with an increased risk of SCD. [118, 119]
A typical pattern found in almost 30% of dilatative cardiomyopathies (DCM) is the intramyocardial fibrosis in the septum, also known as the "mid-wall sign". [120]
HCM typically present a more inhomogeneous LGE distribution pattern. [121]
The study of myocardial viability has shown that ischemic LGE with a transmurality of less than 50% predicts a high rate of functional myocardial recovery, whereas more than 50% transmurality is correlated with poor functional recovery. [122]
The presence of LGE in the setting of myocarditis, DCM and HCM has also been correlated with a higher rate of arrhythmias, heart failure and mortality. [123-125]
To summarize, the extension of LGE has been demonstrated to be an independent important predictor for cardiovascular events. [126]

1.5.4. 3D-LGE imaging methods

3D LGE is a free-breathing technique that can produce high-resolution images in a 3D pattern, making it possible to analyze the whole heart under a single scan using multiplanar reformatting (MPR) software. The main advantages additionally involve the possibility to better analyze the scar complexity, to detect abnormalities in smaller cardiac structures and to better identify peri-infarct areas. Apart from these advantages, the main disadvantages constitute the longer acquisition time and the artefacts in case of arrhythmias and tachycardia. [116, 127, 128]
In order to eliminate artefacts caused by fat tissue or to identify fat infiltration in the myocardium, the 3D LGE fat-water Dixon method was developed. It is based on using pulse frequencies in which fat and water are either in phase or out of it. By separating these signals, two kinds of images are produced, one with only water and one with only fat. [116, 129, 130]
The presence of intramyocardial fat tissue was associated with different diseases, such as ACM, DCM, and lipomatous metaplasia of an ischemic scar. Its presence was described to be of prognostic value, increasing the risk for cardiac events as a substrate for potential arrhythmias. Fat tissue can also be identified in benign or malignant heart tumors, such as lipoma and liposarcoma. [116, 131, 132]

1.5.5. Ventricular strain analysis

Ventricular strain analysis is a CMR technique which permits an objective quantification of contractile myocardial dysfunction. The application of this technique is based on the anatomy and orientation of the muscular fibers of the heart. The subendocardial layer has longitudinal fibers with orientation from base to apex. On the other hand, the subepicardial layer has longitudinal fibers in the opposite orientation of the subendocardial one. The intramyocardial layer has circular fibers. As a result, the contractile motion of the ventricle is a combination of circular and longitudinal shortening, torsion and radial thickening. Consequently, in CMR imaging, a longitudinal, radial and circumferential strain is used to assess the contractile function of the ventricle. [133]

The longitudinal strain evaluates the shortening from the base to the apex of the ventricle, whereas the circumferential one represents the circular shortening observed on the short-axis view. Both of them are given in negative values, but the radial strain, which is the radial deformation of the ventricle directed towards the LV cavity, is given in positive values. [134]

The analysis is made by using tissue tagging or feature tracking. Tissue tagging has already been validated, but it requires predetermined sequences and scan times. Feature tracking can measure segmental and global strain values using the already routinely acquired cines. After manual tracking of the subendocardial and epicardial contours, the software identifies and tracks features moving with every image, calculating the displacement during a heart cycle. The main limitation is the artefacts caused by the features moving outside the plane. [135]

Higher values than -17% for the circumferential and -20% for the longitudinal strain are considered pathologic, whereas lower values than 20% for the radial strain are considered pathologic. The circumferential strain has better reproducibility and the highest consensus, while the radial one has shown higher range differences between studies, hence it is not yet well established in most centers. [136, 137]

Myocardial strain analysis using CMR has been studied in patients with ischemic heart disease, detecting impaired contraction in areas with ischemia, but also providing more information about infarction size and its transmurality. [138, 139]

Non-ischemic heart diseases like myocarditis and chemotherapy-induced cardiotoxicity showed pathologic values in the strain analyses in patients where changes in the ejection fraction were not yet evident. [140, 141] Another application of the strain analysis was found in cardiomyopathies such as DCM (typically characterized by impaired circumferential strain) and HCM (abnormal strain in the hypertrophied areas). [142, 143]

Different studies of patients with suspected cardiomyopathies or also of those without known coronary artery disease showed that impaired longitudinal or circumferential strain was related to a poor outcome (hospitalization, sudden cardiac death and all-cause mortality). [144, 145]

The use of strain analysis in a clinical context is yet to be established. Standardization of the contouring and quality evaluation is needed for the method to be comparable between different studies, in order to bring this technique to routine clinical use. [134]

1.6. Aims of the study

Our study aim is to investigate the degree of myocardial inflammation in patients with chronic bowel disease in different stages of the disease (active disease and in remission) using CMR to gain insights into cardiac involvement and its course.
We aim to detect subclinical changes in these patients and also correlate CMR disease markers with the IBD activity indexes. This may potentially help to earlier identify those patients with IBD who have a higher risk of developing cardiovascular events. Insights gained could help in the future to monitor individual treatment concepts and their response regarding cardiac involvement in chronic inflammatory bowel diseases and incorporate them into treatment decisions.

Our study also aims to investigate the impact on the heart of medications commonly prescribed to patients with IBD. Of particular concern is the potential cardiotoxic effect of mesalazine and new immunomodulatory and immunosuppressive therapies used for IBD. Therefore, our research seeks to shed light on the cardiovascular safety profile of these medications.

2. METHODS

2.1. Study population

This prospective study included 46 adult patients with IBD without known cardiovascular disease (CVD), recruited from a tertiary center. Two patients with arrhythmia were excluded due to non-diagnostic imaging. The patients were either in an active stage of disease and hospitalized for acute IBD flare, or in remission and recruited from the outpatient department. The study also included healthy volunteers as a control group who were matched for age and sex and had no history of CVD or cardiac symptoms. They had no pathologic ECG changes and underwent the same CMR scan protocol as the patients with IBD, but without injection of a contrast agent.

The diagnosis and stage of IBD were determined by a board-certified gastroenterologist using established guidelines. [20] Patients with active disease had an endoscopy and biopsy proof of acute intestinal inflammation. Infectious colitis, including Clostridium difficile, was excluded according to current guidelines. Patients in remission did not undergo repeated invasive endoscopy with biopsy since there was no clinical indication to do so. The distinction between active disease and remission was based on the clinical scores mentioned in the following paragraph (2.2).

Exclusion criteria for the study included contraindications to CMR, known CVD, renal impairment (estimated glomerular filtration rate <30 ml/min), known hypersensitivity to gadolinium, claustrophobia, and pregnancy or lactation for female subjects. Written informed consent was obtained from all participants, and ethical approval was granted by the institutional ethics committee under the number EA1/198/20. The study was registered in the ISRCTN registry (number: 30941346).

Patient screening, clinical assessment, and CMR were performed in the period from the 1st of April 2021 till the 30th of September 2022. The enrollment process was restricted and slowed down due to the Covid-19 pandemic. For safety reasons, patients who took part in the study were tested negative for Sars-Cov-2 infection and had no disease symptoms before the scan.

In the enrolment phase, a physician would go through a standardized questionnaire with each patient to collect information about cardiovascular comorbidities and cardiac-related

symptom history. Patients with ischemic cardiac disease were excluded from the study cohort. The presence of cardiovascular risk factors was noted and information about known arrhythmias such as atrial fibrillation (which could compromise CMR image interpretation) was collected. The presence of other systemic inflammatory diseases was also taken into consideration as a possible confounder.

Part of the questionnaire was additionally on the presence of cardiovascular symptoms such as dyspnea, angina pectoris, fatigue, palpitations and syncope.

In relation to the inflammatory bowel disease, detailed information was documented on: the disease entity and duration; endoscopic, histologic and abdominal MRI findings; and current disease activity scores. (*Tables 1,2*)

The current medications being taken by the patient for the treatment of the chronic inflammatory bowel disease including other non-related medications were noted.

Furthermore, laboratory testing containing reactive protein C (as a marker of local and systemic inflammation), albumin, creatinine and glomerular filtration rate, hemoglobin and hematocrit was taken as standard. (*Table 3*)

The process of enrollment of study participants is described in a strobe diagram as shown below. (*Figure 1*)

Enrollment process:

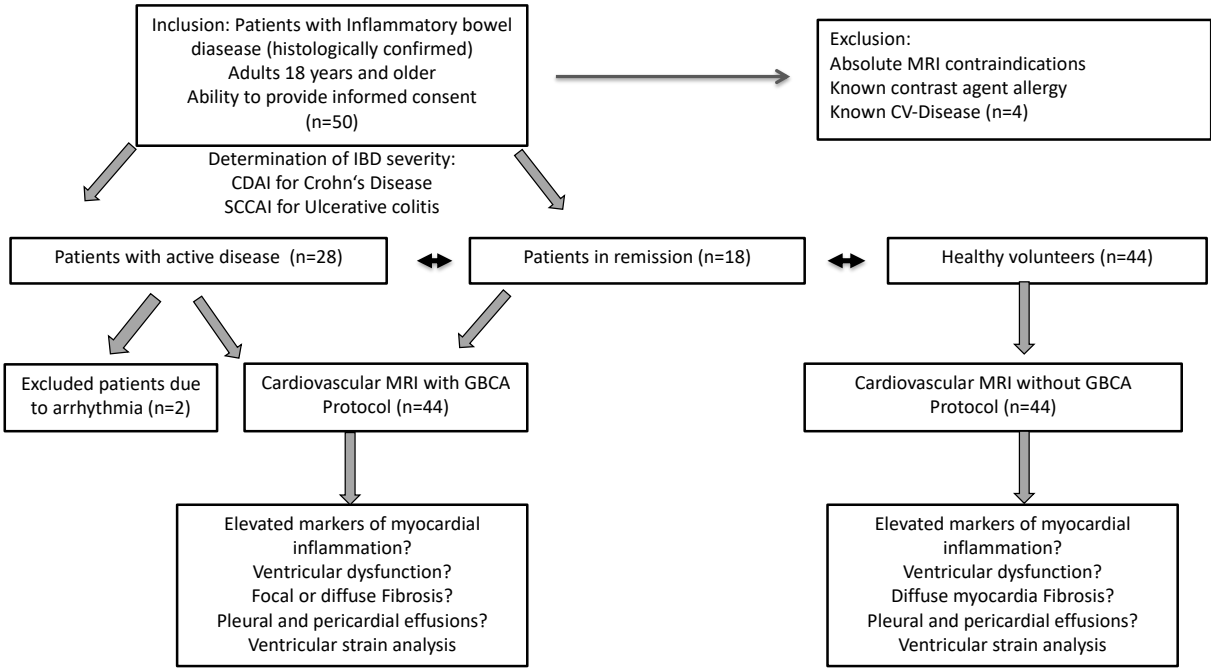

Figure 1. Enrollment diagram with inclusion and exclusion criteria. Representation of the number of patients from each group, the type of MRI test they underwent and the analysed aspects using MRI.

Allgemeine Angaben

Patienten-ID		
Geschlecht		o männlich o weiblich
Alter	[Jahre]	
Größe	[cm]	
Gewicht	[kg]	
BMI	[kg/m^2]	

Einschlusskriterien

Patient ist einwilligungsfähig und in der Lage Wesen und Tragweite der Untersuchungen zu verstehen	○ ja ○ nein
Alter > 18 Jahre	○ ja ○ nein
Einverständniserklärung vorliegend	○ ja ○ nein

Ausschlusskriterien

Absolute Kontraindikation für eine Kardio-MRT Untersuchung z.B. nicht MR-fähige Metallimplantate	○ ja ○ nein

Chronisch Entzündliche Darmerkrankung (CED) gesichert?

CED Entität?	
Erstdiagnose Chronisch entzündliche Darmerkrankung	[MM/YYYY]
Histologie CED vorliegend?	○ ja ○ nein (
Ergebnis Histologie (Datum und Zusammenfassung)	
Gastroskopie/ Koloskopiebefund vorliegend?	○ ja ○ nein
Hinweis für CED in Gastroskopie/Koloskopie (Datum und Zusammenfassung)	
MRT Abdomen vorliegend?	○ ja ○ nein
(MRT: Datum, Hinweis für Inflammation?, Lokalisation)	
Aktivitätsscore? (Name und Punktzahl) CDAI für M. Crohn, Clinician-based Simple Clinical Colitis Activity Index (SCCAI) für Colitis Ulcerosa	

Table 1. General patient information, inclusion and exclusion criteria, IBD medical history and activity scores (German version).

Laborwerte		
Datum der Laborentnahme	[MM/YYYY]	
Troponin (ng/l)	Falls vorliegend	
Nt-pro-BNP (pmol/L)	Falls vorliegend	
Albumin (g/dl)		
Kreatinin (mmol/l)		
GFR (ml/min)		
CRP (mg/dl)		
Hämatokrit (%)		
Hemoglobin (g/dl)		
Calprotectin (Stuhl)		

Nebendiagnosen

Koronare Herzgefäßerkrankung	o ja o nein
Akuter Herzinfarkt in der Anamnese? Falls ja, wann?	o ja o nein _____
Chronische Herzinsuffizienz	o ja o nein
Herzklappenerkrankungen Falls ja: Klappe, Insuffizienz/Stenose, Schweregrad (gering, mittel, schwer)	o ja o nein
Arterieller Hypertonus	o ja o nein
Hyperlipoproteinämie	o ja o nein
pAVK Falls ja: Stadium	o ja o nein _____ nach Fontaine
Vorhofflimmern	o ja o nein
Herzrhythmusstörungen Falls ja, welche?	o ja o nein _____
Diabetes mellitus Typ 1	o ja o nein
Diabetes mellitus Typ 2	o ja o nein
Andere systemische entzündliche Erkrankung	o ja o nein _____
Chronische Niereninsuffizienz? Falls ja: K/DOQI-Stadium	o ja o nein o I o II o III o IV

Table 2. Laboratory findings and secondary diagnosis (German version).

Anamnese

Angina pectoris	o ja o nein
Luftnot (NYHA-Stadium)	o ja o nein o I o II o III o IV
Fatigue	o ja o nein
Palpitationen	o ja o nein
Nikotinabusus (in pack-years)	
Synkope	o ja o nein

Dauermedikation (CED-Medikation)

Substanz [Wirkstoff]	Dosis [mg]	Häufigkeit der Dosis-applikation	Applikations-weg
			o oral o _____
			o oral o _____
			o oral o _____
			o oral o _____
			o oral o _____
			o oral o _____

Table 3. Cardiovascular symptoms and current medical therapies (German version).

2.2. Definition and measurement of inflammatory bowel disease activity indexes

Prior to the CMR scan, disease activity scores were clinically assessed using the Simple Clinical Colitis Activity Index (SCCAI) for patients with UC and the Crohn's Disease Activity Index (CDAI) for patients with CD. The SCCAI is an established questionnaire that assesses symptom severity based on six criteria (*Table 4*) over the last seven days and can detect disease activity in remission. A SCCAI $\leq$ 2.5 was defined as indicating remission. [42] The CDAI is also established in clinical trials to assess the severity of illness in patients with CD using eight clinical criteria (*Table 5*). Scores $\leq$ 150 are considered to indicate remission, while a CDAI > 450 is a marker of severe CD. [45]

For patients with active disease, validated indices were used to measure endoscopic disease activity. The Ulcerative Colitis Endoscopic Index of (UCEIS) was used in UC patients, with remission defined as a score $\leq$ 1 and higher scores indicating active disease up to a maximum of 8 points. [43] The Simple Endoscopic Score for Crohn's Disease (SES-CD) was used in CD patients, with scores higher than 2 points indicating active disease, with the highest severity when over 15 points are calculated. [46] The disease duration of each patient was calculated in days. Day one was considered as the day of IBD diagnosis. When this was uncertain, the first day of the same month was taken. A calculation was done from day one to the date of CMR examination.

To correlate CMR biomarkers (T1, T2, ECV, strain) with clinical activity indices and disease duration, SCCAI and CDAI scores were standardized using Z-scoring to include both UC and CD patients in one model. The standardized activity index was calculated per patient as:

$$\mathrm{Z-Score} = \frac{(\mathrm{CDAI\ or\ SCCAI}) - \mathrm{mean}\ (\mathrm{CDAI\ or\ SCCAI})}{\mathrm{Standard\ deviation}\ (\mathrm{CDAI\ or\ SCCAI})}$$

Kriterium	Gewichtungsfaktor	Punkte
Durchschnittliche Anzahl Stuhlgänge pro Tag	1-3 = 0 4-6 = 1 7-9 = 2 >9 = 3	
Durchschnittliche Anzahl Stuhlgänge pro Nacht	1-3 = 1 4-6 = 2	
Stuhldrang	eilig = 1 sofort = 2 inkontinent = 3	
Blut im Stuhl	Spur = 1 Gelegentlich frisches Blut (< 50% der Stuhlgänge) = 2 meist frisches Blut (>50% der Stuhlgänge) = 3	
Allgemeinbefinden	sehr gut = 0 leicht schlechter als normal = 1 schlecht = 2 sehr schlecht = 3 schrecklich = 4	
Extraintestinale Manifestationen (1 Punkt pro Manifestation)	Leber/Gallengänge: Primär sklerosierende Cholangitis (PSC) Gelenke: Arthritis, Spondylitis ankylosans, Sakroiliitis Haut/Mundveränderungen: Erythema nodosum, Pyoderma gangraenosum, Pyostomatitis vegetans Auge: Iritis, Episkleritis, Uveitis	
	Summe	

Table 4. SCCAI scoring system (German version).

Kriterium	Gewichtungsfaktor	Punkte
Durchschnittliche Anzahl flüssiger oder weicher Stuhlgänge pro Tag innerhalb letzten 7 Tage	14 Punkte/ Stuhlgang	
Verwendung von Diphenoxylat oder Loperimid gegen Durchfall	ja=30 Punkte	
Durchschnittliche Bauchschmerzen-Bewertung über sieben Tage	Keine (0 Punkte) Leichte Schmerzen (35 Punkte) Moderate Schmerzen (70 Punkte) Starke Schmerzen (105 Punkte)	
Allgemeines tägliches Wohlbefinden über sieben Tage	Gut (0 Punkte) Etwas unter Durchschnitt (49 Punkte) Schlecht (98 Punkte) Sehr schlecht (147 Punkte) Furchtbar (196 Punkte)	
Komplikationen	Arthritis oder Arthralgie (20 Punkte)	
	Iritis oder Uveitis (20 Punkte)	
	Erythema nodosum, Pyoderma gangrenosum oder Stomatitis aphthosa (20 Punkte)	
	Analfissur, Fistel oder Abszess (20 Punkte)	
	Andere Fistel (20 Punkte)	
	Temperatur über 37,8 °C (über 100 °F) in der letzten Woche (20 Punkte)	
Befund einer abdominalen Raumforderung	Keine Raumforderung (0 Punkte) Mögliche Raumforderung (20 Punkte) Definitive Raumforderung (50 Punkte)	
Anämie und Gewichtsveränderungen **Gewicht:**	Absolute Hämatokritabweichung von 47% in Männern oder 42% in Frauen (6 Punkte pro Prozentpunkt Abweichung)	
	Abweichung (%) vom Standardgewicht (1 Punkt für jedes Prozent Abweichung)	
Standardgewicht = Normales Gewicht Abweichung vom Standardgewicht beträgt (1 - Gewicht/Standardgewicht) x 100	**Summe**	

Table 5. CDAI scoring system. (German version).

2.3. Image acquisition protocol using cardiovascular magnetic resonance

The study participants were scanned using a 1.5 Tesla CMR scanner (AvantoFit®, Siemens, Erlangen, Germany). ECG gating (alternatively, pulse oximetry wave in case of insufficient ECG signal) and a 32-channel surface phased-array coil were used for image acquisition. Localization of slices was planned using a four-chamber view, with the initial slice encompassing the valvular plane. Subsequently, both the left and right ventricles were imaged all the way to the apex. During mapping analysis, slices featuring artifacts, those within the left ventricular outflow tract, or those at the apex with no discernible blood pool and/or thin walls were excluded from consideration. The left ventricular extent was determined by drawing a line connecting the mitral valve to the apex. Slices were then categorized into basal, midventricular, and apical layers based on the American Heart Association model, with the apical gap excluded.

Similarly, in patients exhibiting focal fibrosis on late gadolinium enhancement images, scar tissue was quantified using a 5 standard deviation approach, yielding segmental scar burden measurements in terms of mass and volume.

For depiction of focal fibrosis and scarring, 3D fat/water imaging using inversion recovery prepared spoiled gradient-echo prototype sequence (SIEMENS WIP 1111) was executed. The acquisition was ECG-gated during free breathing and conducted in a transverse orientation with a resolution of 1.3mm x 1.3mm x 1.3mm. The image navigator was manually positioned directly over the left ventricle. The acquisition parameters were set as follows: TE1= 1.31ms; TE2= 2.81ms; with a flip angle of 15° for 3T MRI and 20° for 1.5T MRI. The inversion time (TI) was individually determined using a TI-Scout (SIEMENS WIP 1090). To accommodate the time delay during image acquisition, up to 130 ms was added (with a mean of 21.01 ms). Trigger delay (TD) and acquisition window were chosen based on automatic detection of the resting phase, relying on CINE images acquired in 4CV immediately before the start of 3D data acquisition. The values suggested by the automatic resting phase detection were then manually adjusted. Acquisition was carried out using an undersampled variable-density golden-step Cartesian trajectory with spiral order sampling (VD-CASPR). K-space data were modulated with a linear shift using motion estimates in the left-right and foot-head directions from the image navigator. The acquired data underwent reconstruction using compressed sensing (CS) with orthogonal Haar wavelets. The cost function for CS was solved using a fast iterative shrinkage-thresholding algorithm (FISTA). After reconstruction, fat-water separation was performed, resulting in four 3D datasets: an in-phase image acquired at TE1, an opposite-phase image acquired at TE2, a water-only image, and a fat-only image.

A dose of 0.2mmol/kg of Gadoteridol (Prohance®, Bracco Imaging, Konstanz, Germany) was given and a whole heart sequence protocol was used. [146] Due to reduced image quality in patients with arrhythmias or heart rates higher than 90 bpm, in 9 patients, motion-corrected 2D LGE imaging was used instead of 3D LGE Dixon. [147] The same scan protocol was used for healthy volunteers, with the exclusion of contrast-media-based imaging. Detailed imaging parameters are listed below and are in line with previously published literature of our research group:

"Balanced steady-state free precession cine imaging:

Long axis*: ECG triggered with retrogating, repetition time (TR) 2.78 ms, 30 reconstructed phases, echo time (TE) 1.19ms, field of view (FOV) 340x276mm^2, matrix 192x156, voxel size 1.8x1.8mm^2, slice thickness (ST) 6mm, flip angle (FA) 74°, GRAPPA acceleration factor 2.*

Short axis: *ECG triggered with retrogating, TR 3.31ms, 30 reconstructed phases, TE 1.44ms, FOV 380x308.75mm^2, matrix 192x156, voxel size 2.0x2.0mm^2, ST 7mm, gap between slices: 0mm, FA 80°, GRAPPA acceleration factor 2.*

T2 mapping: *Balanced steady-state free precession sequence, T2 prep times 0, 25 and 55 ms, 3 recovery heartbeats, TR 2.98ms, TE 1.12ms, FA 70°, FOV 380×288mm^2, matrix 224x170, voxel size 1.7x1.7mm^2, ST 8mm, gap between slices 0mm, GRAPPA acceleration factor 2, motion corrected.*

T1 Mapping: *5(3)3 MOLLI acquisition scheme, TR 3.9ms, TE 1.13ms, FA 35°, TI 180ms, FOV 360×270mm^2, matrix 256x144, voxel size 1.4x1.4mm^2, ST 8 mm, gap between slices: 0mm, GRAPPA acceleration factor 2, motion corrected.*

Late gadolinium enhancement: *PSIR reconstruction, gradient echo sequences, TI 240ms, TR 29.76ms, TE 5.17ms, FA 30°, FOV 350x263mm^2, matrix 256x166, voxel size 1.4x1.4mm^2, ST 7mm, gap between slices 0mm.*

Synthetic Extracellular volume: *Pre-contrast: 5(3)3 MOLLI acquisition scheme, TR 3.9ms, TE 1.13ms, FA 35°, TI 180ms, FOV 360×270mm^2, matrix 256x144, voxel size 1.4x1.4mm^2, ST 6 mm, GRAPPA acceleration factor 2, motion corrected.*

Post-contrast: 4(1)3(1)2 MOLLI acquisition scheme, TR 5ms, TE 1.13ms, FA 35°, TI 260ms, FOV 360×270mm^2, matrix 256x144, voxel size 1.4x1.4mm^2, ST 6 mm, GRAPPA acceleration factor 2, motion corrected." [148]

Protocols are represented below for both IBD patients (*Table 6*) and the healthy volunteers (*Table 7*):

1.5 T Scanprotokoll - „Protokoll I“ Durchführung bei der ersten Untersuchung			
Nr	**Sequenz**	**Serie**	**Kommentare (z.B. freigeatmet etc)**
1.	T2-TRUFI		
2.	**CINE 4 CV**		
	CINE 3 CV		
	CINE 2 CV		
	CINE RV		
3.	T2 map 4CV		
	T2 map SAX basal		
	T2 map SAX midv.		
	T2 map SAX apikal		
4.	T_1 map nativ_4CV		
	T_1 map nativ SAX basal		
	T_1 map nativ SAX midv		
	T_1 map nativ SAX apikal		
Kontrastmittelapplikation (ProHance, Dosis 0,02 mmol/kg KG)			
6.	**Overview**		
7.	**CINE SAX Paket**		
8.	**3D GRE Dixon LGE**		
9.	Post T_1 map 4CV		
	Post-T_1 map SAX basal		
	Post T_1 SAX map midv		
	Post-T_1 map apikal		

Table 6. Protocol with GBCA for IBD patients (German version).

1.5 T Scanprotokoll - „Protokoll II“ Durchführung bei der ersten Untersuchung		
Sequenz	**Serie**	**Kommentare (z.B. freigeatmet etc)**
T2-TRUFI		
CINE 4 CV		
CINE 3 CV		
CINE 2 CV		
CINE RV		
T2 map 4CV		
T2 map SAX basal		
T2 map SAX midv.		
T2 map SAX apikal		
T_1 map nativ_4CV		
T_1 map nativ SAX basal		
T_1 map nativ SAX midv		
T_1 map nativ SAX apikal		
CINE SAX CS Paket		

Table 7. Protocol without GBCA for healthy volunteers (German version).

2.4. Image analysis

Two experienced readers independently analyzed all CMR images and maps. The software used was CVI42® (version 5.13.0, Circle Cardiovascular Imaging, Calgary, Canada), and image analysis was based on current recommendations. [94] Cine SAX and LAX images were used for biventricular function and dimension assessment. For left ventricular function assessment, papillary muscles were included in the myocardial mass during diastole and systole in SAX. Using a biplanar approach, the left atrial dimensions were evaluated in cine four- and two-chamber views, whereas the surface of the right atrium was measured in four-chamber view.

By contouring the endocardial and epicardial border of the left ventricular myocardium with an automatic 5% safety contour offset, a 16-segment American Heart Association (AHA) model was produced, with the exclusion of the apical cap. This permits a quantitative appreciation of mapping images. Segments with focal fibrosis, fat or artefacts detected on 3D imaging were excluded from the analysis. Slices that were too thin and did not permit endo- and epicardial contouring were also excluded. The mean value of corresponding AHA segments was calculated for global, basal, midventricular, and apical T1, T2, and ECV values. The assessment of LGE and fat/water image analysis for the presence and location of focal scars and myocardial fat infiltration was done visually. T1 and T2 weighted localizer images and cine images were used to visually detect pleural and pericardial effusion. More than 4 mm of pericardial fluid during end-diastole was considered pathologic. [149]

Strain analysis using feature tracking (FT) was used to assess myocardial deformation and function by analyzing the global longitudinal (GLS), circumferential (GCS), and radial (GRS) strain. Radial and longitudinal strain were measured in three different long-axis views: four-, three-, and two-chamber views. Circumferential strain and radial strain in the short axis were assessed using the full coverage of the short axis. During the end-diastole, the endo- and epicardial contours were manually outlined. The end-diastolic phase was consistent across all short- and long-axis slices for each subject. Contouring did not include trabeculae, papillary muscles, pericardium, or epicardial fat. The left ventricular outflow tract was excluded from all the short-axis slices. The left ventricle segmentation followed the AHA 17-segment model, with the apex excluded from the analysis, adopting the 16-segment model. Bulls-eye plots were generated to visualize segmental strain values. [135, 137]

A third, more experienced reader (JSM, > 25 years of experience) performed a consensus read. An interobserver comparison was done for the first 20 cases, which were analyzed independently by the two readers, and Bland-Altman analysis was used for this purpose.

2.5. Statistical analysis

Patient recruitment numbers were predefined, and the statistical results were verified by certified statisticians of the Charite Medical School. Data collection was made using the Excel program (Version 16.15, 2018 Microsoft) and the statistical analysis (including graphs) was done using Matlab R2021b, Update 3 software (The MathWorks, Inc.).

Continuous variables were given as mean with standard deviation or median and interquartile range according to their distribution. Categorical variables were given as absolute frequencies and percentages. Q-Q plots and the Shapiro–Wilk test were used for the assessment of normal distribution. The Kruskal–Wallis method or one-way ANOVA were used for the comparison of continuous variables. This was followed by Dunn’s or Bonferroni's post hoc testing. In the case of not normal distribution, the correlation analysis was based on Kendall's Tau (τ) coefficient. The Chi-square or Fisher’s exact tests were used for the comparison of categorical variables. A p-value lower than 0.05 was considered statistically significant.

3. RESULTS

3.1. Baseline characteristics

The final analysis included 88 datasets, with 46 scans from IBD patients. Of these, 44 were eligible for final image analysis, since 2 patients were excluded due to low image quality because of arrhythmias. Additionally, one patient refused the administration of contrast agent, so only native imaging was performed. 26 of the patients had active disease and 18 were in remission. Forty-four control healthy volunteers were matched with IBD patients for age, sex, and body mass index (BMI). No significant differences regarding age, sex, BMI, comorbidities, or cardiovascular symptom history were seen between the active and remission group. The IBD patient population consisted of 54.55% females and the average age was 39.5 years. 30 of the patients were diagnosed with CD, 12 of them with CU and 2 patients with IC. Laboratory testing results showed relevant differences, with significantly lower hemoglobin, hematocrit and albumin levels in patients with active disease compared to those in remission. Interestingly, no relevant difference was seen when considering the CRP levels between these two groups.

Baseline characteristics can be found in *Table 8*, and cardiac-related symptom history in *Table 9*.

Compared to patients in remission, those with active disease had significantly higher clinical disease activity scores (CDAI: 343 (217-508) vs. 107 (77-168), $p < 0.001$; SCCAI: 10 (7-12) vs. 2 (1-2), $p < 0.001$), and the disease duration was shorter in this group (587 days (69 - 5237) vs. 2958 (1282-7743), $p = 0.006$). The timing between endoscopy and CMR of the active group was a median of 7 (IQR 1-12) days. Patients with active disease were more often under systemic therapy with steroids (active disease: 20/26 (76.92 %) vs. remission: 2/18 (11.11 %); $p < 0.001$) than those in remission. From the active group, six patients were diagnosed for the first time with IBD. Medical therapy assignments did not differ significantly between the two disease groups, as shown in *Table 10*.

Baseline characteristics of the study population

	All patients (n=44)	Control group (n=44)	Active (n=26)	Remission (n=18)	P
Demographic features and comorbidity					
Male	20 (45.45)	20 (45.45)	10 (38.46)	10 (55.56)	0.262
Age	39.50 (31.50-58.00)	38.50 (30.50-53.50)	38.50 (27.00-56.00	42.00 (35.00-62.00	0.48
BMI, kg/m^2	24.22 (20.45-26.59)	24.05 (21.57-26.22)	23.48 (20.08-26.78	24.87 (20.45-26.37	0.99
Diabetes mellitus	1	--	0	1	--
Arterial hypertension	7	--	3	4	0.419*
Hyperlipidemia	6	--	3	3	0.676*
Smoker	21	--	13	8	0.717*
Disease type and activity					
Crohn's disease	30 (68.18)	--	17 (65.38)	13 (72.22)	0.748*
Ulcerative colitis	12 (27.27)	--	8 (30.77)	4 (22.22)	0.734*
Indeterminate colitis	2 (4.54)	--	1 (3.84)	1 (5.56)	--
CDAI§	195 (117-364)	--	343 (217-508)	107 (77-168)	<0.001*
SCCAI§	7 (2-10)	--	10 (7-12)	2 (1 -2)	<0.001*
Days since initial diagnosis	1436 (151-6542)	--	587 (69 - 5237)	2958 (1282 - 7743)	0.006*
Endoscopy results					
Days between endoscopy and CMR, n			7 (1-12)		
SES-CD			18 (8-24)		
UCEIS			7 (5-8)		

Laboratory results					
CRP, mg/l	2.72 ± 3.44	--	3.23 ± 3.66	1.85 ± 2.91	0.228*
Hemoglobin, g/dl	12.63 ± 2.30	--	11.77 ± 2.30	13.94 ± 1.60	0.002*
Hematocrit, %	37.60 ± 6.35	--	35.27 ± 6.62	41.18 ± 3.86	0.003*
Albumin, g/dl	3.42 ± 0.74	--	3.16 ± 0.71	4.01 ± 0.37	0.002*
Glomerular filtration rate, ml/min	99.23 ± 26.19	--	101.19 ± 26.80	96.24 ± 25.74	0.568*

Table 8. Baseline characteristics of the study population. Values are n (%), mean ± SD, or median (IQR). Comparison was made between control, active and remission using the ANOVA or Kruskal-Wallis test for continuous variables or Chi-square test for categorical variables. * Comparison between active and remission was performed using the Student's t-test or Mann-Whitney U test for continuous variables and Chi-square or Fisher's exact test for categorical variables.

Symptom history

	CED (n=44)	Control group (n=44)	Active (n=26)	Remission (n=18)	P
Fatigue	33 (75)	0	20 (76.92)	13 (72.22)	0.723
NYHA I	28 (63.64)	0 (0)	17 (65.38)	11 (61.11)	0.534
NYHA II	8 (18.18)	0	4 (15.38)	4 (22.22)	0.697
NYHA III	7 (7 (15.91))	0	5 (19.23)	2 (11.11)	0.681
NYHA IV	1 (2.27)	0	0 (0)	1 (5.56)	/
Syncope	11 (25.00)	0	5	6	0.314
Chest pain	10 (22.73)	0	7 (26.92)	3 (16.67)	0.489
Palpitation	18 (40.91)	0	11 (42.31)	7 (38.89)	0.821

Table 9. Symptom history. Values indicate number (percentage), categorial variables compared using Chi-square or Fisher's exact test as appropriate.

Medical therapy

	CED (n=44)	Control group (n=44)	Active (n=26)	Remission (n=18)	P
Topical steroids	3 (6.82)	--	2 (7.69)	1 (5.56)	1
Systemic steroids	22 (50)	--	20 (76.92)	2 (11.11)	< 0.001
Mesalazine	10 (22.72)	--	7 (26.92)	3 (16.67)	0.489
Azathioprin	3 (6.81)	--	2 (7.69)	1 (5.56)	1
Monoclonal antibody	17 (38.64)	--	7 (26.92)	10 (55.56)	0.055

Table 10. Medical therapy. Values indicate the number of patients (percentage), active and remission, compared using Fisher's exact test or Chi-square test as appropriate.

3.2 Left and right ventricular function and dimensions

No significant difference was seen regarding the left and right ventricular dimensions, stroke volumes, or ejection fraction between patients with active disease, remission and the control group (*Table 11*). Patients in remission, however, had significantly higher myocardial mass indices compared to the control group. Such a difference was not evident when the active group was compared with the healthy volunteers (Active: 48.90 ± 8.13, Remission: 56.09 ± 9.86, HV: 47.83 ± 11.32; R vs. HV p = 0.018). *Figure 2* and *Figure 3* demonstrate visually how the contouring and measurements were made.

Ventricular and atrial dimensions and function

	CED (n=44)	Control group (n=44)	Active (n=26)	Remission (n=18)	P
LV-EF, %	61.67 ± 4.58	63.41 ± 4.26	61.98 ± 4.36	61.23 ± 4.96	0.167
LV-EDV indexed to BSA, ml/m^2	79.56 ± 16.43	80.49 ± 18.27	75.73 ±15.88	84.87 ± 16.10	0.226
LV-EDV indexed to height, m	84.88 ± 16.34	85.99 ± 19.62	80.54 ± 14.92	90.90 ± 16.70	0.169

LV-SV indexed to BSA, ml/m^2	48.95 ± 10.07	50.88 ± 11.28	46.92 ± 10.11	51.77 ± 9.56	0.240
LV-Mass indexed to BSA, g/m^2	49.97 (44.09-59.89)	45.73 (40.24-52.66)	45.78 (43.51-54.61)	54.76 (48.43-60.78)	0.006/ < 0.01
LV-Mass indexed to height, m	56.01± 12.44	51.44± 13.64	52.78± 11.23	60.50± 12.94	0.021/ 0.043
LA biplane area, cm^2	19.63 (17.29-22.84)	21.05 (18.72-22.70)	19.40 (17.00-22.03	19.88 (18.15-23.55	0.309
RV-EF	55.17 ± 5.03	54.06 ± 5.28	55.83 ± 5.14	54.21 ± 4.84	0.361
RV-EDV indexed to BSA, ml/m^2	86.37 (74.50-99.58)	87.26 (77.86-101.84	86.37 (75.51-95.63	86.42 (73.50-99.64	0.639
RV-SV indexed to BSA, ml/m^2	47.11 ± 9.63	48.84 ± 10.68	47.53 ± 7.87	46.50 ± 11.95	0.695
RA area, cm^2	20.26 ± 4.16	20.86 ± 3.17	19.78 ± 3.88	20.95 ± 4.56	0.444

Table 11. Ventricular and atrial dimensions and function. The comparison between control, active and remission was made by using ANOVA or Kruskal-Wallis test for continuous variables, or Chi-square test for categorical variables. For $P < 0.05$, a post-hoc testing was performed. All second values indicate active vs. control, other tests were not significant.

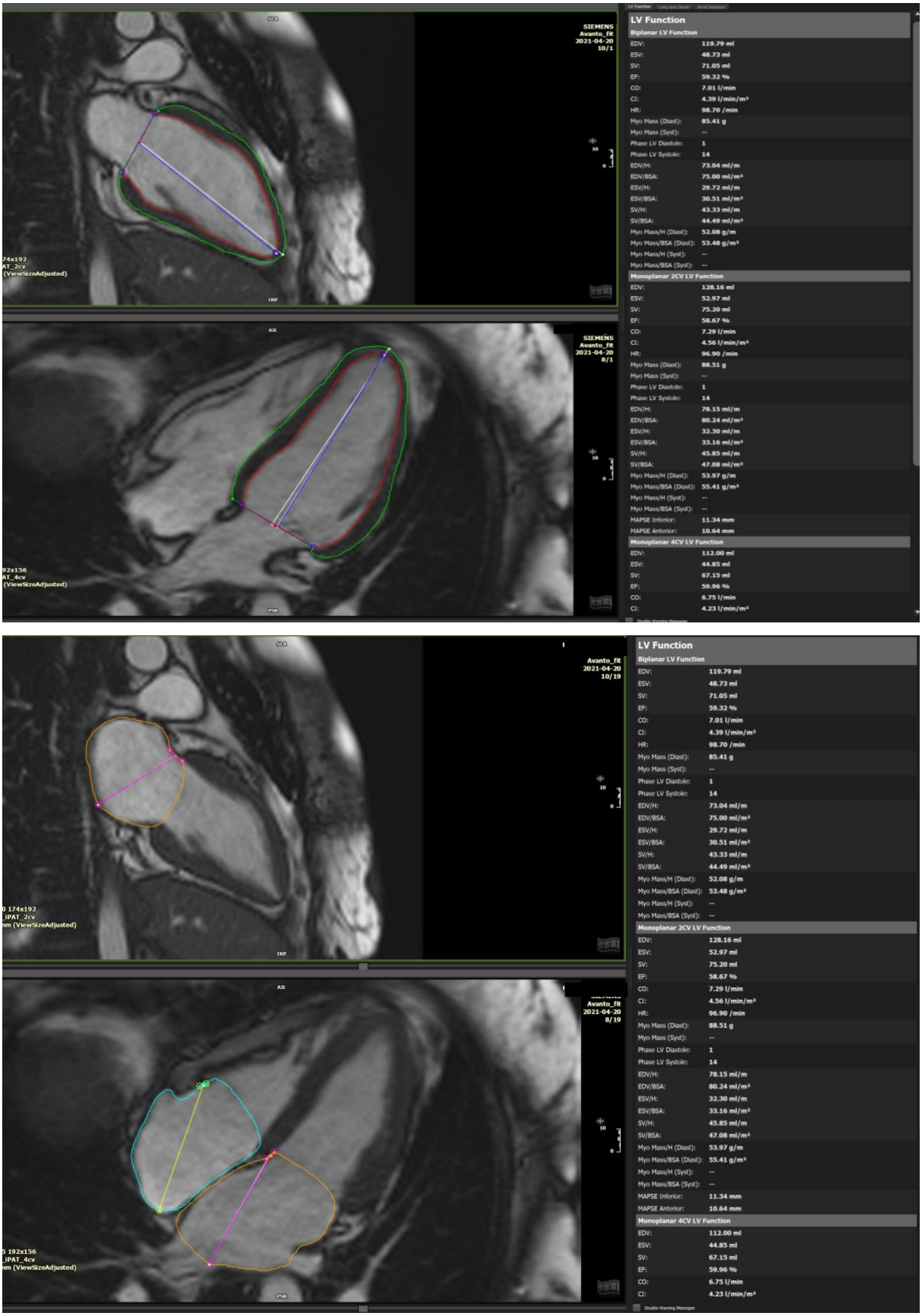

Figure 2. Cine long-axis view (LAX) of two- and four-chamber view a study patient used to calculate atrial and ventricular volumes, surface area, mass and LVEF. The contouring of the atria is done after the maximal filling of the atria with closed mitral valve. The contouring of the left ventricle is done in the end-diastole and end-systole.

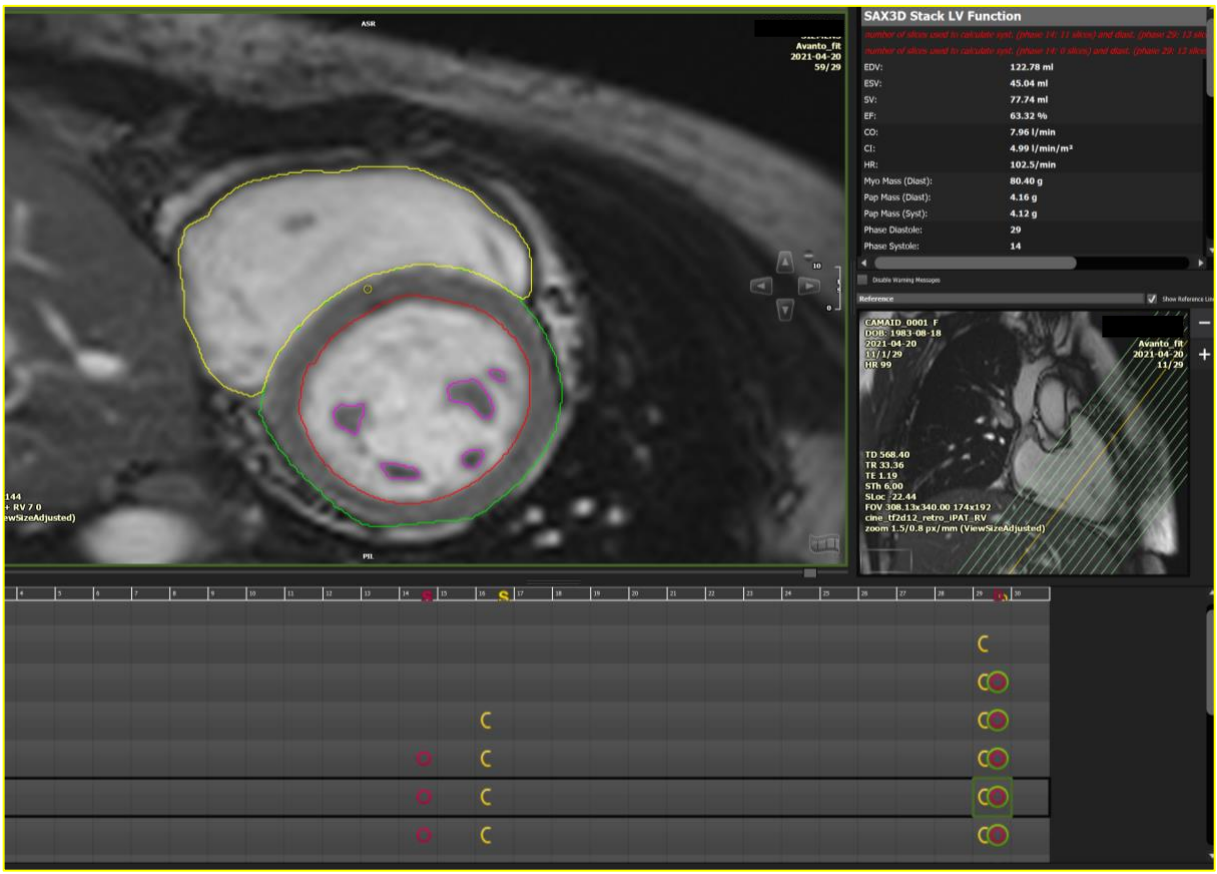

Figure 3. Cine short-axis view (SAX) with contouring of the left and right ventricle in end-diastole and end-systole for the measurement of ventricular volumes, mass, LVEF and RVEF using multiple slices from the base to the ventricular apex in a study patient. Papillary muscles were included in the myocardial mass during diastole and systole.

3.3. T2 mapping

Segments with artefacts, fibrosis, or fat infiltration were excluded from the analysis. As a result, 1397 out of 1408 native T2 segments (99.2%) were analyzed. Patients in active and remission stages showed no significant differences regarding T2 values when compared with each other and healthy volunteers. No difference was seen either globally or at a slice level (Active disease: T2 global 49.33 ± 2.37, Remission: 48.67 ± 1.85, H V: 49.27 ± 2.50; p = 0.605) (*Table 12*). Even after dividing the two IBD groups of patients based on the CDAI- and SCCAI score cut-offs, no relevant differences were seen (T2 global: active disease: 49.33 ± 2.29, remission: 48.33 ± 1.77, HV: 49.27 ± 2.50; p = 0.453). Additionally, we saw no difference in T2 values when patients were compared based on the presence in the therapy of mesalazine (p = 0.389) or monoclonal antibody (p = 0.871) (*Figure 4*).

T2 Mapping

	CED (n=44)	Control group (n=44)	Active (n=26)	Remission (n=18)	P
Average basal T2, ms	48.63 ± 2.31	48.78 ± 2.44	48.75 ± 2.53	48.45 ± 2.01	0.877
Average medial T2, ms	49.03 ± 2.36	49.33 ± 2.58	49.25 ± 2.64	48.70 ± 1.91	0.649
Apical T2, ms	49.81 ± 2.64	49.88 ± 2.86	50.26 ± 2.78	49.12 ± 2.31	0.407

Table 12. T2 Mapping. The comparison between control, active and remission was made by using ANOVA or Kruskal-Wallis tests for continuous variables or the Chi-square test for categorical variables. For P < 0.05, a post-hoc testing was performed

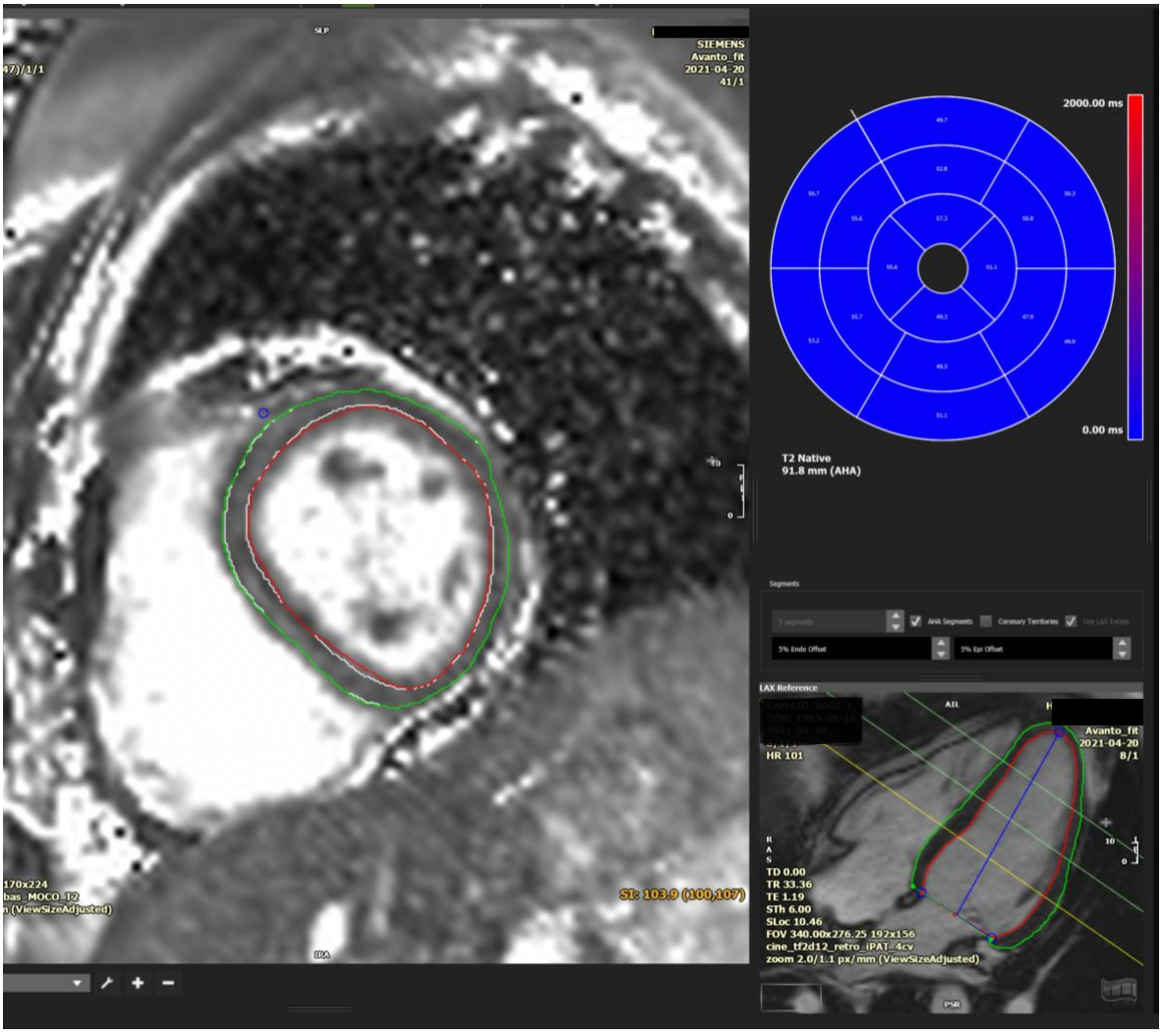

Figure 4. Quantification of T2 mapping in a study patient using endo- and epicardial contouring with 5% offset at three different levels (basal, midventricular and apical) with results shown after segmentation in 16 AHA segments in the bull's eye diagram.

3.4. Native T1 mapping and ECV

A total of 1270 out of 1408 native T1 segments (90.2 %) underwent analysis after exclusion of segments for the presence of artefacts, fibrosis or fat infiltration. Patients with active disease, but not those in remission, had significantly higher global T1 values compared with healthy volunteers (Active 1022.0 ± 34.83 ms, Remission: 1010.10 ± 32.88 ms, HV: 990.61 ± 29.35, $P < 0.001$ between active and HV, other NS). These differences were consistent also when comparing T1 values of each of the three myocardial slices individually: basal ($p= 0.002$), midventricular ($p= 0.002$) and apical ($p = 0.006$). This was reflected in *Table 13*. ECV was performed only on the IBD patients, since the healthy volunteers did not undergo administration of contrast media. ECV values did not differ between patients in active and in remission disease at a global or slice level (global ECV, active: 24.11 ± 2.56, remission: 23.04 ± 3.55, $p = 0.283$). After dividing the IBD patients into active and remission stage by using CDAI- and SCCAI score cut-offs, the analysis of T1 and ECV values was still consistent (active disease: T1 global 1023.8 ± 35.07 ms, remission: T1 global 1001.4 ± 27.08 ms, HV: 990.61 ± 29.35, $P < 0.001$ between active and healthy, other NS; ECV global: Active disease: 24.12 ± 3.28, remission: 22.57 ± 2.16; $p = 0.132$). Global T1 and ECV showed no correlation with the duration of disease (T1: $r\tau = 0.051$, $p = 0.64$; ECV: $r\tau = 0.097$, $p = 0.39$) or with the age of patients (T1: $r\tau = -0.031$, $p = 0.78$; ECV: $r\tau = -0.034$, $p = 0.77$). Five patients, who were considered clinically in remission, had slightly higher scores than the predefined threshold (SCCAI: 3; CDAI: 168, 173, 181, 198). Even after considering these patients in the active group, there was no relevant difference in the results shown above. Additionally, we saw no significant difference between male and female IBD patients when considering global T1 and ECV values (T1: $p = 0.523$; ECV: $p = 0.745$). No difference was seen in global T1 and ECV values when IBD patients were compared based on the presence of mesalazine (T1: $p = 0.265$; ECV: $p = 0.138$) or monoclonal antibody therapies (T1: $p = 0.592$; ECV: $p = 0.639$) in their treatment regimen. *Figure 5* shows the quantification method.

Native T1 Mapping and ECV

	CED (n=44)	Control group (n=44)	Active (n=26)	Remission (n=18)	P
Average basal T1, ms	1019.13 ± 34.24	995.73 ± 26.24	1022.44 ± 33.49	1014.54 ± 35.71	0.002 / 0.002
Average medial T1, ms	1018.26 ± 38.58	992.11 ± 29.18	1022.71 ± 40.64	1011.72 ± 35.50	0.002/ < 0.01
Apical T1, ms	1010.33 ± 52.74	980.23 ± 47.85	1024.53 ± 49.91	987.61 ± 50.60	0.003/ < 0.01
Basal ECV, %	22.87 ± 2.79	--	23.41 ± 2.36	22.07 ± 3.26	0.167
Medial ECV, %	23.40 ± 2.97	--	24.14 ± 2.68	22.20 ± 3.13	0.063
Apical ECV, %	25.46 ± 4.25	--	26.17 ± 4.71	24.42 ± 3.40	0.302

Table 13. Native T1 mapping and ECV. The comparison between control, active and remission was made by using ANOVA or Kruskal-Wallis tests for continuous variables or the Chi-square test for categorical variables. For $P < 0.05$, a post-hoc testing was performed. All second values indicate active vs. control, other tests were not significant. For ECV, only the comparison between active and remission was performed.

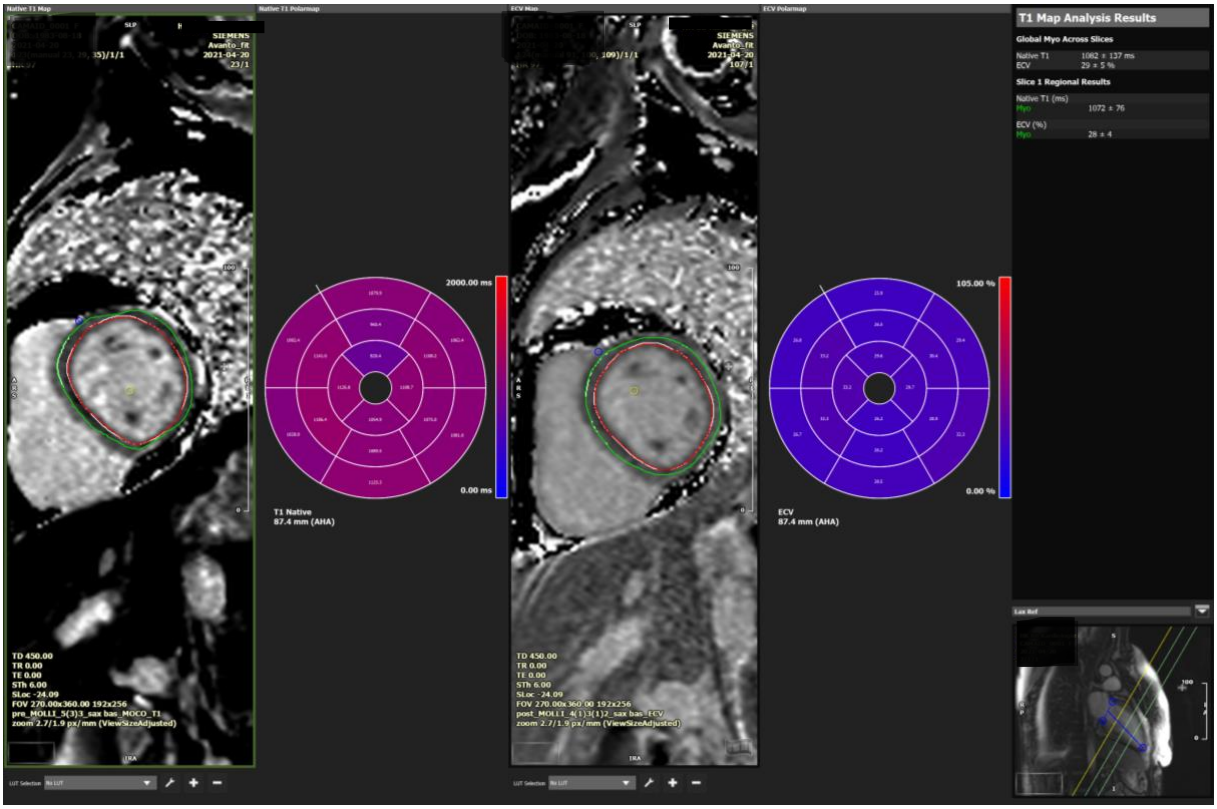

Figure 5. Quantification of parametric T1 mapping (before contrast agent) and synthetic extracellular volume (after contrast agent) in a study patient. The subendocardial and epicardial contouring with 5% offset of the left ventricular myocardium is done in three slices (basal, midventricular and apical) and the results are shown after segmentation in 16 AHA segments in the bull's eye diagram.

3.5. Myocardial segments with concomitant elevation of T1 and T2 values

Our analysis showed high T1 values in 83/351 (23.6%) segments of the patients with active disease, 40/242 (16.5%) segments in those in remission and 31/678 (4.6%) segments in the healthy volunteers group. The number of patients with active disease who had at least one segment with concomitant high T1 and T2 values in the same position was significantly higher (8/26, 30.8%) in comparison to those in remission stage (0/18) and healthy volunteers (1/44, 2.3%, P<0.001). The total number of concomitant high T1 and T2 values in the same AHA segments was the following for the three groups of participants: active IBD 20/350 (5.7%), remission IBD 0/238 (0%) and healthy volunteers 1/678 (0.4%).

3.6. Focal myocardial fibrosis and fat infiltration

LGE imaging was acquired in 43 patients and fat imaging was available in 44 patients. One patient from the active group refused the administration of contrast agent. 3D Dixon LGE imaging was available in 31 patients, while 2D fat (n=13) and 2D LGE (n=12) images were obtained in the remaining patients. 3D imaging was not possible and was substituted from 2D imaging for the following reasons: heart rate > 90 bpm and/or arrhythmia (n= 9) with consequent low image quality, technical problems with the MRI scanner (n=2), patient wish to stop the scanning due to long duration (n=1). We found positive LGE findings in 7/43 patients (16.3%), all of them with a non-ischemic pattern. No significant difference (p = 0.427) was seen when comparing the presence of LGE between patients in active (3/24, 12%) and remission (4/18, 22.2%) stages of the disease. A comparison with healthy volunteers was not possible, since this group did not undergo contrast agent administration. We detected fat infiltration in the myocardium in 5/44 (11.4%) of all patients, with no significant difference (p = 0.634) between patients with active disease and those in remission (*Table 14*).
Figure 6 shows the 3D visualization and localization of LGE using MPR.

LGE and fat infiltration

	CED (n=44)	Control group (n=44)	Active (n=26)	Remission (n=18)	P
LGE presence	7/43*	--	3 (12)	4 (22.22)	0.427
LGE pattern non-ischemic	7/43*	--	3 (12)	4 (22.22)	0.427
Fat presence	5/44		4 (15.38)	1 (5.56)	0.634

Table 14. Focal myocardial fibrosis and fat infiltration. * One patient refused contrast agent administration. For the comparison between active and remission group t-test, Chi-square or Fisher's exact test as appropriate were used.

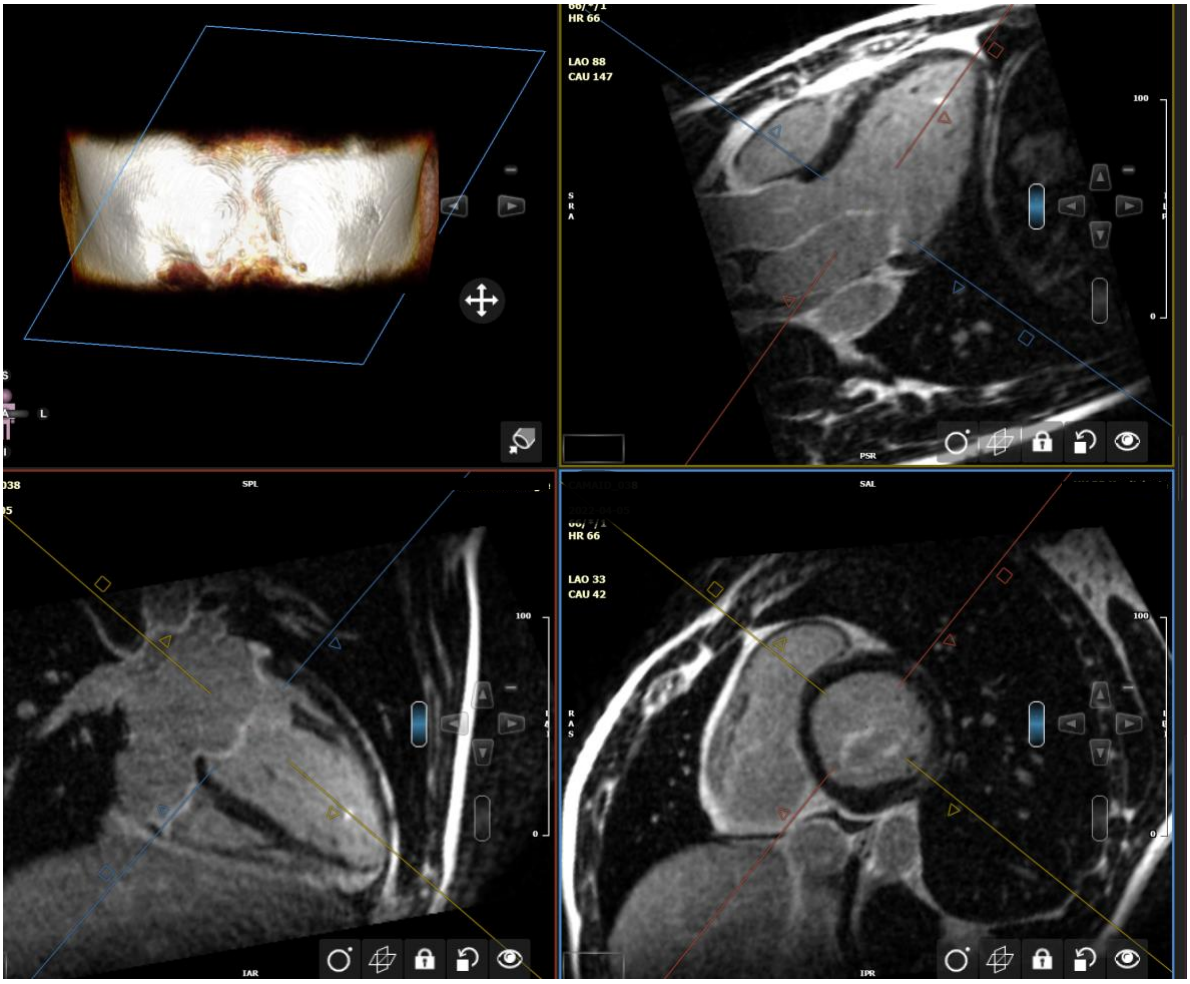

Figure 6. 3D LGE Dixon imaging using MPR to visualize the heart in three two-dimensional slices. Normal myocardium is shown as hypointense, and the presence of localized fibrotic tissue is shown as hyperintensity basal, inferolateral in a study patient (after contrast media injection). This method permits an accurate localization of fibrosis or fat tissue with a high spatial resolution.

3.7. Pericardial and pleural effusions

The presence of pericardial effusion was identified in exactly half of the patients with active disease, whereas in only one-third of patients in remission was the presence of pericardial effusion confirmed. The comparison of these two groups with the control group showed a higher prevalence of pericardial effusion in patients with active disease, but not in those in remission, when compared to the control group. This difference was statistically relevant (p: 0.017).

Although there was a trend toward a higher frequency of pleural effusions in the active group, the difference did not reach statistical significance (p: 0.059) (*Table 15*).
Figure 7 and *Figure 8* show how pericardial and pleural effusions can be identified.

Pericardial and pleural effusions

	CED (n=44)	Control group (n=44)	Active (n=26)	Remission (n=18)	P
Pericardial effusion	19 (43.18)	8 (18.18)	13 (50)	6 (33.33)	0.005/ 0.017
Pleural effusion	10 (22.72)	13 (29.55)	8 (30.77)	2 (11.11)	0.059

Table 15. Pericardial and pleural effusions. The comparison between control, active and remission was made by using ANOVA or Kruskal-Wallis tests for continuous variables or the Chi-square test for categorical variables. For $P < 0.05$, a post-hoc testing was performed. All second values indicate active vs. control, other tests were not significant.

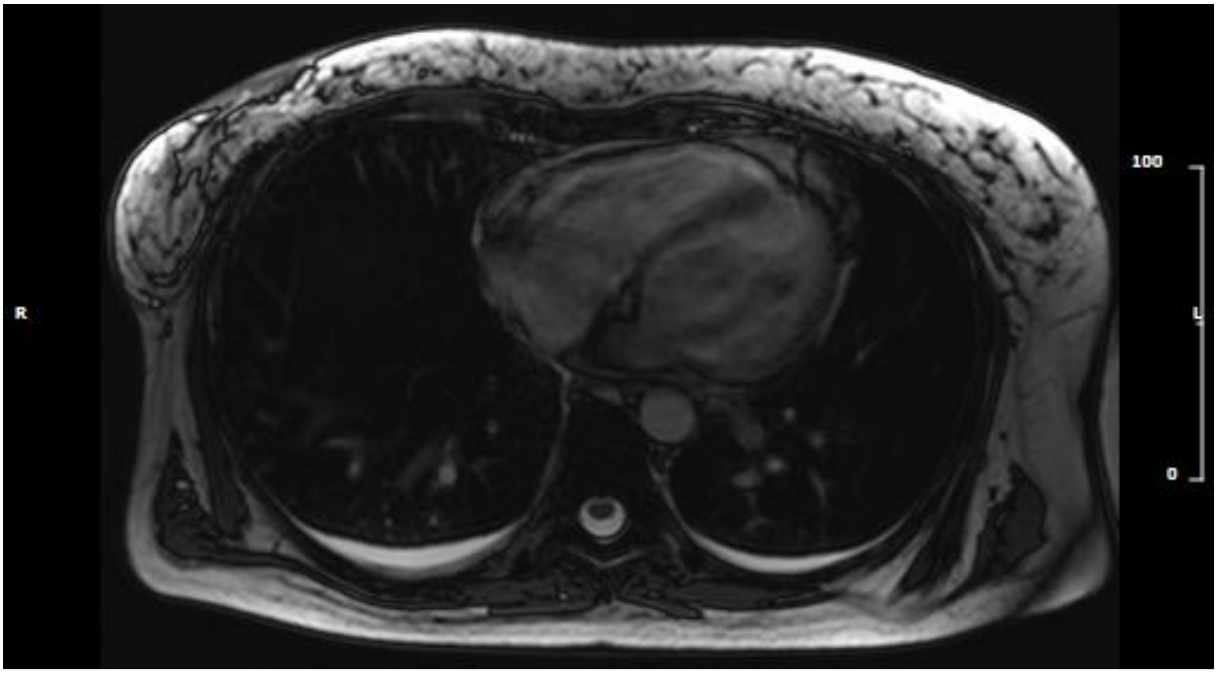

Figure 7. T2-weighted localizer axial image of a study patient showing hyperintense areas located posteriorly and at a basal level of the lungs, representing pleural effusions.

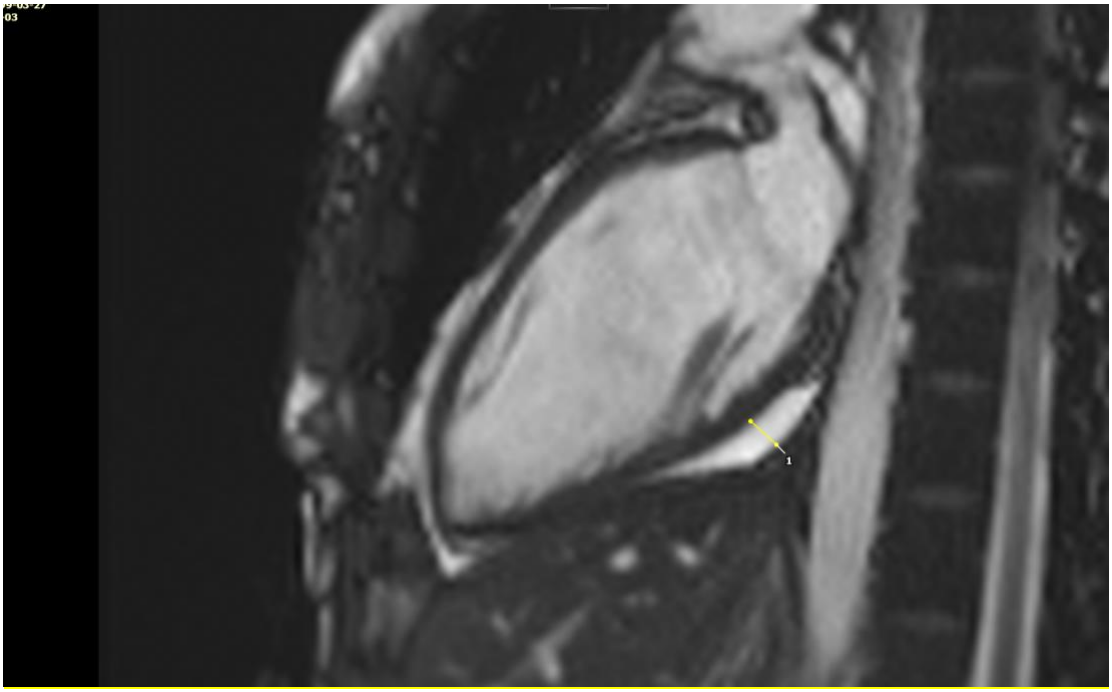

Figure 8. Cine imaging of a two-chamber view showing a hyperintensity inferior and basal, corresponding to pericardial effusion in a study patient.

3.8. Strain analysis

Compared to healthy volunteers, patients with active disease had significantly lower global radial and global circumferential strain values. This difference was not relevant when comparing patients in remission with healthy volunteers (GRS: Active: 23.40 ± 5.34, Remission: 24.64 ± 5.78, HV: 28.06 ± 4.92; active vs. remission P= 0.002; GCS: - 15.31 ± 2.38 vs. - 15.93 ± 2.65 vs. - 17.48 ± 2.02, p < 0.001). Global longitudinal strain analysis showed no relevant differences between all three groups, as shown in *Table 16*.
Figure 9 shows how the contouring and quantification was done.

Strain analysis

	CED (n=44)	Control group (n=44)	Active (n=26)	Remission (n=18)	P
Global longitudinal strain	-17.38 ± 2.83	- 17.79 ± 2.15	- 17.30 ± 3.26	- 17.49 ± 2.16	0.725
Global radial strain	23.87 ± 5.48	28.06 ± 4.92	23.40 ± 5.34	24.64 ± 5.78	0.001 / 0.002
Global circumferential strain	- 15.55 ± 2.48	- 17.48 ± 2.02	- 15.31 ± 2.38	- 15.93 ± 2.65	< 0.001 / < 0.001

Table 16. Strain analysis. The comparison between control, active and remission was made by using ANOVA or Kruskal-Wallis tests for continuous variables or the Chi-square test for categorical variables. For P < 0.05, a post-hoc testing was performed. All second values indicate active vs. control, other tests were not significant.

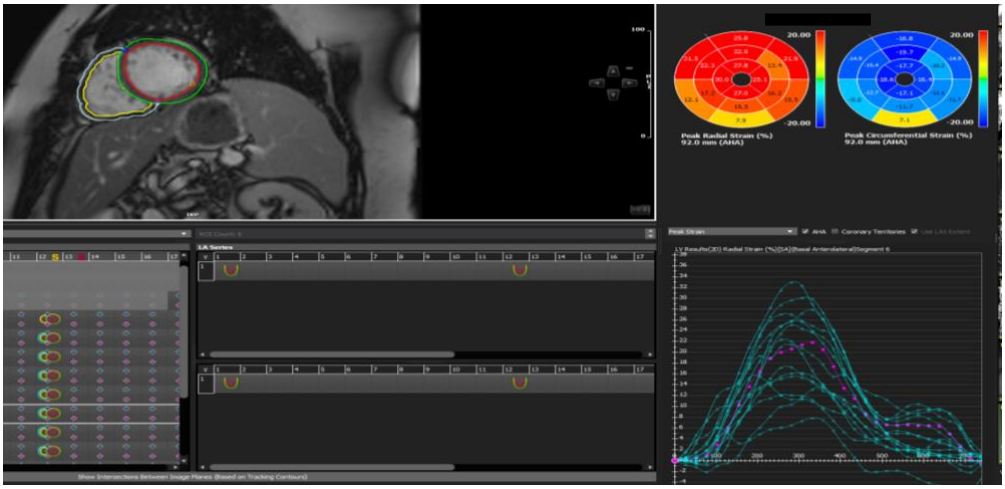

Figure 9. Strain imaging of a study patient obtained by contouring the endocardial and epicardial part of the myocardium in short axis view (SAX), and two- and four chamber view. On the right of the picture is the bull's eye with radial and circumferential strain divided in 16 AHA segments.

3.9. Correlation with disease activity

We used the Z-Score to correlate CMR biomarkers with clinical scores by unifying all IBD patients in one model. The Z-Score of Clinical Disease Activity showed a moderate correlation with global T1 values ($r_\tau = 0.21$, $p = 0.049$) and global ECV ($r_\tau = 0.23$, $p = 0.042$). No correlation was seen between the Z-Score and GRS or GCS (GRS: $r_\tau = -0.08$, $p = 0.49$;

GCS: $r_\tau = 0.08$, $p = 0.49$). Additionally, global T2 values showed no significant correlation with the Z-Score of activity index ($r_\tau = 0.11$, $p = 0.288$).

3.10. Interobserver variability

The image analysis was done by two experienced readers (MF with 5 years of experience and EA with 2 years of experience). For the first 20 patients, an analysis of interobserver variability was done. The compared parameters were the ventricular and atrial dimensions, as well as LVEF and RVEF, followed by the comparison of parametric mapping, such as T1 and T2 mapping. The comparison was made between mean values with standard deviation and Bland-Altman plots were used to show the differences. The T1 and T2 maps were compared not only as a global mean value with standard deviation but also at a segmental level.
The comparison of all the above-mentioned parameters showed that no relevant differences were seen between the two readers and the values measured were inside the tolerance range. The following tables and figures reflect the specific differences between the two readers:

Atrial area differences

Clinical Result (mean±std)	R1	R2	Difference
4CV_RAESAREA [cm^2]	19.3 (4.5)	19.9 (4.7)	-0.6 (0.7)
4CV_RAEDAREA [cm^2]	19.3 (4.5)	19.9 (4.7)	-0.6 (0.7)
4CV_LAESAREA [cm^2]	20.8 (3.6)	21.2 (3.7)	-0.4 (0.9)
4CV_LAEDAREA [cm^2]	20.8 (3.6)	21.2 (3.7)	-0.4 (0.9)
2CV_LAESAREA [cm^2]	18.9 (4.2)	18.8 (4.4)	0.1 (1.4)
2CV_LAEDAREA [cm^2]	18.9 (4.2)	18.8 (4.4)	0.1 (1.4)
LAESP_4CV [#]	14.3 (2.0)	14.1 (2.1)	0.5 (0.8)
LAEDP_4CV [#]	14.3 (2.0)	14.1 (2.1)	0.5 (0.8)
LAESP_2CV [#]	14.3 (2.0)	14.1 (2.1)	0.5 (0.8)
LAEDP_2CV [#]	14.3 (2.0)	14.1 (2.1)	0.5 (0.8)
RAESP_4CV [#]	14.3 (2.0)	14.1 (2.1)	0.5 (0.8)
RAEDP_4CV [#]	14.3 (2.0)	14.1 (2.1)	0.5 (0.8)

Table 17. Atrial area differences. This table shows the clinical parameter names in the first column. The other columns show statistics concerning the parameters. The first and second readers' means (stds) are shown in the second and third column, respectively. The mean and std of the differences between both readers is presented in the fourth column. The mean differences of both readers' ± 95% confidence intervals are shown in parentheses, with ±tolerance ranges thereafter. This provides information on whether the 95% estimate of the mean difference between both readers is within an acceptable limit.

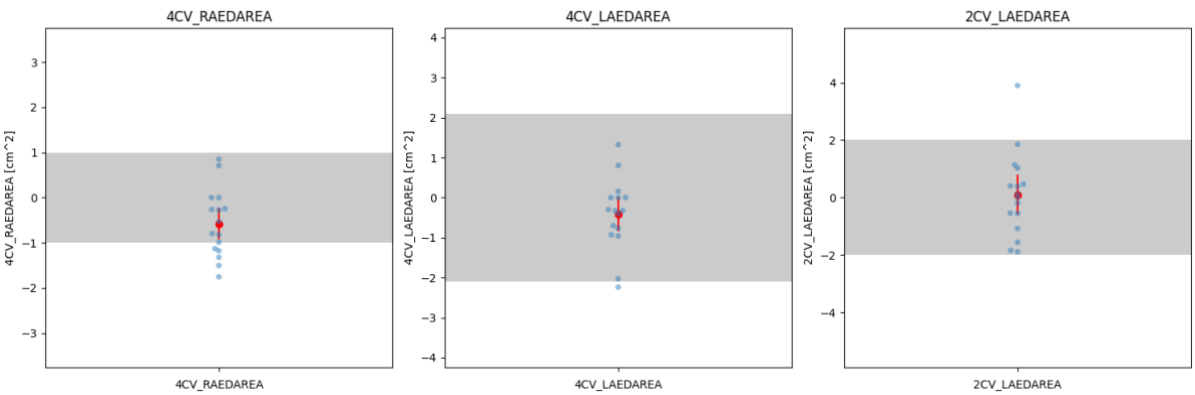

Figure 10. Confidence intervals and tolerance ranges of atria areas: each subfigure references an atrial area, from left to right: 4CV RA, 4CV LA, 2CV LA. Tolerance intervals are shown as gray bars and represent ±1.96 standard deviation of an expert intrareader deviation. The 95% confidence intervals of the mean area difference are represented as an error bar in red. Individual area differences per contour are plotted in blue. Legend: CV: Chamber view, RA: Right Atrium, LA: Left Atrium.

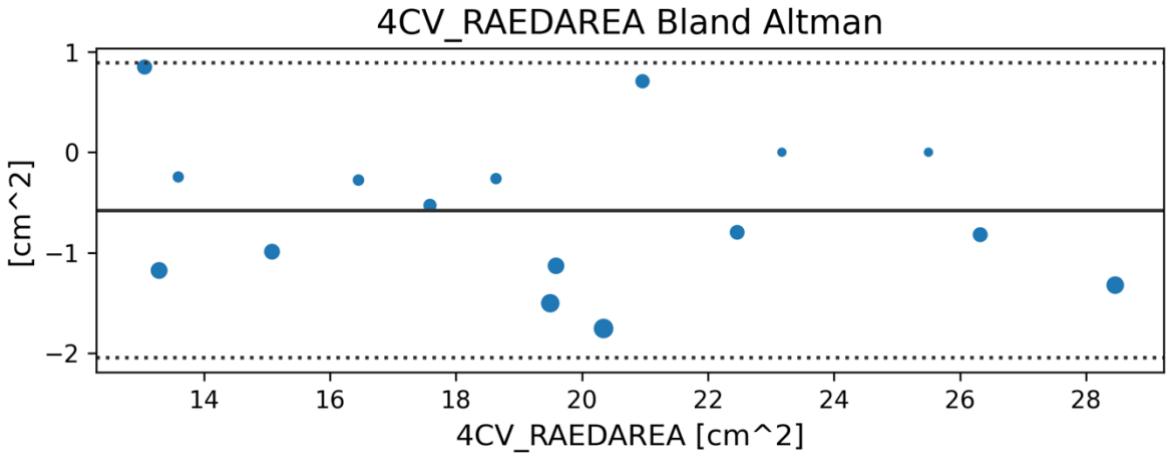

Figure 11. Bland-Altman plot of the atrial surface in four chamber-view showing all parameters inside the tolerance range.

Ventricular dimensions and function

Clinical Result (mean±std)	R1	R2	Difference
LVESV [ml]	59.9 (10.8)	57.0 (12.5)	2.9 (6.1)
LVEDV [ml]	149.6 (21.7)	151.7 (23.0)	-2.1 (6.7)
RVESV [ml]	76.9 (17.3)	73.5 (16.7)	3.4 (7.1)
RVEDV [ml]	165.1 (32.3)	162.2 (29.9)	2.9 (12.2)
LVSV [ml]	88.5 (14.2)	93.8 (14.2)	-5.3 (4.6)
LVEF [%]	58.3 (4.3)	60.6 (4.2)	-2.3 (2.9)
RVSV [ml]	88.2 (16.9)	88.7 (14.6)	-0.5 (7.6)
RVEF [%]	53.5 (3.8)	55.0 (3.3)	-1.4 (2.9)
LVM [g]	85.1 (16.3)	87.7 (18.4)	-2.5 (5.3)
RVM [g]	0.0 (0.0)	0.0 (0.0)	0.0 (0.0)
LVESPAPMUM [g]	3.5 (1.4)	4.3 (1.5)	-0.9 (0.7)
LVEDPAPMUM [g]	2.2 (1.0)	3.4 (1.4)	-1.2 (1.7)
LVESP [#]	11.7 (1.3)	11.4 (1.1)	0.3 (0.6)
RVESP [#]	12.3 (1.6)	11.6 (1.4)	0.7 (1.0)
LVEDP [#]	25.0 (9.8)	26.7 (7.1)	0.3 (0.6)
RVEDP [#]	26.9 (7.2)	26.7 (7.1)	0.3 (0.5)
NrSlices [#]	17.0 (1.0)	17.0 (1.0)	0.0 (0.0)

Table 18. Ventricular dimensions and function. This table shows the clinical parameter names in the first column. The other columns show statistics concerning the parameters. The first and second readers' means (stds) are shown in the second and third column, respectively. The mean and std of the differences between both readers is presented in the fourth column. The mean differences of both readers' ± 95% confidence intervals are shown in parentheses, with ±tolerance ranges thereafter. This provides information on whether the 95% estimate of the mean difference between both readers is within an acceptable limit.

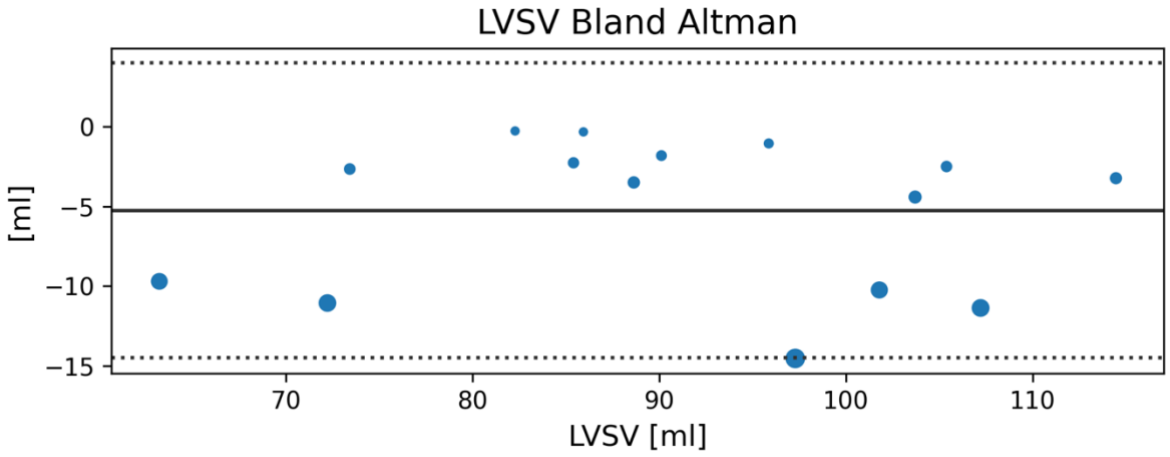

Figure 12. Bland-Altman plot of left ventricular systolic volume with overall parameters in the tolerance range.

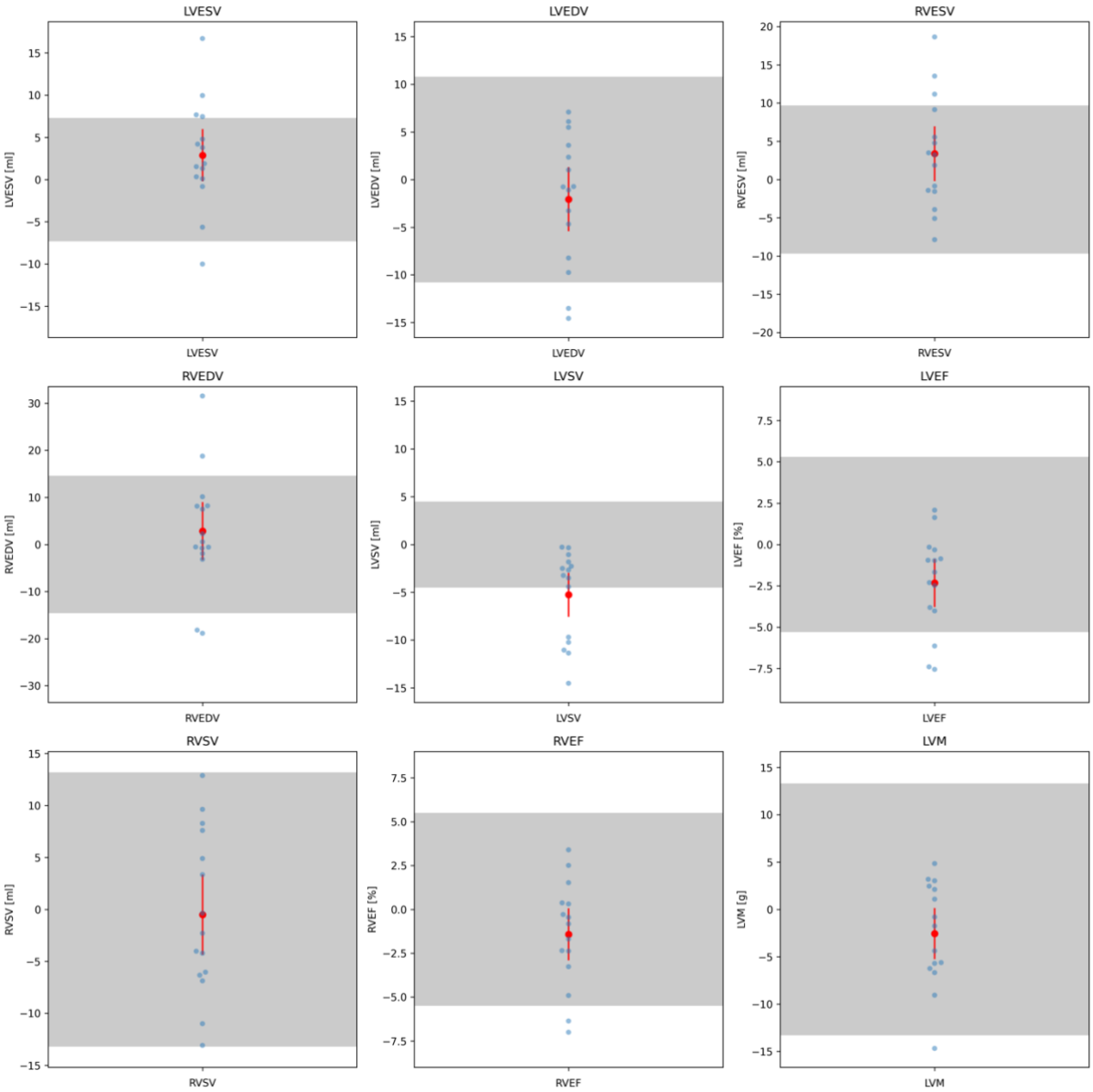

Figure 13. Tolerance ranges and confidence intervals: each subfigure references a clinical parameter. Tolerance intervals are shown as gray bars and represent ±1.96 standard deviation of an expert intrareader deviation as derived in another publication (see below). The 95% confidence intervals of the mean value are represented as an error bar in red. Individual clinical parameter differences per case are plotted in blue. Legend: LV: Left ventricle, RV: Right ventricle, ESV: end-systolic volume, EDV: end-diastolic volume, EF: ejection fraction, LVM: Left ventricular myocardium.

T1 values

Clinical Result (mean±std)	R1	R2	Difference
GLOBAL_T1 [ms]	1008.1 (47.1)	1004.1 (45.5)	-1.1 (11.4)

Table 19. T1 values. This table shows the clinical parameter names in the first column. The other columns show statistics concerning the parameters. The first and second readers' means (stds) are shown in the second and third column, respectively. The mean and std of the differences between both readers is presented in the fourth column. The mean differences of

both readers' ± 95% confidence intervals are shown in parentheses, with ±tolerance ranges thereafter. This provides information on whether the 95% estimate of the mean difference between both readers is within an acceptable limit.

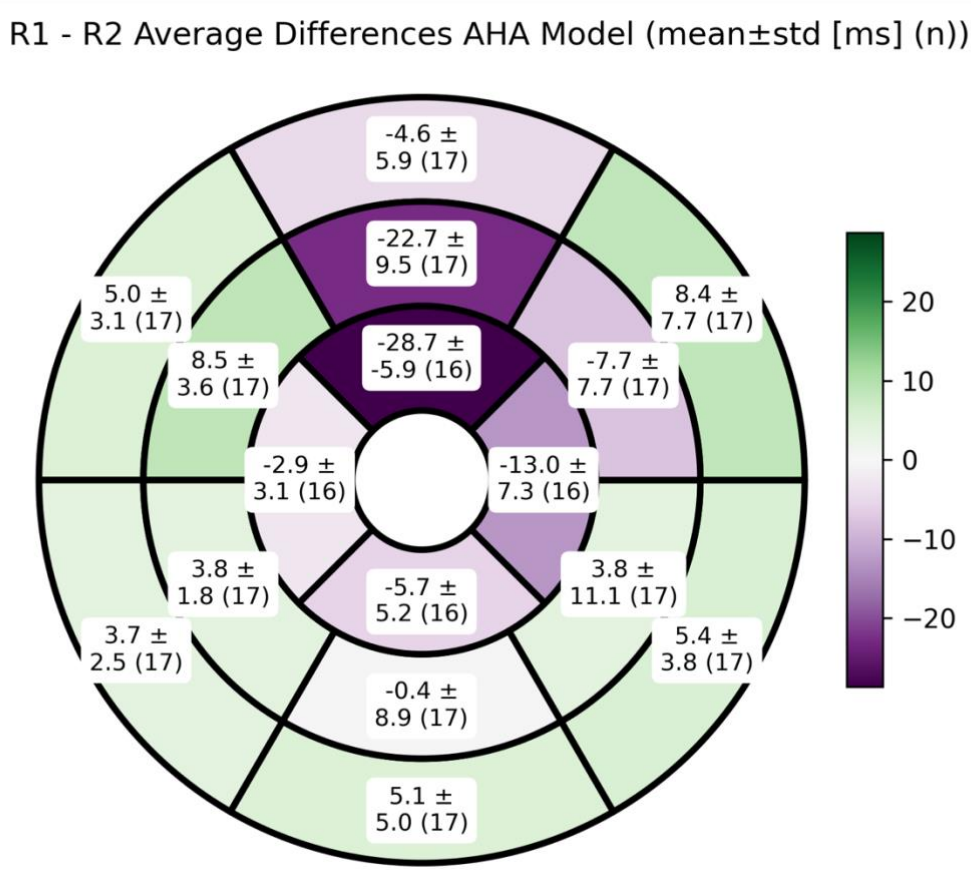

Figure 14. T1 values and average differences in the AHA model: the AHA model is plotted for 16 segments reflecting the basal (6 outer segments), midventricular (6 middle segments) and apical (4 inner segments). Each segment contains a label with the mean±standard deviation (n). The mean and standard deviation pertains to the pixel value differences per segment between the two readers. In parentheses, the number of cases that provided values to the respective segment by both readers is shown. Legend: AHA: American Heart Association.

T2 values

Clinical Result (mean±std)	R1	R2	Difference
GLOBAL_T2 [ms]	48.6 (2.2)	48.6 (2.3)	-0.0 (0.4)

Table 20. T2 values. This table shows the clinical parameter names in the first column. The other columns show statistics concerning the parameters. The first and second readers' means (stds) are shown in the second and third column, respectively. The mean and std of the differences between both readers is presented in the fourth column. The mean differences of both readers' ± 95% confidence intervals are shown in parentheses, with ±tolerance ranges thereafter. This provides information on whether the 95% estimate of the mean difference between both readers is within an acceptable limit.

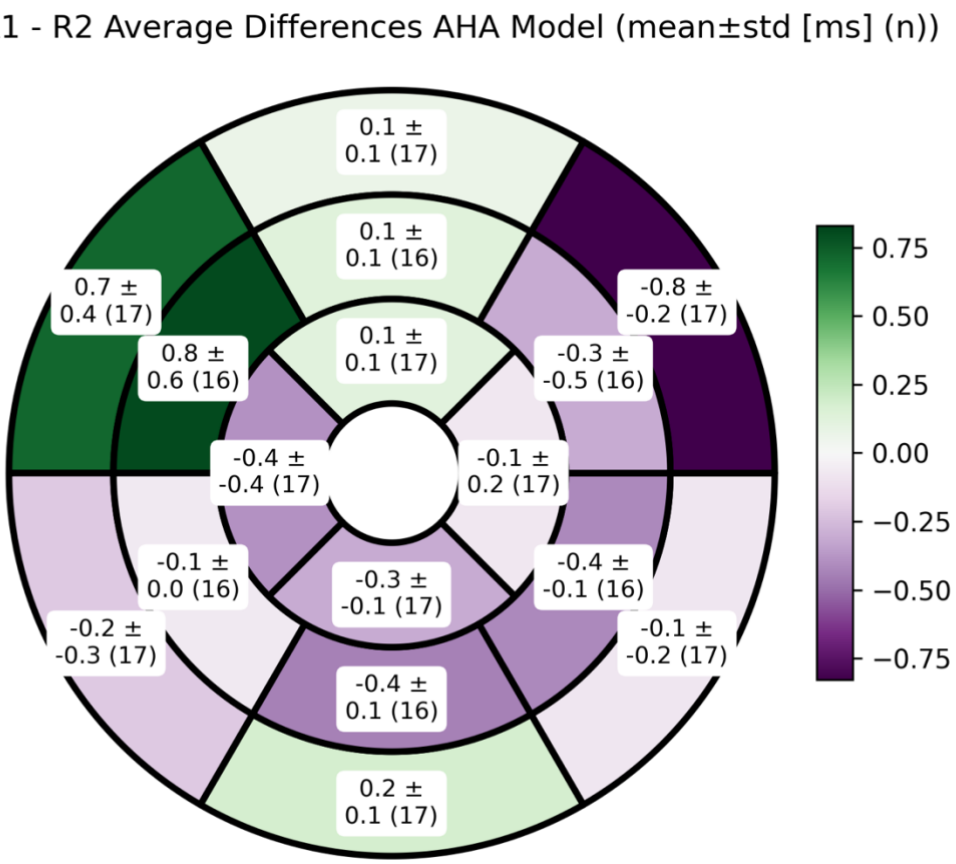

Figure 15. T2 values and average differences in the AHA model: the AHA model is plotted for 16 segments reflecting the basal (6 outer segments), midventricular (6 middle segments) and apical (4 inner segments). Each segment contains a label with the mean±standard deviation (n). The mean and standard deviation pertains to the pixel value differences per segment between the two readers. In parentheses, the number of cases that provided values to the respective segment by both readers is shown. Legend: AHA: American Heart Association.

4. DISCUSSION

Pathophysiological explanation of the main findings

No significant differences regarding age, sex, BMI, comorbidities, or cardiovascular symptom history were seen between the active and remission groups. Regarding the cardiovascular symptoms, the relatively young average age of 39.5 years of the study participants, and the fact that patients with ischemic heart disease were excluded, should be taken into consideration while interpreting these results.

Laboratory testing results showed relevant differences, with significantly lower hemoglobin, hematocrit and albumin levels in patients with active disease compared to those in remission. This is probably explainable considering that during the active phase of the disease, patients may experience gastrointestinal bleeding of various degrees and there is also an activation of acute phase proteins. All this could lead to inflammation-associated anemia and lower albumin levels. [77] Interestingly, no relevant differences were seen when comparing the CRP levels between these two groups. One possible explanation could be the immunosuppressive therapy, which had already been started in patients with active disease before the CMR study was performed and may have lowered CRP levels. Changes in the CRP values under immunosuppressive therapy may happen earlier compared to the other above-mentioned lab values. [48]

The comparison of the left and right ventricular function showed no significant differences between the three analyzed groups. The LVEF and RVEF was preserved in all three groups. Left ventricular dimensions and stroke volumes also showed no differences in all three participant groups.

When considering the myocardial mass indices, these were significantly higher in patients in remission compared to those in the control group. This difference was not relevant when comparing patients with active disease and the control group. Since the left ventricular mass is a known parameter that can predict the risk for cardiovascular events, higher mass indices could reflect a higher risk of developing these events in this group of patients. [150]

Although the reason for this difference in LV mass indices is unclear, one hypothesis may be related to the use of corticosteroids. The effect of this therapy on inducing left ventricular hypertrophy has been previously studied. [151, 152] In our study, patients in remission had significantly longer disease duration than those with active disease, therefore they might have been subjected to higher accumulative steroid doses through the course of the disease, causing an increase in left ventricular mass indices.

The strain analysis showed lower values of global circumferential and radial strain in patients with active disease, but not in those in remission. Whereas global longitudinal strain analysis showed no relevant differences between all three groups, circumferential strain has better reproducibility and has been established in many CMR research centers. [153] These differences were evident, although the LVEF was preserved. The subclinical effect of reduced strain with still preserved ejection fraction may represent an early stage of ventricular dysfunction in patients with active (systemic) inflammation involving the heart. [154]
The analysis of the study data showed significantly higher native T1 values in the group of patients with active disease, but not those in remission, when compared to the control group. This was consistent not only when considering the global average value, but also when different myocardial slices (basal, midventricular and apical) were analyzed separately. Increased native T1 values are seen in the setting of edema (myocarditis, myocardial infarction), focal or diffuse fibrosis, or amyloidosis. The increase of native T1 did not reflect the values seen in patients with amyloidosis (>1100ms). [155] Furthermore, segments of focal fibrosis and fat accumulation areas were excluded from the mapping analysis. The T2 values were not significantly elevated in the active group compared with the other two groups. Since the latter are more specific for edema, a combination of higher T1- and normal T2 values might correlate in this case with diffuse fibrosis. [12]
When considering a concomitant increase of native T1 and T2 in the same segments, the number of patients with active disease (30.8%) presenting this pattern was significantly higher in comparison to those in remission stage and control group. This shows a certain degree of active inflammation in this group of patients.
An elevation of T1 values was seen also in other CMR studies of patients with known systemic inflammatory diseases, such as rheumatoid arthritis or systemic sclerosis with heart involvement. [16, 156] Furthermore, it is unclear if an isolated elevation of T1 values reflects an active inflammation. We could hypothesize that after an acute myocardial injury, there is a slight reduction of T1 values in time, though these continue to be higher than normal. Chronically higher T1 values were also observed in other studies with follow-up of patients with myocarditis. [106]
Different studies observed higher levels of proinflammatory cytokines like TNF-α, IFN-γ and IL-12 in patients with IBD and active stage of disease. [31] This correlates with higher levels of inflammation in the gut and on a systemic level. It is reasonable to assume that such a systemic inflammation can affect also the myocardial tissue. It was hypothesized that these

subclinical changes might be a precursor of cardiac remodeling and diastolic dysfunction. [157, 158]

ECV was obtained only in IBD patients, since the healthy volunteers did not undergo GBCA administration. ECV values did not differ between patients in active and in remission disease at a global or slice level. After dividing the IBD patients into active and remission stage by using CDAI- and SCCAI–score cut-offs, the analysis of T1 and ECV values was still consistent. The small sample size may be one explanation for the lack of statistical significance. Furthermore, average ECV values of the entire myocardium may not reflect segmental changes, hence they can be underrepresented when undergoing statistical analysis. Finally, a significant difference between patients with active disease and healthy volunteers was the presence of pericardial effusions. As much as 50% of the patients with active disease developed a pericardial effusion, whereas pericardial effusions were detected in only 33% of patients in remission. The comparison of these two groups with the control group showed a higher prevalence of pericardial effusion in patients with active disease but not in those in remission, when compared to the control group. This difference was statistically significant. In none of these patients was a hemodynamically relevant pericardial effusion observed. Regarding pleural effusions, although there was a trend toward a higher prevalence of pleural effusions in the active group, the difference did not reach statistical significance (p: 0.059). Pericardial effusions are a known sign of cardiac involvement in systemic disease, and their association has also been described in patients with inflammatory bowel disease. The presence of pericardial effusion further strengthens the suspicion of cardiac involvement, particularly during the active phase of IBD. [159-162]

Focal myocardial fibrosis and fat infiltration

Our study participants had a mean age of 39.5 years and had no known ischemic heart disease. A comparison between IBD patients with healthy volunteers was not possible, since this group did not undergo GBCA administration. We found positive LGE findings in 16.3% of IBD patients, all of them with a non-ischemic pattern. No significant difference was seen when comparing the presence of LGE between patients in active and remission stages of the disease. There is evidence of a correlation between ischemic heart disease and inflammatory bowel disease. [5] In our study, however, we did not see any ischemic LGE pattern. This might be related to the relatively young age of our study participants, with few risk factors for coronary artery disease. Other factors such as chronic inflammation and prolonged use of

corticosteroids may play a role in the long term in developing coronary artery disease in patients with IBD. [38]

The detected LGE was of an intramyocardial or subepicardial pattern. This kind of distribution is usually seen in patients with inflammatory myocardial changes such as in the setting of myocarditis. Focal fibrosis represented by the detected LGE is mostly a sign of irreversible myocardial damage, and it usually persists indefinitely after the acute inflammation and myocardial injury has occurred. [106] The small sample size should be an aspect to take into consideration when interpreting the results of the statistical analysis.

We detected fat infiltration in the myocardium in 11.4% of all IBD patients, with no significant difference between patients with active disease and those in remission. The presence of intramyocardial fat tissue was associated with ischemic and non-ischemic cardiomyopathies. Fat infiltration can also be of prognostic value by increasing the risk for potential arrhythmias and SCD. [131, 132] If we interpret the distribution of fat infiltration by also taking into consideration the LGE pattern, we did not see an ischemic type of distribution, but rather a non-ischemic one. The impact of this finding is currently unclear and was not addressed in our study design, but as is the case for focal fibrosis, it could represent chronic tissue injury.

Relation with disease activity

The clinical assessment and differentiation between an acute flare of IBD and remission were made by board-certified gastroenterologists. For our study, the Crohn's Disease Activity Index (CDAI) was used for CD patients, and the Simple Clinical Colitis Activity Index (SCCAI) for UC patients. An active flare was assigned for scores of CDAI> 150 and SCCAI>2.5, based on other clinical trials on IBD therapies. [163]

Patients with clinical scores surpassing these thresholds, considered as having active disease, exhibited significantly higher native T1 and ECV values compared to the remission group. However, no such correlation was observed when considering T2 mapping and strain imaging. Furthermore, the increased ECV values reinforce the suspicion of diffuse myocardial fibrosis. [16, 164] Finally, global T1 and ECV showed no correlation with the duration of the disease.

These results reflect a correlation between subclinical myocardial changes and disease activity.

IBD therapies and possible effects on subclinical myocardial changes

There is evidence of a higher incidence of myocarditis in patients undergoing treatment with mesalazine. [165, 166] In our study, however, we did not find any significant differences in T1, T2 and ECV values when comparing patients with and without long-term mesalazine treatment.

The effects on the heart of immunosuppressive and immunomodulating therapies, including modern monoclonal treatments, have been considered and studied. Some data supports a higher incidence of myocardial and pericardial inflammation in patients undergoing therapy with infliximab, methotrexate, azathioprine, etanercept, and adalimumab. [23-25, 82-84]

In our study, we did not see a higher incidence of myocardial inflammation, in correlation with the use of these drug regimens. However, it is important to mention that the sample size was small and led to insufficient power to detect possible differences.

Patients in the active stage of the disease had a higher frequency of systemic steroid use compared to those in remission, and this difference was statistically significant. At the time of the CMR study, these patients were already receiving immunosuppressive therapy with corticosteroids. The potential subclinical effects of this treatment on T1 mapping, T2 mapping, and ECV are not yet fully understood. What is already known, however, is that long-term therapies with corticosteroids can increase the LV mass. [151, 152] As mentioned above, this was also observed in our study, with an increased LV mass index in patients in remission. These patients, having a longer disease duration than those with active flares, may have been treated more often with corticosteroids to induce remission, hence an accumulated dose effect of steroids could have increased the LV mass indices.

5. LIMITATIONS

One limitation of this study was the impossibility of performing endoscopy on patients in remission or healthy volunteers for obvious ethical reasons. This would have given us further insights into the staging of the disease and correlations with disease activity. Clinically, however, there was no indication to perform such an invasive test on these patients.
Another limitation was the lack of ECV and LGE imaging in healthy volunteers. Due to ethical reasons, no GBCA was given to this group of participants.
Since all the patients in remission were seen only in a gastroenterologist ambulatory setting, no routine cardiac markers (troponin, CK-MB, NT-proBNP) were obtained, which made them unavailable for our study. These lab tests could have given us more information about possible cardiac involvement.
Finally, it was not possible to recruit a large enough number of patients with different IBD therapies and who were therapy-naive, in order to statistically appreciate possible effects of these therapies on the heart. This was mainly due to the large heterogenicity of therapies for IBD and the limited number of patients who could be included in our study from one tertiary center.

6. CONCLUSIONS

This study showed subclinical myocardial changes with preserved ejection fraction in patients with active IBD compared to healthy volunteers. These alterations were not only of a structural nature, reflected by the diffuse myocardial fibrosis, but also functional, with reduced ventricular circumferential and radial strain.
The detected myocardial changes suggest a certain degree of myocardial involvement in the setting of systemic inflammation in IBD patients. Even though the prevalence of cardiovascular complications in patients with IBD is not high, CMR could help select patients at a higher risk of developing such complications and follow them up more closely. In order to address this matter, further research in this area is needed.
More investigation is also warranted to determine the impact on myocardial injury of different therapy regimens, including mesalazine, immunosuppressive agents, and immunomodulating therapies.

7. BIBLIOGRAPHY

[1] A. Garber, and M. Regueiro, “Extraintestinal Manifestations of Inflammatory Bowel Disease: Epidemiology, Etiopathogenesis, and Management,” *Curr Gastroenterol Rep,* vol. 21, no. 7, pp. 31, May 16, 2019.

[2] S. R. Vavricka, L. Brun, P. Ballabeni, V. Pittet, B. M. Prinz Vavricka, J. Zeitz, G. Rogler, and A. M. Schoepfer, “Frequency and risk factors for extraintestinal manifestations in the Swiss inflammatory bowel disease cohort,” *Am J Gastroenterol,* vol. 106, no. 1, pp. 110-9, Jan, 2011.

[3] R. J. Belin, A. Ghasemiesfe, J. Carr, F. H. Miller, C. Parada, and N. Akhter, “Crohn's colitis-induced myocarditis,” *J Cardiol Cases,* vol. 14, no. 1, pp. 4-7, Jul, 2016.

[4] S. Aniwan, D. S. Pardi, W. J. Tremaine, and E. V. Loftus, Jr., “Increased Risk of Acute Myocardial Infarction and Heart Failure in Patients With Inflammatory Bowel Diseases,” *Clin Gastroenterol Hepatol,* vol. 16, no. 10, pp. 1607-1615 e1, Oct, 2018.

[5] W. Feng, G. Chen, D. Cai, S. Zhao, J. Cheng, and H. Shen, “Inflammatory Bowel Disease and Risk of Ischemic Heart Disease: An Updated Meta-Analysis of Cohort Studies,” *J Am Heart Assoc,* vol. 6, no. 8, Aug 2, 2017.

[6] S. L. Kristensen, O. Ahlehoff, J. Lindhardsen, R. Erichsen, G. V. Jensen, C. Torp-Pedersen, O. H. Nielsen, G. H. Gislason, and P. R. Hansen, “Disease activity in inflammatory bowel disease is associated with increased risk of myocardial infarction, stroke and cardiovascular death--a Danish nationwide cohort study,” *PLoS One,* vol. 8, no. 2, pp. e56944, 2013.

[7] G. Caio, L. Lungaro, F. Caputo, M. Muccinelli, M. C. Marcello, E. Zoli, U. Volta, R. De Giorgio, and G. Zoli, “Recurrent myocarditis in a patient with active ulcerative colitis: a case report and review of the literature,” *BMJ Open Gastroenterol,* vol. 8, no. 1, Mar, 2021.

[8] B. Berlot, I. Harries, and C. Bucciarelli-Ducci, “Connection between the heart and the gut,” *Heart,* vol. 105, no. 15, pp. 1148-1196, Aug, 2019.

[9] F. von Knobelsdorff-Brenkenhoff, and J. Schulz-Menger, “Cardiovascular magnetic resonance in the guidelines of the European Society of Cardiology: a comprehensive summary and update,” *Journal of Cardiovascular Magnetic Resonance,* vol. 25, no. 1, pp. 42, 2023/07/24, 2023.

[10] T. Leiner, J. Bogaert, M. G. Friedrich, R. Mohiaddin, V. Muthurangu, S. Myerson, A. J. Powell, S. V. Raman, and D. J. Pennell, “SCMR Position Paper (2020) on clinical indications for cardiovascular magnetic resonance,” *J Cardiovasc Magn Reson,* vol. 22, no. 1, pp. 76, Nov 9, 2020.

[11] F. von Knobelsdorff-Brenkenhoff, and J. Schulz-Menger, “Role of cardiovascular magnetic resonance in the guidelines of the European Society of Cardiology,” *J Cardiovasc Magn Reson,* vol. 18, pp. 6, Jan 22, 2016.

[12] D. R. Messroghli, J. C. Moon, V. M. Ferreira, L. Grosse-Wortmann, T. He, P. Kellman, J. Mascherbauer, R. Nezafat, M. Salerno, E. B. Schelbert, A. J. Taylor, R. Thompson, M. Ugander, R. B. van Heeswijk, and M. G. Friedrich, “Clinical recommendations for cardiovascular magnetic resonance mapping of T1, T2, T2* and extracellular volume: A consensus statement by the Society for Cardiovascular Magnetic Resonance (SCMR) endorsed by the European Association for Cardiovascular Imaging (EACVI),” *J Cardiovasc Magn Reson,* vol. 19, no. 1, pp. 75, Oct 9, 2017.

[13] M. Saeed, O. Weber, R. Lee, L. Do, A. Martin, D. Saloner, P. Ursell, P. Robert, C. Corot, and C. B. Higgins, “Discrimination of myocardial acute and

chronic (scar) infarctions on delayed contrast enhanced magnetic resonance imaging with intravascular magnetic resonance contrast media," *J Am Coll Cardiol,* vol. 48, no. 10, pp. 1961-8, Nov 21, 2006.
[14] J. Schulz-Menger, "Diagnostic Accuracy of CMR in Biopsy-Proven Acute Myocarditis∗," *JACC: Cardiovascular Imaging,* vol. 7, no. 3, pp. 264-266, 2014/03/01/, 2014.
[15] R. J. Kim, E. Wu, A. Rafael, E. L. Chen, M. A. Parker, O. Simonetti, F. J. Klocke, R. O. Bonow, and R. M. Judd, "The use of contrast-enhanced magnetic resonance imaging to identify reversible myocardial dysfunction," *N Engl J Med,* vol. 343, no. 20, pp. 1445-53, Nov 16, 2000.
[16] N. A. B. Ntusi, S. K. Piechnik, J. M. Francis, V. M. Ferreira, P. M. Matthews, M. D. Robson, P. B. Wordsworth, S. Neubauer, and T. D. Karamitsos, "Diffuse Myocardial Fibrosis and Inflammation in Rheumatoid Arthritis: Insights From CMR T1 Mapping," *JACC Cardiovasc Imaging,* vol. 8, no. 5, pp. 526-536, May, 2015.
[17] A. Barison, L. Gargani, D. De Marchi, G. D. Aquaro, S. Guiducci, E. Picano, M. M. Cerinic, and A. Pingitore, "Early myocardial and skeletal muscle interstitial remodelling in systemic sclerosis: insights from extracellular volume quantification using cardiovascular magnetic resonance," *Eur Heart J Cardiovasc Imaging,* vol. 16, no. 1, pp. 74-80, Jan, 2015.
[18] A. L. P. Caforio, Y. Adler, C. Agostini, Y. Allanore, A. Anastasakis, M. Arad, M. Bohm, P. Charron, P. M. Elliott, U. Eriksson, S. B. Felix, P. Garcia-Pavia, E. Hachulla, S. Heymans, M. Imazio, K. Klingel, R. Marcolongo, M. Matucci Cerinic, A. Pantazis, S. Plein, V. Poli, A. Rigopoulos, P. Seferovic, Y. Shoenfeld, J. L. Zamorano, and A. Linhart, "Diagnosis and management of myocardial involvement in systemic immune-mediated diseases: a position statement of the European Society of Cardiology Working Group on Myocardial and Pericardial Disease," *Eur Heart J,* vol. 38, no. 35, pp. 2649-2662, Sep 14, 2017.
[19] H. Abdel-Aty, N. Siegle, A. Natusch, E. Gromnica-Ihle, R. Wassmuth, R. Dietz, and J. Schulz-Menger, "Myocardial tissue characterization in systemic lupus erythematosus: value of a comprehensive cardiovascular magnetic resonance approach," *Lupus,* vol. 17, no. 6, pp. 561-7, Jun, 2008.
[20] C. A. Lamb, N. A. Kennedy, T. Raine, P. A. Hendy, P. J. Smith, J. K. Limdi, B. Hayee, M. C. E. Lomer, G. C. Parkes, C. Selinger, K. J. Barrett, R. J. Davies, C. Bennett, S. Gittens, M. G. Dunlop, O. Faiz, A. Fraser, V. Garrick, P. D. Johnston, M. Parkes, J. Sanderson, H. Terry, D. R. Gaya, T. H. Iqbal, S. A. Taylor, M. Smith, M. Brookes, R. Hansen, and A. B. Hawthorne, "British Society of Gastroenterology consensus guidelines on the management of inflammatory bowel disease in adults," *Gut,* vol. 68, no. Suppl 3, pp. s1-s106, Dec, 2019.
[21] K. Cesa, C. Cunningham, T. Harris, and W. Sunseri, "A Review of Extraintestinal Manifestations & Medication-Induced Myocarditis and Pericarditis in Pediatric Inflammatory Bowel Disease," *Cureus,* vol. 14, no. 6, pp. e26366, Jun, 2022.
[22] G. C. Kaiser, D. E. Milov, N. A. Erhart, and D. J. Bailey, "Massive pericardial effusion in a child following the administration of mesalamine," *J Pediatr Gastroenterol Nutr,* vol. 25, no. 4, pp. 435-8, Oct, 1997.
[23] J. Devasahayam, U. Pillai, and A. Lacasse, "A rare case of pericarditis, complication of infliximab treatment for Crohn's disease," *J Crohns Colitis,* vol. 6, no. 6, pp. 730-1, Jul, 2012.

[24] C. Cudzilo, A. Aragaki, J. Guitron, and S. Benzaquen, “Methotrexate-induced pleuropericarditis and eosinophilic pleural effusion,” *J Bronchology Interv Pulmonol,* vol. 21, no. 1, pp. 90-2, Jan, 2014.
[25] C. D. Simpson, “Azathioprine-induced pericarditis in a patient with ulcerative colitis,” *Can J Gastroenterol,* vol. 11, no. 3, pp. 217-9, Apr, 1997.
[26] M. Guindi, and R. H. Riddell, “Indeterminate colitis,” *J Clin Pathol,* vol. 57, no. 12, pp. 1233-44, Dec, 2004.
[27] W. J. Tremaine, “Review article: Indeterminate colitis--definition, diagnosis and management,” *Aliment Pharmacol Ther,* vol. 25, no. 1, pp. 13-7, Jan 1, 2007.
[28] T. Hammer, and E. Langholz, “The epidemiology of inflammatory bowel disease: balance between East and West? A narrative review,” *Digestive Medicine Research,* vol. 3, 2020.
[29] M. Zhao, L. Gönczi, P. L. Lakatos, and J. Burisch, “The Burden of Inflammatory Bowel Disease in Europe in 2020,” *Journal of Crohn's and Colitis,* vol. 15, no. 9, pp. 1573-1587, 2021.
[30] S. C. Shah, H. Khalili, C. Gower-Rousseau, O. Olen, E. I. Benchimol, E. Lynge, K. R. Nielsen, P. Brassard, M. Vutcovici, A. Bitton, C. N. Bernstein, D. Leddin, H. Tamim, T. Stefansson, E. V. Loftus, Jr., B. Moum, W. Tang, S. C. Ng, R. Gearry, B. Sincic, S. Bell, B. E. Sands, P. L. Lakatos, Z. Vegh, C. Ott, G. G. Kaplan, J. Burisch, and J. F. Colombel, “Sex-Based Differences in Incidence of Inflammatory Bowel Diseases-Pooled Analysis of Population-Based Studies From Western Countries,” *Gastroenterology,* vol. 155, no. 4, pp. 1079-1089 e3, Oct, 2018.
[31] J. Kikut, N. Konecka, M. Ziętek, and M. Szczuko, “Inflammatory Bowel Disease Etiology: Current Knowledge,” *Pteridines,* vol. 29, no. 1, pp. 206-214, 2018.
[32] C. Mowat, A. Cole, A. Windsor, T. Ahmad, I. Arnott, R. Driscoll, S. Mitton, T. Orchard, M. Rutter, L. Younge, C. Lees, G. T. Ho, J. Satsangi, S. Bloom, and I. B. D. S. o. t. B. S. o. Gastroenterology, “Guidelines for the management of inflammatory bowel disease in adults,” *Gut,* vol. 60, no. 5, pp. 571-607, May, 2011.
[33] R. M. Feakins, and G. British Society of, “Inflammatory bowel disease biopsies: updated British Society of Gastroenterology reporting guidelines,” *J Clin Pathol,* vol. 66, no. 12, pp. 1005-26, Dec, 2013.
[34] J. E. Lennard-Jones, “Classification of inflammatory bowel disease,” *Scand J Gastroenterol Suppl,* vol. 170, pp. 2-6; discussion 16-9, 1989.
[35] V. G. Nóbrega, I. N. N. Silva, B. S. Brito, J. Silva, M. Silva, and G. O. Santana, “THE ONSET OF CLINICAL MANIFESTATIONS IN INFLAMMATORY BOWEL DISEASE PATIENTS,” *Arq Gastroenterol,* vol. 55, no. 3, pp. 290-295, Jul-Sep, 2018.
[36] C. W. Chang, J. M. Wong, C. C. Tung, I. L. Shih, H. Y. Wang, and S. C. Wei, “Intestinal stricture in Crohn's disease,” *Intest Res,* vol. 13, no. 1, pp. 19-26, Jan, 2015.
[37] M. Zhao, B. Z. S. Lo, M. K. Vester-Andersen, I. Vind, F. Bendtsen, and J. Burisch, “A 10-Year Follow-up Study of the Natural History of Perianal Crohn's Disease in a Danish Population-Based Inception Cohort,” *Inflamm Bowel Dis,* vol. 25, no. 7, pp. 1227-1236, Jun 18, 2019.
[38] S. Wu, S. Xie, C. Yuan, Z. Yang, S. Liu, Q. Zhang, F. Sun, J. Wu, S. Zhan, S. Zhu, and S. Zhang, “Inflammatory Bowel Disease and Long-term Risk of Cancer: A Prospective Cohort Study Among Half a Million Adults in UK Biobank,” *Inflamm Bowel Dis,* vol. 29, no. 3, pp. 384-395, Mar 1, 2023.

[39] R. W. Stidham, and P. D. R. Higgins, “Colorectal Cancer in Inflammatory Bowel Disease,” *Clin Colon Rectal Surg,* vol. 31, no. 3, pp. 168-178, May, 2018.
[40] L. Lakatos, T. Pandur, G. David, Z. Balogh, P. Kuronya, A. Tollas, and P. L. Lakatos, “Association of extraintestinal manifestations of inflammatory bowel disease in a province of western Hungary with disease phenotype: results of a 25-year follow-up study,” *World J Gastroenterol,* vol. 9, no. 10, pp. 2300-7, Oct, 2003.
[41] S. R. Vavricka, G. Rogler, C. Gantenbein, M. Spoerri, M. Prinz Vavricka, A. A. Navarini, L. E. French, E. Safroneeva, N. Fournier, A. Straumann, F. Froehlich, M. Fried, P. Michetti, F. Seibold, P. L. Lakatos, L. Peyrin-Biroulet, and A. M. Schoepfer, “Chronological Order of Appearance of Extraintestinal Manifestations Relative to the Time of IBD Diagnosis in the Swiss Inflammatory Bowel Disease Cohort,” *Inflamm Bowel Dis,* vol. 21, no. 8, pp. 1794-800, Aug, 2015.
[42] M. Bewtra, C. M. Brensinger, V. T. Tomov, T. B. Hoang, C. E. Sokach, C. A. Siegel, and J. D. Lewis, “An optimized patient-reported ulcerative colitis disease activity measure derived from the Mayo score and the simple clinical colitis activity index,” *Inflamm Bowel Dis,* vol. 20, no. 6, pp. 1070-8, Jun, 2014.
[43] S. P. Travis, D. Schnell, P. Krzeski, M. T. Abreu, D. G. Altman, J. F. Colombel, B. G. Feagan, S. B. Hanauer, G. R. Lichtenstein, P. R. Marteau, W. Reinisch, B. E. Sands, B. R. Yacyshyn, P. Schnell, C. A. Bernhardt, J. Y. Mary, and W. J. Sandborn, “Reliability and initial validation of the ulcerative colitis endoscopic index of severity,” *Gastroenterology,* vol. 145, no. 5, pp. 987-95, Nov, 2013.
[44] J. S. Lee, E. S. Kim, and W. Moon, “Chronological Review of Endoscopic Indices in Inflammatory Bowel Disease,” *Clin Endosc,* vol. 52, no. 2, pp. 129-136, 3, 2019.
[45] W. R. Best, J. M. Becktel, J. W. Singleton, and F. Kern, Jr., “Development of a Crohn's disease activity index. National Cooperative Crohn's Disease Study,” *Gastroenterology,* vol. 70, no. 3, pp. 439-44, Mar, 1976.
[46] M. Daperno, G. D'Haens, G. Van Assche, F. Baert, P. Bulois, V. Maunoury, R. Sostegni, R. Rocca, A. Pera, A. Gevers, J.-Y. Mary, J.-F. Colombel, and P. Rutgeerts, “Development and validation of a new, simplified endoscopic activity score for Crohn's disease: the SES-CD,” *Gastrointestinal Endoscopy,* vol. 60, no. 4, pp. 505-512, 2004.
[47] R. Khanna, G. Zou, L. Stitt, B. G. Feagan, W. J. Sandborn, P. Rutgeerts, J. W. D. McDonald, E. Dubcenco, R. Fogel, R. Panaccione, V. Jairath, S. Nelson, L. M. Shackelton, B. Huang, Q. Zhou, A. M. Robinson, B. G. Levesque, and G. D'Haens, “Responsiveness of Endoscopic Indices of Disease Activity for Crohn’s Disease,” *Official journal of the American College of Gastroenterology | ACG,* vol. 112, no. 10, pp. 1584-1592, 2017.
[48] J.-F. Colombel, R. Panaccione, P. Bossuyt, M. Lukas, F. Baert, T. Vaňásek, A. Danalioglu, G. Novacek, A. Armuzzi, X. Hébuterne, S. Travis, S. Danese, W. Reinisch, W. J. Sandborn, P. Rutgeerts, D. Hommes, S. Schreiber, E. Neimark, B. Huang, Q. Zhou, P. Mendez, J. Petersson, K. Wallace, A. M. Robinson, R. B. Thakkar, and G. D'Haens, “Effect of tight control management on Crohn's disease (CALM): a multicentre, randomised, controlled phase 3 trial,” *The Lancet,* vol. 390, no. 10114, pp. 2779-2789, 2017.

[49] B. Christensen, and D. T. Rubin, “Understanding Endoscopic Disease Activity in IBD: How to Incorporate It into Practice,” *Current Gastroenterology Reports,* vol. 18, no. 1, pp. 5, 2016/01/12, 2016.
[50] A. P. Saxena, J. K. Limdi, and F. A. Farraye, “Zeroing in on endoscopic and histologic mucosal healing to reduce the risk of colorectal neoplasia in inflammatory bowel disease,” *Gastrointestinal Endoscopy,* vol. 86, no. 6, pp. 1012-1014, 2017.
[51] L. Peyrin-Biroulet, W. Sandborn, B. E. Sands, W. Reinisch, W. Bemelman, R. V. Bryant, G. D'Haens, I. Dotan, M. Dubinsky, B. Feagan, G. Fiorino, R. Gearry, S. Krishnareddy, P. L. Lakatos, E. V. J. Loftus, P. Marteau, P. Munkholm, T. B. Murdoch, I. Ordás, R. Panaccione, R. H. Riddell, J. Ruel, D. T. Rubin, M. Samaan, C. A. Siegel, M. S. Silverberg, J. Stoker, S. Schreiber, S. Travis, G. Van Assche, S. Danese, J. Panes, G. Bouguen, S. O'Donnell, B. Pariente, S. Winer, S. Hanauer, and J.-F. Colombel, “Selecting Therapeutic Targets in Inflammatory Bowel Disease (STRIDE): Determining Therapeutic Goals for Treat-to-Target,” *Official journal of the American College of Gastroenterology | ACG,* vol. 110, no. 9, pp. 1324-1338, 2015.
[52] B. G. Feagan, and J. K. Macdonald, “Oral 5-aminosalicylic acid for induction of remission in ulcerative colitis,” *Cochrane Database Syst Rev,* vol. 10, pp. CD000543, Oct 17, 2012.
[53] S. C. Truelove, G. Watkinson, and G. Draper, “Comparison of Corticosteroid and Sulphasalazine Therapy in Ulcerative Colitis,” *British Medical Journal,* vol. 2, no. 5321, pp. 1708-1711, 1962.
[54] G. R. D'Haens, Á. Kovács, P. Vergauwe, F. Nagy, T. Molnár, Y. Bouhnik, W. Weiss, H. Brunner, A. Lavergne-Slove, D. Binelli, A. F. D. Di Stefano, and P. Marteau, “Clinical trial: Preliminary efficacy and safety study of a new Budesonide-MMX ® 9 mg extended-release tablets in patients with active left-sided ulcerative colitis,” *Journal of Crohn's and Colitis,* vol. 4, no. 2, pp. 153-160, 2010.
[55] G. Van Assche, F. Manguso, M. Zibellini, J. L. C. Nuño, A. Goldis, E. Tkachenko, G. Varoli, D. Kleczkowski, V. Annese, F. D'Heygere, A. Balzano, and o. b. o. t. B. s. p. centers, “Oral Prolonged Release Beclomethasone Dipropionate and Prednisone in the Treatment of Active Ulcerative Colitis: Results From a Double-Blind, Randomized, Parallel Group Study,” *Official journal of the American College of Gastroenterology | ACG,* vol. 110, no. 5, pp. 708-715, 2015.
[56] K. J. Khan, M. C. Dubinsky, A. C. Ford, T. A. Ullman, N. J. Talley, and P. Moayyedi, “Efficacy of Immunosuppressive Therapy for Inflammatory Bowel Disease: A Systematic Review and Meta-Analysis,” *Official journal of the American College of Gastroenterology | ACG,* vol. 106, no. 4, pp. 630-642, 2011.
[57] P. Rutgeerts, W. J. Sandborn, B. G. Feagan, W. Reinisch, A. Olson, J. Johanns, S. Travers, D. Rachmilewitz, S. B. Hanauer, G. R. Lichtenstein, W. J. S. de Villiers, D. Present, B. E. Sands, and J. F. Colombel, “Infliximab for Induction and Maintenance Therapy for Ulcerative Colitis,” *New England Journal of Medicine,* vol. 353, no. 23, pp. 2462-2476, 2005.
[58] W. J. Sandborn, A. Sakuraba, A. Wang, D. Macaulay, W. Reichmann, S. Wang, J. Chao, and M. Skup, “Comparison of real-world outcomes of adalimumab and infliximab for patients with ulcerative colitis in the United States,” *Current Medical Research and Opinion,* vol. 32, no. 7, pp. 1233-1241, 2016/07/02, 2016.

[59] B. G. Feagan, P. Rutgeerts, B. E. Sands, S. Hanauer, J.-F. Colombel, W. J. Sandborn, G. Van Assche, J. Axler, H.-J. Kim, S. Danese, I. Fox, C. Milch, S. Sankoh, T. Wyant, J. Xu, and A. Parikh, “Vedolizumab as Induction and Maintenance Therapy for Ulcerative Colitis,” *New England Journal of Medicine,* vol. 369, no. 8, pp. 699-710, 2013.

[60] “Late breaking abstracts,” *United European Gastroenterology Journal,* vol. 6, no. 10, pp. 1586-1597, 2018.

[61] B. E. Sands, A. C. Moss, A. Armuzzi, J. K. Marshall, J. O. Lindsay, W. J. Sandborn, S. Danese, K. Tsilkos, N. Lawendy, H. Zhang, G. S. Friedman, G. Chan, D. W. Krichbaum, and C. Su, “DOP026 Efficacy and safety of dose escalation to tofacitinib 10 mg BID for patients with ulcerative colitis following loss of response on tofacitinib 5 mg BID maintenance therapy: results from OCTAVE open,” *Journal of Crohn's and Colitis,* vol. 12, no. supplement_1, pp. S049-S049, 2018.

[62] N. H. Hyman, P. Cataldo, and T. Osler, “Urgent Subtotal Colectomy for Severe Inflammatory Bowel Disease,” *Diseases of the Colon & Rectum,* vol. 48, no. 1, pp. 70-73, 2005.

[63] R. Fornaro, M. Caratto, G. Barbruni, F. Fornaro, A. Salerno, D. Giovinazzo, C. Sticchi, and E. Caratto, “Surgical and medical treatment in patients with acute severe ulcerative colitis,” *Journal of Digestive Diseases,* vol. 16, no. 10, pp. 558-567, 2015.

[64] V. W. Fazio, R. P. Kiran, F. H. Remzi, J. C. Coffey, H. M. Heneghan, H. T. Kirat, E. Manilich, B. Shen, and S. T. Martin, “Ileal Pouch Anal Anastomosis: Analysis of Outcome and Quality of Life in 3707 Patients,” *Annals of Surgery,* vol. 257, no. 4, pp. 679-685, 2013.

[65] S. Bar-Meir, Y. Chowers, A. Lavy, D. Abramovitch, A. Sternberg, G. Leichtmann, R. Reshef, S. Odes, M. Moshkovitz, R. Bruck, R. Eliakim, E. Maoz, and U. Mittmann, “Budesonide versus prednisone in the treatment of active Crohn's disease. The Israeli Budesonide Study Group,” *Gastroenterology,* vol. 115, no. 4, pp. 835-40, Oct, 1998.

[66] A. Rezaie, M. E. Kuenzig, E. I. Benchimol, A. M. Griffiths, A. R. Otley, A. H. Steinhart, G. G. Kaplan, and C. H. Seow, “Budesonide for induction of remission in Crohn's disease,” *Cochrane Database Syst Rev*, no. 6, pp. CD000296, Jun 3, 2015.

[67] L. Beaugerie, P. Seksik, I. Nion–Larmurier, J. P. Gendre, and J. Cosnes, “Predictors of Crohn’s Disease,” *Gastroenterology,* vol. 130, no. 3, pp. 650-656, 2006.

[68] C. Y. Ponsioen, E. J. de Groof, E. J. Eshuis, T. J. Gardenbroek, P. M. M. Bossuyt, A. Hart, J. Warusavitarne, C. J. Buskens, A. A. van Bodegraven, M. A. Brink, E. C. J. Consten, B. A. van Wagensveld, M. C. M. Rijk, R. M. P. H. Crolla, C. G. Noomen, A. P. J. Houdijk, R. C. Mallant, M. Boom, W. A. Marsman, H. B. Stockmann, B. Mol, A. J. de Groof, P. C. Stokkers, G. R. D'Haens, W. A. Bemelman, K. Bruin, J. Maring, T. van Ditzhuijsen, H. Prins, J. van den Brande, P. Kingma, A. van Geloven, N. de Boer, D. van der Peet, J. Jansen, M. Gerhards, J. van der Woude, R. Schouten, B. Oldenburg, R. van Hillegersberg, R. West, G. Mannaerts, M. Spanier, E. J. Spillenaar Bilgen, R. Lieverse, E. van der Zaag, A. Depla, A. van de Laar, C. Bolwerk, H. Brouwer, N. Mahmmod, E. Hazebroek, J. Vecht, R. Pierik, G. Dijkstra, S. Hofker, T. Uiterwaal, Q. Eijsbouts, L. Oostenbrug, M. Sosef, D. Cahen, S. van der Werff, A. Marinelli, J. Peters, H. Cense, N. Talstra, and P. Morar, “Laparoscopic ileocaecal resection versus infliximab for terminal ileitis in Crohn's disease: a

randomised controlled, open-label, multicentre trial," *The Lancet Gastroenterology & Hepatology,* vol. 2, no. 11, pp. 785-792, 2017.
[69] D. McGonagle, and M. F. McDermott, "A proposed classification of the immunological diseases," *PLoS Med,* vol. 3, no. 8, pp. e297, Aug, 2006.
[70] D. L. Mann, "The emerging role of innate immunity in the heart and vascular system: for whom the cell tolls," *Circ Res,* vol. 108, no. 9, pp. 1133-45, Apr 29, 2011.
[71] K. F. Kusano, and K. Satomi, "Diagnosis and treatment of cardiac sarcoidosis," *Heart,* vol. 102, no. 3, pp. 184-90, Feb, 2016.
[72] P. Richardson, W. McKenna, M. Bristow, B. Maisch, B. Mautner, J. O'Connell, E. Olsen, G. Thiene, J. Goodwin, I. Gyarfas, I. Martin, and P. Nordet, "Report of the 1995 World Health Organization/International Society and Federation of Cardiology Task Force on the Definition and Classification of cardiomyopathies," *Circulation,* vol. 93, no. 5, pp. 841-2, Mar 1, 1996.
[73] A. L. Caforio, S. Pankuweit, E. Arbustini, C. Basso, J. Gimeno-Blanes, S. B. Felix, M. Fu, T. Heliö, S. Heymans, R. Jahns, K. Klingel, A. Linhart, B. Maisch, W. McKenna, J. Mogensen, Y. M. Pinto, A. Ristic, H. P. Schultheiss, H. Seggewiss, L. Tavazzi, G. Thiene, A. Yilmaz, P. Charron, and P. M. Elliott, "Current state of knowledge on aetiology, diagnosis, management, and therapy of myocarditis: a position statement of the European Society of Cardiology Working Group on Myocardial and Pericardial Diseases," *Eur Heart J,* vol. 34, no. 33, pp. 2636-48, 2648a-2648d, Sep, 2013.
[74] A. Faccini, J. C. Kaski, and P. G. Camici, "Coronary microvascular dysfunction in chronic inflammatory rheumatoid diseases," *Eur Heart J,* vol. 37, no. 23, pp. 1799-806, Jun 14, 2016.
[75] T. A. McDonagh, M. Metra, M. Adamo, R. S. Gardner, A. Baumbach, M. Böhm, H. Burri, J. Butler, J. Čelutkienė, O. Chioncel, J. G. F. Cleland, A. J. S. Coats, M. G. Crespo-Leiro, D. Farmakis, M. Gilard, S. Heymans, A. W. Hoes, T. Jaarsma, E. A. Jankowska, M. Lainscak, C. S. P. Lam, A. R. Lyon, J. J. V. McMurray, A. Mebazaa, R. Mindham, C. Muneretto, M. Francesco Piepoli, S. Price, G. M. C. Rosano, F. Ruschitzka, A. Kathrine Skibelund, and E. S. D. Group, "2021 ESC Guidelines for the diagnosis and treatment of acute and chronic heart failure: Developed by the Task Force for the diagnosis and treatment of acute and chronic heart failure of the European Society of Cardiology (ESC) With the special contribution of the Heart Failure Association (HFA) of the ESC," *European Heart Journal,* vol. 42, no. 36, pp. 3599-3726, 2021.
[76] S. Prasada, A. Rivera, A. Nishtala, A. E. Pawlowski, A. Sinha, J. D. Bundy, S. A. Chadha, F. S. Ahmad, S. S. Khan, C. Achenbach, F. J. Palella, Jr., R. Ramsey-Goldman, Y. C. Lee, J. I. Silverberg, B. O. Taiwo, S. J. Shah, D. M. Lloyd-Jones, and M. J. Feinstein, "Differential Associations of Chronic Inflammatory Diseases With Incident Heart Failure," *JACC Heart Fail,* vol. 8, no. 6, pp. 489-498, Jun, 2020.
[77] D. M. Bunu, C. E. Timofte, M. Ciocoiu, M. Floria, C. C. Tarniceriu, O. B. Barboi, and D. M. Tanase, "Cardiovascular Manifestations of Inflammatory Bowel Disease: Pathogenesis, Diagnosis, and Preventive Strategies," *Gastroenterol Res Pract,* vol. 2019, pp. 3012509, 2019.
[78] H. T. Sørensen, and K. M. Fonager, "Myocarditis and inflammatory bowel disease. A 16-year Danish nationwide cohort study," *Dan Med Bull,* vol. 44, no. 4, pp. 442-4, Sep, 1997.

[79] S. Aniwan, D. S. Pardi, W. J. Tremaine, and E. V. Loftus, Jr., “Increased Risk of Acute Myocardial Infarction and Heart Failure in Patients With Inflammatory Bowel Diseases,” *Clin Gastroenterol Hepatol,* vol. 16, no. 10, pp. 1607-1615.e1, Oct, 2018.
[80] G. Brown, “5-Aminosalicylic Acid-Associated Myocarditis and Pericarditis: A Narrative Review,” *Can J Hosp Pharm,* vol. 69, no. 6, pp. 466-472, Nov-Dec, 2016.
[81] T. A. Sentongo, and D. A. Piccoli, “Recurrent pericarditis due to mesalamine hypersensitivity: a pediatric case report and review of the literature,” *J Pediatr Gastroenterol Nutr,* vol. 27, no. 3, pp. 344-7, Sep, 1998.
[82] M. H. Edwards, and A. M. Leak, “Pericardial effusions on anti-TNF therapy for rheumatoid arthritis--a drug side effect or uncontrolled systemic disease?,” *Rheumatology (Oxford),* vol. 48, no. 3, pp. 316-7, Mar, 2009.
[83] M. C. Soh, H. H. Hart, and M. Corkill, “Pericardial effusions with tamponade and visceral constriction in patients with rheumatoid arthritis on tumour necrosis factor (TNF)-inhibitor therapy,” *Int J Rheum Dis,* vol. 12, no. 1, pp. 74-7, Apr, 2009.
[84] H. Ozkan, A. S. Cetinkaya, T. Yildiz, and T. Bozat, “A Rare Side Effect due to TNF-Alpha Blocking Agent: Acute Pleuropericarditis with Adalimumab,” *Case Rep Rheumatol,* vol. 2013, pp. 985914, 2013.
[85] S. Mavrogeni, G. Karabela, E. Stavropoulos, E. Gialafos, E. Sfendouraki, L. Kyrou, and G. Kolovou, “Imaging patterns of heart failure in rheumatoid arthritis evaluated by cardiovascular magnetic resonance,” *Int J Cardiol,* vol. 168, no. 4, pp. 4333-5, Oct 9, 2013.
[86] R. G. Assomull, D. J. Pennell, and S. K. Prasad, “Cardiovascular magnetic resonance in the evaluation of heart failure,” *Heart,* vol. 93, no. 8, pp. 985-92, Aug, 2007.
[87] C. M. Kramer, J. Barkhausen, C. Bucciarelli-Ducci, S. D. Flamm, R. J. Kim, and E. Nagel, “Standardized cardiovascular magnetic resonance imaging (CMR) protocols: 2020 update,” *J Cardiovasc Magn Reson,* vol. 22, no. 1, pp. 17, Feb 24, 2020.
[88] N. Kawel-Boehm, S. J. Hetzel, B. Ambale-Venkatesh, G. Captur, C. J. Francois, M. Jerosch-Herold, M. Salerno, S. D. Teague, E. Valsangiacomo-Buechel, R. J. van der Geest, and D. A. Bluemke, “Reference ranges (“normal values”) for cardiovascular magnetic resonance (CMR) in adults and children: 2020 update,” *Journal of Cardiovascular Magnetic Resonance,* vol. 22, no. 1, pp. 87, 2020/12/14, 2020.
[89] S. G. Myerson, N. G. Bellenger, and D. J. Pennell, “Assessment of left ventricular mass by cardiovascular magnetic resonance,” *Hypertension,* vol. 39, no. 3, pp. 750-5, Mar 1, 2002.
[90] N. G. Bellenger, M. I. Burgess, S. G. Ray, A. Lahiri, A. J. Coats, J. G. Cleland, and D. J. Pennell, “Comparison of left ventricular ejection fraction and volumes in heart failure by echocardiography, radionuclide ventriculography and cardiovascular magnetic resonance; are they interchangeable?,” *Eur Heart J,* vol. 21, no. 16, pp. 1387-96, Aug, 2000.
[91] C. A. Papanastasiou, M. A. Bazmpani, D. G. Kokkinidis, T. Zegkos, G. Efthimiadis, A. Tsapas, H. Karvounis, A. Ziakas, A. P. Kalogeropoulos, C. M. Kramer, and T. D. Karamitsos, “The prognostic value of right ventricular ejection fraction by cardiovascular magnetic resonance in heart failure: A systematic review and meta-analysis,” *Int J Cardiol,* vol. 368, pp. 94-103, Dec 1, 2022.

[92] B. Bernhard, A. Schnyder, D. Garachemani, K. Fischer, G. Tanner, Y. Safarkhanlo, A. W. Stark, J. Schütze, M. Pavlicek-Bahlo, S. Greulich, C. Johner, A. Wahl, D. C. Benz, R. Y. Kwong, and C. Gräni, “Prognostic Value of Right Ventricular Function in Patients With Suspected Myocarditis Undergoing Cardiac Magnetic Resonance,” *JACC Cardiovasc Imaging,* vol. 16, no. 1, pp. 28-41, Jan, 2023.

[93] F. I. Marcus, W. J. McKenna, D. Sherrill, C. Basso, B. Bauce, D. A. Bluemke, H. Calkins, D. Corrado, M. G. Cox, J. P. Daubert, G. Fontaine, K. Gear, R. Hauer, A. Nava, M. H. Picard, N. Protonotarios, J. E. Saffitz, D. M. Sanborn, J. S. Steinberg, H. Tandri, G. Thiene, J. A. Towbin, A. Tsatsopoulou, T. Wichter, and W. Zareba, “Diagnosis of arrhythmogenic right ventricular cardiomyopathy/dysplasia: proposed modification of the task force criteria,” *Circulation,* vol. 121, no. 13, pp. 1533-41, Apr 6, 2010.

[94] J. Schulz-Menger, D. A. Bluemke, J. Bremerich, S. D. Flamm, M. A. Fogel, M. G. Friedrich, R. J. Kim, F. von Knobelsdorff-Brenkenhoff, C. M. Kramer, D. J. Pennell, S. Plein, and E. Nagel, “Standardized image interpretation and post-processing in cardiovascular magnetic resonance - 2020 update : Society for Cardiovascular Magnetic Resonance (SCMR): Board of Trustees Task Force on Standardized Post-Processing,” *J Cardiovasc Magn Reson,* vol. 22, no. 1, pp. 19, Mar 12, 2020.

[95] D. R. Messroghli, K. Walters, S. Plein, P. Sparrow, M. G. Friedrich, J. P. Ridgway, and M. U. Sivananthan, “Myocardial T1 mapping: application to patients with acute and chronic myocardial infarction,” *Magn Reson Med,* vol. 58, no. 1, pp. 34-40, Jul, 2007.

[96] R. Fernandez-Jimenez, J. Sanchez-Gonzalez, J. Aguero, M. Del Trigo, C. Galan-Arriola, V. Fuster, and B. Ibanez, “Fast T2 gradient-spin-echo (T2-GraSE) mapping for myocardial edema quantification: first in vivo validation in a porcine model of ischemia/reperfusion,” *J Cardiovasc Magn Reson,* vol. 17, pp. 92, Nov 4, 2015.

[97] T. D. Karamitsos, S. K. Piechnik, S. M. Banypersad, M. Fontana, N. B. Ntusi, V. M. Ferreira, C. J. Whelan, S. G. Myerson, M. D. Robson, P. N. Hawkins, S. Neubauer, and J. C. Moon, “Noncontrast T1 mapping for the diagnosis of cardiac amyloidosis,” *JACC Cardiovasc Imaging,* vol. 6, no. 4, pp. 488-97, Apr, 2013.

[98] D. M. Sado, S. K. White, S. K. Piechnik, S. M. Banypersad, T. Treibel, G. Captur, M. Fontana, V. Maestrini, A. S. Flett, M. D. Robson, R. H. Lachmann, E. Murphy, A. Mehta, D. Hughes, S. Neubauer, P. M. Elliott, and J. C. Moon, “Identification and assessment of Anderson-Fabry disease by cardiovascular magnetic resonance noncontrast myocardial T1 mapping,” *Circ Cardiovasc Imaging,* vol. 6, no. 3, pp. 392-8, May 1, 2013.

[99] S. Dass, J. J. Suttie, S. K. Piechnik, V. M. Ferreira, C. J. Holloway, R. Banerjee, M. Mahmod, L. Cochlin, T. D. Karamitsos, M. D. Robson, H. Watkins, and S. Neubauer, “Myocardial tissue characterization using magnetic resonance noncontrast t1 mapping in hypertrophic and dilated cardiomyopathy,” *Circ Cardiovasc Imaging,* vol. 5, no. 6, pp. 726-33, Nov, 2012.

[100] L. J. Anderson, S. Holden, B. Davis, E. Prescott, C. C. Charrier, N. H. Bunce, D. N. Firmin, B. Wonke, J. Porter, J. M. Walker, and D. J. Pennell, “Cardiovascular T2-star (T2*) magnetic resonance for the early diagnosis of myocardial iron overload,” *Eur Heart J,* vol. 22, no. 23, pp. 2171-9, Dec, 2001.

[101] V. M. Ferreira, C. J. Holloway, S. K. Piechnik, T. D. Karamitsos, and S. Neubauer, “Is it really fat? Ask a T1-map,” *Eur Heart J Cardiovasc Imaging,* vol. 14, no. 11, pp. 1060, Nov, 2013.
[102] P. Haaf, P. Garg, D. R. Messroghli, D. A. Broadbent, J. P. Greenwood, and S. Plein, “Cardiac T1 Mapping and Extracellular Volume (ECV) in clinical practice: a comprehensive review,” *Journal of Cardiovascular Magnetic Resonance,* vol. 18, no. 1, pp. 89, 2016/11/30, 2016.
[103] V. M. Ferreira, S. K. Piechnik, E. Dall'Armellina, T. D. Karamitsos, J. M. Francis, N. Ntusi, C. Holloway, R. P. Choudhury, A. Kardos, M. D. Robson, M. G. Friedrich, and S. Neubauer, “Native T1-mapping detects the location, extent and patterns of acute myocarditis without the need for gadolinium contrast agents,” *J Cardiovasc Magn Reson,* vol. 16, no. 1, pp. 36, May 23, 2014.
[104] V. M. Ferreira, J. Schulz-Menger, G. Holmvang, C. M. Kramer, I. Carbone, U. Sechtem, I. Kindermann, M. Gutberlet, L. T. Cooper, P. Liu, and M. G. Friedrich, “Cardiovascular Magnetic Resonance in Nonischemic Myocardial Inflammation: Expert Recommendations,” *J Am Coll Cardiol,* vol. 72, no. 24, pp. 3158-3176, Dec 18, 2018.
[105] P. Lurz, C. Luecke, I. Eitel, F. Fohrenbach, C. Frank, M. Grothoff, S. de Waha, K. P. Rommel, J. A. Lurz, K. Klingel, R. Kandolf, G. Schuler, H. Thiele, and M. Gutberlet, “Comprehensive Cardiac Magnetic Resonance Imaging in Patients With Suspected Myocarditis: The MyoRacer-Trial,” *J Am Coll Cardiol,* vol. 67, no. 15, pp. 1800-1811, Apr 19, 2016.
[106] F. von Knobelsdorff-Brenkenhoff, J. Schuler, S. Doganguzel, M. A. Dieringer, A. Rudolph, A. Greiser, P. Kellman, and J. Schulz-Menger, “Detection and Monitoring of Acute Myocarditis Applying Quantitative Cardiovascular Magnetic Resonance,” *Circ Cardiovasc Imaging,* vol. 10, no. 2, Feb, 2017.
[107] S. Bohnen, U. K. Radunski, G. K. Lund, E. Tahir, M. Avanesov, C. Stehning, B. Schnackenburg, G. Adam, S. Blankenberg, and K. Muellerleile, “T1 mapping cardiovascular magnetic resonance imaging to detect myocarditis-Impact of slice orientation on the diagnostic performance,” *Eur J Radiol,* vol. 86, pp. 6-12, Jan, 2017.
[108] U. K. Radunski, G. K. Lund, D. Saring, S. Bohnen, C. Stehning, B. Schnackenburg, M. Avanesov, E. Tahir, G. Adam, S. Blankenberg, and K. Muellerleile, “T1 and T2 mapping cardiovascular magnetic resonance imaging techniques reveal unapparent myocardial injury in patients with myocarditis,” *Clin Res Cardiol,* vol. 106, no. 1, pp. 10-17, Jan, 2017.
[109] M. Fontana, S. M. Banypersad, T. A. Treibel, A. Abdel-Gadir, V. Maestrini, T. Lane, J. A. Gilbertson, D. F. Hutt, H. J. Lachmann, C. J. Whelan, A. D. Wechalekar, A. S. Herrey, J. D. Gillmore, P. N. Hawkins, and J. C. Moon, “Differential Myocyte Responses in Patients with Cardiac Transthyretin Amyloidosis and Light-Chain Amyloidosis: A Cardiac MR Imaging Study,” *Radiology,* vol. 277, no. 2, pp. 388-97, Nov, 2015.
[110] J. Schulz-Menger, D. A. Bluemke, J. Bremerich, S. D. Flamm, M. A. Fogel, M. G. Friedrich, R. J. Kim, F. von Knobelsdorff-Brenkenhoff, C. M. Kramer, D. J. Pennell, S. Plein, and E. Nagel, “Standardized image interpretation and post processing in cardiovascular magnetic resonance: Society for Cardiovascular Magnetic Resonance (SCMR) board of trustees task force on standardized post processing,” *J Cardiovasc Magn Reson,* vol. 15, no. 1, pp. 35, May 1, 2013.

[111] A. S. Bojer, M. H. Sørensen, N. Vejlstrup, J. P. Goetze, P. Gæde, and P. L. Madsen, “Distinct non-ischemic myocardial late gadolinium enhancement lesions in patients with type 2 diabetes,” *Cardiovasc Diabetol,* vol. 19, no. 1, pp. 184, Oct 22, 2020.
[112] R. S. Oakes, T. J. Badger, E. G. Kholmovski, N. Akoum, N. S. Burgon, E. N. Fish, J. J. Blauer, S. N. Rao, E. V. DiBella, N. M. Segerson, M. Daccarett, J. Windfelder, C. J. McGann, D. Parker, R. S. MacLeod, and N. F. Marrouche, “Detection and quantification of left atrial structural remodeling with delayed-enhancement magnetic resonance imaging in patients with atrial fibrillation,” *Circulation,* vol. 119, no. 13, pp. 1758-67, Apr 7, 2009.
[113] T. G. Neilan, O. R. Coelho-Filho, S. B. Danik, R. V. Shah, J. A. Dodson, D. J. Verdini, M. Tokuda, C. A. Daly, U. B. Tedrow, W. G. Stevenson, M. Jerosch-Herold, B. B. Ghoshhajra, and R. Y. Kwong, “CMR quantification of myocardial scar provides additive prognostic information in nonischemic cardiomyopathy,” *JACC Cardiovasc Imaging,* vol. 6, no. 9, pp. 944-54, Sep, 2013.
[114] H. Mahrholdt, A. Wagner, R. M. Judd, and U. Sechtem, “Assessment of myocardial viability by cardiovascular magnetic resonance imaging,” *Eur Heart J,* vol. 23, no. 8, pp. 602-19, Apr, 2002.
[115] P. Kellman, and A. E. Arai, “Cardiac imaging techniques for physicians: late enhancement,” *J Magn Reson Imaging,* vol. 36, no. 3, pp. 529-42, Sep, 2012.
[116] R. J. Holtackers, T. Emrich, R. M. Botnar, M. E. Kooi, J. E. Wildberger, and K. F. Kreitner, “Late Gadolinium Enhancement Cardiac Magnetic Resonance Imaging: From Basic Concepts to Emerging Methods,” *Rofo,* vol. 194, no. 5, pp. 491-504, May, 2022.
[117] J. Uhlig, O. Al-Bourini, R. Salgado, M. Francone, R. Vliegenthart, J. Bremerich, J. Lotz, and M. Gutberlet, “Gadolinium-based Contrast Agents for Cardiac MRI: Use of Linear and Macrocyclic Agents with Associated Safety Profile from 154 779 European Patients,” *Radiology: Cardiothoracic Imaging,* vol. 2, no. 5, pp. e200102, 2020.
[118] A. S. Flett, J. Hasleton, C. Cook, D. Hausenloy, G. Quarta, C. Ariti, V. Muthurangu, and J. C. Moon, “Evaluation of techniques for the quantification of myocardial scar of differing etiology using cardiac magnetic resonance,” *JACC Cardiovasc Imaging,* vol. 4, no. 2, pp. 150-6, Feb, 2011.
[119] A. Mentias, P. Raeisi-Giglou, N. G. Smedira, K. Feng, K. Sato, O. Wazni, M. Kanj, S. D. Flamm, M. Thamilarasan, Z. B. Popovic, H. M. Lever, and M. Y. Desai, “Late Gadolinium Enhancement in Patients With Hypertrophic Cardiomyopathy and Preserved Systolic Function,” *Journal of the American College of Cardiology,* vol. 72, no. 8, pp. 857-870, 2018/08/21/, 2018.
[120] R. G. Assomull, S. K. Prasad, J. Lyne, G. Smith, E. D. Burman, M. Khan, M. N. Sheppard, P. A. Poole-Wilson, and D. J. Pennell, “Cardiovascular magnetic resonance, fibrosis, and prognosis in dilated cardiomyopathy,” *J Am Coll Cardiol,* vol. 48, no. 10, pp. 1977-85, Nov 21, 2006.
[121] A. M. Maceira, J. Joshi, S. K. Prasad, J. C. Moon, E. Perugini, I. Harding, M. N. Sheppard, P. A. Poole-Wilson, P. N. Hawkins, and D. J. Pennell, “Cardiovascular magnetic resonance in cardiac amyloidosis,” *Circulation,* vol. 111, no. 2, pp. 186-93, Jan 18, 2005.
[122] J. B. Selvanayagam, A. Kardos, J. M. Francis, F. Wiesmann, S. E. Petersen, D. P. Taggart, and S. Neubauer, “Value of delayed-enhancement cardiovascular magnetic resonance imaging in predicting myocardial viability after surgical revascularization,” *Circulation,* vol. 110, no. 12, pp. 1535-41, Sep 21, 2004.

[123] S. Kuruvilla, N. Adenaw, A. B. Katwal, M. J. Lipinski, C. M. Kramer, and M. Salerno, “Late gadolinium enhancement on cardiac magnetic resonance predicts adverse cardiovascular outcomes in nonischemic cardiomyopathy: a systematic review and meta-analysis,” *Circ Cardiovasc Imaging,* vol. 7, no. 2, pp. 250-258, Mar, 2014.
[124] S. A. Abbasi, A. Ertel, R. V. Shah, V. Dandekar, J. Chung, G. Bhat, A. A. Desai, R. Y. Kwong, and A. Farzaneh-Far, “Impact of cardiovascular magnetic resonance on management and clinical decision-making in heart failure patients,” *J Cardiovasc Magn Reson,* vol. 15, no. 1, pp. 89, Oct 1, 2013.
[125] Z. Weng, J. Yao, R. H. Chan, J. He, X. Yang, Y. Zhou, and Y. He, “Prognostic Value of LGE-CMR in HCM: A Meta-Analysis,” *JACC Cardiovasc Imaging,* vol. 9, no. 12, pp. 1392-1402, Dec, 2016.
[126] S. A. Lee, Y. E. Yoon, J. E. Kim, J. J. Park, I. Y. Oh, C. H. Yoon, J. W. Suh, J. S. Kim, E. J. Chun, Y. S. Cho, T. J. Youn, C. Lim, G. Y. Cho, I. H. Chae, K. H. Park, D. J. Choi, and S. I. Choi, “Long-Term Prognostic Value of Late Gadolinium-Enhanced Magnetic Resonance Imaging in Patients With and Without Left Ventricular Dysfunction Undergoing Coronary Artery Bypass Grafting,” *Am J Cardiol,* vol. 118, no. 11, pp. 1647-1654, Dec 1, 2016.
[127] M. Fenski, T. H. Grandy, D. Viezzer, S. Kertusha, M. Schmidt, C. Forman, and J. Schulz-Menger, “Isotropic 3D compressed sensing (CS) based sequence is comparable to 2D-LGE in left ventricular scar quantification in different disease entities,” *The International Journal of Cardiovascular Imaging,* vol. 38, no. 8, pp. 1837-1850, 2022/08/01, 2022.
[128] S. Toupin, T. Pezel, A. Bustin, and H. Cochet, “Whole-Heart High-Resolution Late Gadolinium Enhancement: Techniques and Clinical Applications,” *Journal of Magnetic Resonance Imaging,* vol. 55, no. 4, pp. 967-987, 2022.
[129] D. Hernando, P. Kellman, J. P. Haldar, and Z. P. Liang, “Robust water/fat separation in the presence of large field inhomogeneities using a graph cut algorithm,” *Magn Reson Med,* vol. 63, no. 1, pp. 79-90, Jan, 2010.
[130] S. B. Reeder, B. A. Hargreaves, H. Yu, and J. H. Brittain, “Homodyne reconstruction and IDEAL water-fat decomposition,” *Magn Reson Med,* vol. 54, no. 3, pp. 586-93, Sep, 2005.
[131] G. Cannavale, M. Francone, N. Galea, F. Vullo, A. Molisso, I. Carbone, and C. Catalano, “Fatty Images of the Heart: Spectrum of Normal and Pathological Findings by Computed Tomography and Cardiac Magnetic Resonance Imaging,” *Biomed Res Int,* vol. 2018, pp. 5610347, 2018.
[132] P. Kellman, D. Hernando, and A. E. Arai, “Myocardial Fat Imaging,” *Curr Cardiovasc Imaging Rep,* vol. 3, no. 2, pp. 83-91, Apr, 2010.
[133] M. S. Amzulescu, M. De Craene, H. Langet, A. Pasquet, D. Vancraeynest, A. C. Pouleur, J. L. Vanoverschelde, and B. L. Gerber, “Myocardial strain imaging: review of general principles, validation, and sources of discrepancies,” *Eur Heart J Cardiovasc Imaging,* vol. 20, no. 6, pp. 605-619, Jun 1, 2019.
[134] A. Scatteia, A. Baritussio, and C. Bucciarelli-Ducci, “Strain imaging using cardiac magnetic resonance,” *Heart Fail Rev,* vol. 22, no. 4, pp. 465-476, Jul, 2017.
[135] J. Gröschel, J. Kuhnt, D. Viezzer, T. Hadler, S. Hormes, P. Barckow, J. Schulz-Menger, and E. Blaszczyk, “Comparison of manual and artificial intelligence based quantification of myocardial strain by feature tracking—a cardiovascular MR study in health and disease,” *European Radiology*, 2023/08/18, 2023.

[136] P. Claus, A. M. S. Omar, G. Pedrizzetti, P. P. Sengupta, and E. Nagel, “Tissue Tracking Technology for Assessing Cardiac Mechanics: Principles, Normal Values, and Clinical Applications,” *JACC Cardiovasc Imaging,* vol. 8, no. 12, pp. 1444-1460, Dec, 2015.
[137] C. Lim, E. Blaszczyk, L. Riazy, S. Wiesemann, J. Schüler, F. von Knobelsdorff-Brenkenhoff, and J. Schulz-Menger, “Quantification of myocardial strain assessed by cardiovascular magnetic resonance feature tracking in healthy subjects-influence of segmentation and analysis software,” *Eur Radiol,* vol. 31, no. 6, pp. 3962-3972, Jun, 2021.
[138] A. M. Shetye, S. A. Nazir, N. A. Razvi, N. Price, J. N. Khan, F. Y. Lai, I. B. Squire, G. P. McCann, and J. R. Arnold, “Comparison of global myocardial strain assessed by cardiovascular magnetic resonance tagging and feature tracking to infarct size at predicting remodelling following STEMI,” *BMC Cardiovasc Disord,* vol. 17, no. 1, pp. 7, Jan 5, 2017.
[139] C. McComb, D. Carrick, J. D. McClure, R. Woodward, A. Radjenovic, J. E. Foster, and C. Berry, “Assessment of the relationships between myocardial contractility and infarct tissue revealed by serial magnetic resonance imaging in patients with acute myocardial infarction,” *Int J Cardiovasc Imaging,* vol. 31, no. 6, pp. 1201-9, Aug, 2015.
[140] S. Nakano, M. Takahashi, F. Kimura, T. Senoo, T. Saeki, S. Ueda, J. Tanno, T. Senbonmatsu, T. Kasai, and S. Nishimura, “Cardiac magnetic resonance imaging-based myocardial strain study for evaluation of cardiotoxicity in breast cancer patients treated with trastuzumab: A pilot study to evaluate the feasibility of the method,” *Cardiol J,* vol. 23, no. 3, pp. 270-80, 2016.
[141] B. Baeßler, F. Schaarschmidt, A. Dick, G. Michels, D. Maintz, and A. C. Bunck, “Diagnostic implications of magnetic resonance feature tracking derived myocardial strain parameters in acute myocarditis,” *Eur J Radiol,* vol. 85, no. 1, pp. 218-227, Jan, 2016.
[142] A. H. Aletras, G. S. Tilak, L. Y. Hsu, and A. E. Arai, “Heterogeneity of intramural function in hypertrophic cardiomyopathy: mechanistic insights from MRI late gadolinium enhancement and high-resolution displacement encoding with stimulated echoes strain maps,” *Circ Cardiovasc Imaging,* vol. 4, no. 4, pp. 425-34, Jul, 2011.
[143] R. J. Taylor, F. Umar, E. L. Lin, A. Ahmed, W. E. Moody, W. Mazur, B. Stegemann, J. N. Townend, R. P. Steeds, and F. Leyva, “Mechanical effects of left ventricular midwall fibrosis in non-ischemic cardiomyopathy,” *J Cardiovasc Magn Reson,* vol. 18, pp. 1, Jan 5, 2016.
[144] S. J. Buss, K. Breuninger, S. Lehrke, A. Voss, C. Galuschky, D. Lossnitzer, F. Andre, P. Ehlermann, J. Franke, T. Taeger, L. Frankenstein, H. Steen, B. Meder, E. Giannitsis, H. A. Katus, and G. Korosoglou, “Assessment of myocardial deformation with cardiac magnetic resonance strain imaging improves risk stratification in patients with dilated cardiomyopathy,” *Eur Heart J Cardiovasc Imaging,* vol. 16, no. 3, pp. 307-15, Mar, 2015.
[145] I. Mordi, H. Bezerra, D. Carrick, and N. Tzemos, “The Combined Incremental Prognostic Value of LVEF, Late Gadolinium Enhancement, and Global Circumferential Strain Assessed by CMR,” *JACC Cardiovasc Imaging,* vol. 8, no. 5, pp. 540-549, May, 2015.
[146] C. Munoz, A. Bustin, R. Neji, K. P. Kunze, C. Forman, M. Schmidt, R. Hajhosseiny, P. G. Masci, M. Zeilinger, W. Wuest, R. M. Botnar, and C. Prieto, “Motion-corrected 3D whole-heart water-fat high-resolution late gadolinium

enhancement cardiovascular magnetic resonance imaging," *J Cardiovasc Magn Reson,* vol. 22, no. 1, pp. 53, Jul 20, 2020.
[147] A. A. Peters, B. Wagner, G. Spano, F. Haupt, L. Ebner, K. P. Kunze, M. Schmidt, R. Neji, R. Botnar, C. Prieto, B. Jung, A. Christe, C. Grani, and A. T. Huber, "Myocardial scar detection in free-breathing Dixon-based fat- and water-separated 3D inversion recovery late-gadolinium enhancement whole heart MRI," *Int J Cardiovasc Imaging,* vol. 39, no. 1, pp. 135-144, Jan, 2023.
[148] J. Groschel, Y. Bhoyroo, E. Blaszczyk, R. F. Trauzeddel, D. Viezzer, H. Saad, M. Fenski, and J. Schulz-Menger, "Different Impacts on the Heart After COVID-19 Infection and Vaccination: Insights From Cardiovascular Magnetic Resonance," *Front Cardiovasc Med,* vol. 9, pp. 916922, 2022.
[149] J. Bogaert, and M. Francone, "Cardiovascular magnetic resonance in pericardial diseases," *J Cardiovasc Magn Reson,* vol. 11, no. 1, pp. 14, May 4, 2009.
[150] A. Suinesiaputra, D. A. Bluemke, B. R. Cowan, M. G. Friedrich, C. M. Kramer, R. Kwong, S. Plein, J. Schulz-Menger, J. J. M. Westenberg, A. A. Young, and E. Nagel, "Quantification of LV function and mass by cardiovascular magnetic resonance: multi-center variability and consensus contours," *Journal of Cardiovascular Magnetic Resonance,* vol. 17, no. 1, pp. 63, 2015/07/28, 2015.
[151] T. F. Ismail, P. J. Angell, A. Jabbour, G. Smith, R. Wage, B. Hewins, N. Mistry, A. L. Dahl, S. Clark, B. Cowley, K. George, G. Whyte, D. J. Pennell, and S. K. Prasad, "Cardiac effects of anabolic steroid use amongst recreational body builders - a CMR study," *Journal of Cardiovascular Magnetic Resonance,* vol. 14, no. 1, pp. P186, 2012/02/01, 2012.
[152] A. Kanzaki, M. Kadoya, S. Katayama, and H. Koyama, "Cardiac Hypertrophy and Related Dysfunctions in Cushing Syndrome Patients—Literature Review," *Journal of Clinical Medicine,* vol. 11, no. 23, pp. 7035, 2022.
[153] G. Pedrizzetti, P. Claus, P. J. Kilner, and E. Nagel, "Principles of cardiovascular magnetic resonance feature tracking and echocardiographic speckle tracking for informed clinical use," *J Cardiovasc Magn Reson,* vol. 18, no. 1, pp. 51, Aug 26, 2016.
[154] X. Chen, H. Hu, J. Pan, J. Shu, Y. Hu, and R. Yu, "Performance of cardiovascular magnetic resonance strain in patients with acute myocarditis," *Cardiovasc Diagn Ther,* vol. 10, no. 4, pp. 725-737, Aug, 2020.
[155] R. Kranzusch, F. Aus dem Siepen, S. Wiesemann, L. Zange, S. Jeuthe, T. Ferreira da Silva, T. Kuehne, B. Pieske, C. Tillmanns, M. G. Friedrich, J. Schulz-Menger, and D. R. Messroghli, "Z-score mapping for standardized analysis and reporting of cardiovascular magnetic resonance modified Look-Locker inversion recovery (MOLLI) T1 data: Normal behavior and validation in patients with amyloidosis," *J Cardiovasc Magn Reson,* vol. 22, no. 1, pp. 6, Jan 20, 2020.
[156] N. A. B. Ntusi, S. K. Piechnik, J. M. Francis, V. M. Ferreira, A. B. S. Rai, P. M. Matthews, M. D. Robson, J. Moon, P. B. Wordsworth, S. Neubauer, and T. D. Karamitsos, "Subclinical myocardial inflammation and diffuse fibrosis are common in systemic sclerosis – a clinical study using myocardial T1-mapping and extracellular volume quantification," *Journal of Cardiovascular Magnetic Resonance,* vol. 16, no. 1, pp. 21, 2014/03/04, 2014.
[157] C. Jellis, J. Martin, J. Narula, and T. H. Marwick, "Assessment of nonischemic myocardial fibrosis," *J Am Coll Cardiol,* vol. 56, no. 2, pp. 89-97, Jul 6, 2010.
[158] A. Moreo, G. Ambrosio, B. De Chiara, M. Pu, T. Tran, F. Mauri, and S. V. Raman, "Influence of myocardial fibrosis on left ventricular diastolic function:

noninvasive assessment by cardiac magnetic resonance and echo," *Circ Cardiovasc Imaging,* vol. 2, no. 6, pp. 437-43, Nov, 2009.
[159] M. Imazio, and Y. Adler, "Management of pericardial effusion," *European Heart Journal,* vol. 34, no. 16, pp. 1186-1197, 2012.
[160] A. Kontzias, A. Barkhodari, and Q. Yao, "Pericarditis in Systemic Rheumatologic Diseases," *Curr Cardiol Rep,* vol. 22, no. 11, pp. 142, Sep 10, 2020.
[161] B. B. Das, M. Dodson, and A. Guzman, "Recurrent pericarditis in an adolescent with Crohn's colitis," *Ann Pediatr Cardiol,* vol. 13, no. 3, pp. 256-259, Jul-Sep, 2020.
[162] D. Bansal, G. Chahoud, K. Ison, E. Gupta, M. Montgomery, L. Garza, and J. L. Mehta, "Pleuropericarditis and pericardial tamponade associated with inflammatory bowel disease," *J Ark Med Soc,* vol. 102, no. 1, pp. 16-9, Jul, 2005.
[163] P. D. Higgins, M. Schwartz, J. Mapili, I. Krokos, J. Leung, and E. M. Zimmermann, "Patient defined dichotomous end points for remission and clinical improvement in ulcerative colitis," *Gut,* vol. 54, no. 6, pp. 782-8, Jun, 2005.
[164] S. Won, C. Davies-Venn, S. Liu, and D. A. Bluemke, "Noninvasive imaging of myocardial extracellular matrix for assessment of fibrosis," *Curr Opin Cardiol,* vol. 28, no. 3, pp. 282-9, May, 2013.
[165] L. Garcia-Ferrer, J. Estornell, and V. Palanca, "Myocarditis by mesalazine with cardiac magnetic resonance imaging," *Eur Heart J,* vol. 30, no. 8, pp. 1015, Apr, 2009.
[166] C. Galvao Braga, J. Martins, C. Arantes, V. Ramos, C. Vieira, A. Salgado, S. Magalhaes, and A. Correia, "Mesalamine-induced myocarditis following diagnosis of Crohn's disease: a case report," *Rev Port Cardiol,* vol. 32, no. 9, pp. 717-20, Sep, 2013.

8. DECLARATION ON OATH (Eidesstattliche Versicherung)

„Ich, Endri Abazi, versichere an Eides statt durch meine eigenhändige Unterschrift, dass ich die vorgelegte Dissertation mit dem Thema: Evaluation of the cardiac involvement of chronic inflammatory bowel diseases using cardiovascular magnetic resonance. / Evaluierung der kardialen Mitbeteiligung chronisch entzündlicher Darmerkrankungen mittels kardiovaskulärer Magnetresonanztomographie; selbstständig und ohne nicht offengelegte Hilfe Dritter verfasst und keine anderen als die angegebenen Quellen und Hilfsmittel genutzt habe.

Alle Stellen, die wörtlich oder dem Sinne nach auf Publikationen oder Vorträgen anderer Autoren/innen beruhen, sind als solche in korrekter Zitierung kenntlich gemacht. Die Abschnitte zu Methodik (insbesondere praktische Arbeiten, Laborbestimmungen, statistische Aufarbeitung) und Resultaten (insbesondere Abbildungen, Graphiken und Tabellen) werden von mir verantwortet.

Ich versichere ferner, dass ich die in Zusammenarbeit mit anderen Personen generierten Daten, Datenauswertungen und Schlussfolgerungen korrekt gekennzeichnet und meinen eigenen Beitrag sowie die Beiträge anderer Personen korrekt kenntlich gemacht habe (siehe Anteilserklärung). Texte oder Textteile, die gemeinsam mit anderen erstellt oder verwendet wurden, habe ich korrekt kenntlich gemacht.

Meine Anteile an etwaigen Publikationen zu dieser Dissertation entsprechen denen, die in der untenstehenden gemeinsamen Erklärung mit der Erstbetreuerin, angegeben sind. Für sämtliche im Rahmen der Dissertation entstandenen Publikationen wurden die Richtlinien des ICMJE (International Committee of Medical Journal Editors; www.icmje.og) zur Autorenschaft eingehalten. Ich erkläre ferner, dass ich mich zur Einhaltung der Satzung der Charité – Universitätsmedizin Berlin zur Sicherung Guter Wissenschaftlicher Praxis verpflichte.

Weiterhin versichere ich, dass ich diese Dissertation weder in gleicher noch in ähnlicher Form bereits an einer anderen Fakultät eingereicht habe.

Die Bedeutung dieser eidesstattlichen Versicherung und die strafrechtlichen Folgen einer unwahren eidesstattlichen Versicherung (§§156, 161 des Strafgesetzbuches) sind mir bekannt und bewusst.“

_____ _____

Datum Unterschrift

9. STATISTICAL CERTIFICATE (Statistische Bescheinigung)

CHARITÉ

CharitéCentrum für Human- und Gesundheitswissenschaften

Charité | Campus Charité Mitte | 10117 Berlin

Institut für Biometrie und klinische Epidemiologie (iBikE)

Direktor: Prof. Dr. Frank Konietschke

Postanschrift:
Charitéplatz 1 | 10117 Berlin
Besucheranschrift:
Reinhardtstr. 58 | 10117 Berlin

Tel. +49 (0)30 450 562171
frank.konietschke@charite.de
https://biometrie.charite.de/

Name, Vorname: Abazi, Endri
Emailadresse: endri.abazi@charite.de
Matrikelnummer: 9122000
PromotionsbetreuerIn: Prof. Dr. med. J. Schulz-Menger
Promotionsinstitution / Klinik: ECRC/ Charite (Campus Buch)

Bescheinigung

Hiermit bescheinige ich, dass *Herr Endri Abazi* innerhalb der Service Unit Biometrie des Instituts für Biometrie und klinische Epidemiologie (iBikE) bei mir eine statistische Beratung zu einem Promotionsvorhaben wahrgenommen hat. Folgende Beratungstermine wurden wahrgenommen:

- *Termin 1: 11.04.2023*

Folgende wesentliche Ratschläge hinsichtlich einer sinnvollen Auswertung und Interpretation der Daten wurden während der Beratung erteilt:

- Klarer herausstellen, welche Tests wann Anwendung finden
- Ggf. Mann-Whitney Test als nichtparametrische Alternative zu t-Test
- Präsentation der Ergebnisse deutlicher machen

Diese Bescheinigung garantiert nicht die richtige Umsetzung der in der Beratung gemachten Vorschläge, die korrekte Durchführung der empfohlenen statistischen Verfahren und die richtige Darstellung und Interpretation der Ergebnisse. Die Verantwortung hierfür obliegt allein dem Promovierenden. Das Institut für Biometrie und klinische Epidemiologie übernimmt hierfür keine Haftung.

Datum:_____ Name des Beraters/ der Beraterin:

_____

Unterschrift BeraterIn, Institutsstempel

10. CURRICULUM VITAE

(MEIN LEBENSLAUF WIRD AUS DATENSCHUTZRECHTLICHEN GRÜNDEN IN DER ELEKTRONISCHEN VERSION MEINER ARBEIT NICHT VERÖFFENTLICHT)